NTIA Report 85-184

Millimeter-Wave Urban and Suburban Propagation Measurements Using Narrow and Wide Bandwidth Channel Probes

E.J. Violette
R.H. Espeland
G.R. Hand

U.S. DEPARTMENT OF COMMERCE
Malcolm Baldrige, Secretary

Rodney L. Joyce, Acting Assistant Secretary
for Communications and Information

November 1985

PREFACE

The propagation studies and analysis described in this report were sponsored by the Department of the Army Communication-Electronics Command (CECOM), Fort Monmouth, New Jersey. The technical guidance and advice provided by Dr. Felix Schwering of CECOM are gratefully acknowledged.

A literature search for published information concerning millimeter-wave propagation in urban-suburban environments and a discussion of findings were performed by F. Kenneth Steele of NTIA, which avoided a duplication of effort in the work performed.

TABLE OF CONTENTS

LIST OF FIGURES

LIST OF FIGURES (continued)

LIST OF FIGURES (continued)

LIST OF TABLES

MILLIMETER-WAVE URBAN AND SUBURBAN PROPAGATION MEASUREMENTS USING NARROW AND WIDE BANDWIDTH CHANNEL PROBES

E. J. Violette, R. H. Espeland, and G. R. Hand*

Measurements reported are part of a study of propagation characteristics for millimeter-wave communication links operating in an urban-suburban environment. Absorption data were collected for signals propagated through some common building materials at 9.6 (reference frequency), 28.8, and 57.6 GHz. At these same channel frequencies, paths at street level obstructed by office buildings and residential properties were examined in terms of received signal levels resulting from direct penetration and/or propagation by diffraction modes with terminal separation of from 0.1 to 1.2 km. Signal fading was measured for line-of-sight paths up to 0.9 km as the transmitter terminal, operating at 11.4, 28.8, and 30.3 GHz, traveled down an urban street. Narrow- and wide-beam antenna patterns and both modes of linear antenna polarization were used to compare multipath fading characteristics. A unique 30.3 GHz wide bandwidth channel impulse probe was used to record multipath signal amplitudes and delay times, relative to the direct path, for the same antenna parameters indicated above. Impulse response measurements were recorded at about 10 m intervals as the transmitter traveled along the urban street.

Key words: impulse; millimeter waves; multipath; propagation; urban-suburban

1. INTRODUCTION

Urban and suburban environments present a wide variety of situations for communication links in the millimeter-wave spectrum. An ideal link for the compact size of millimeter-wave equipment with small, yet narrow, beamwidth antennas would be from rooftop to rooftop of the tallest buildings. The only conceivable propagation problem with a line-of-sight (LOS) link of this type would be excessive attenuation from rain in the path or gaseous absorption (in a molecular resonance band) for a long path (> 1 km). If, however, a link is required for operation at street level and if it operates from portable terminals, many problems can confront the user. One of the major concerns is interference between reflected signals and direct LOS signals. Reflected signals from street surfaces and from building walls, vehicles, street signs, etc. can cause deep fades. For wide bandwidth links (high data rate, for

*The authors are with the Institute for Telecommunication Sciences, National Telecommunications and Information Administration, U.S. Department of Commerce, Boulder, CO 80303.

example), distortion results from time-delayed, reflected multipath signals that will affect the efficient transmission of information. The severity of these problems depends upon such link parameters as length of path, antenna beamwidths, frequency, and path clearance.

Studies of millimeter-wave propagation conducted by the Institute for Telecommunication Sciences have included on-site measurements in urban and suburban settings. Measurements performed in FY 83 provided information at 9.6, 28.8, and 57.6 GHz regarding the reflection properties of buildings and street surfaces. Also, for the same frequencies, data were taken on LOS paths with narrow beamwidth scanning antennas to separate multipath components and on non-LOS paths to analyze reflected and diffracted components. The results of these mesurements made in the Denver, Colorado, metropolitan area were described in the U.S. Army Technical Report CECOM-83-3, "Urban Millimeter Wave Propagation Studies" (Violette et al., 1983a).

The reported results suggest that reliable millimeter-wave voice links could be established for an LOS path along a city street if a 30 dB clear air fade margin (above the free-space level) is provided. When one or more of the terminals are in motion, problems that are related to equipment design occur in establishing and holding a millimeter-wave voice link. Proper design of the response times of automatic gain control and frequency locking functions is critical due to the high signal fade rates resulting from multipath interference at these short radio-frequency (rf) wavelengths. In addition, if narrow antenna beamwidths are used, which is a prime benefit of the millimeter-wave band, rapid lock-up response time is necessary to detect the period when antenna coupling is achieved.

Measurements made on non-LOS paths showed that proper use of reflecting and diffracting surfaces can complete a link. In a random selection of terminal locations for non-LOS paths, arbitrary pointing of the transmitter antenna (other than vertical) produced detectable signals at the receiver without attempting to optimize antenna pointing. This test was performed for terminal separation of up to 500 m in downtown Denver. These signals arrived at the receiver by complex multireflections (from building surfaces, street signs, and other reflecting surfaces), by edge scattering, and/or by penetration through obstructions. In most cases, these signal levels were very small and would be usable only by sophisticated state-of-the-art equipment.

The purpose of the FY 84 studies was to further examine the propagation characteristics of millimeter-wave communication links operating in an urban environment. Two phases of study were conducted. The first emphasized the measurement of propagation loss on paths obstructed by common building materials, by commercial buildings of various types, and by typical suburban dwellings and street foliage. A continuous-wave (cw) probe operating at 9.6, 28.8, and 57.6 GHz (nearly the same system as used for the previously sited measurements) was used for this phase of the study. In the second phase of the study, the wideband high data-rate diagnostic probe (30.3 GHz) with cw channels at 11.4 and 28.8 GHz was used to make line-of-sight measurements along a section (approximately 1 km) of 17th Street in downtown Denver, Colorado. Signal amplitudes were sampled at about 0.1 m intervals, and an impulse response was recorded at approximately 10 m intervals along the street path. Amplitude and time delay of multipath signals relative to the direct path resulted from the impulse response measurements.

The results of this study will allow a better description of the effects of the urban and suburban environments on the propagation of millimeter waves by measuring propagation losses and by recording amplitude and delay features of multipath signals in urban and suburban settings.

To determine the available data base, a literature search of work done at frequencies above 10 GHz pertinent to suburban-urban propagation was conducted. Only two publications were located on the subject. Propagation properties of three types of building materials (plasterboard, chipboard, and aerated concrete blocks) were reported using 60 GHz (Huish et al., 1983), and Reudink (1972) made field strength measurements at 11.2 GHz with a mobile receiver and fixed transmitting antennas at heights of 120 m in an urban area (Manhattan, NY) and 60 m in a suburban area (New Providence, NY) with smaller buildings and houses. He found that the cumulative amplitude probability distribution for ranges up to about 1.6 km was nearly Ricean for both areas and that the signals in the suburban area were on the whole 10 dB higher than in the urban area.

2. MILLIMETER-WAVE MEASUREMENTS OF PROPAGATION LOSS THROUGH MATERIALS, BUILDINGS, AND FOR VARIOUS STREET SCENARIOS AT 9.6, 28.8, AND 57.6 GHZ

The propagation loss measurements were of three types. The first type compared the free space loss on a calibration path to the loss on the same path when obstructed by various types of building materials. The materials used for these measurements were plywood, drywall, and aluminum sheeting. These losses were also compared to the propagation loss through a commercially manufactured absorbing material.

The second type of propagation loss measurements was performed with buildings as path obstructions. Building types included solid concrete, brick with windows, and buildings with exterior walls constructed mainly of coated glass windows.

The third type of propagation loss measurements was in suburban residential areas. These settings included dense residential areas, sparse residential areas, and sparse residential areas with the receiver terminal at a location that was elevated relative to the transmitter terminal locations. These measurements were made during the summer months when the trees were in full foliage.

2.1 Equipment Description

The equipment used for the FY 83 measurements (Violette et al., 1983a) was redesigned in the IF and phase-locking sections only and used for the propagation loss measurements described in this report. The principal modification was the inclusion of low-noise amplifiers and very narrow, multipole crystal filters at each frequency in the receiver to increase the fade margin by a minimum of 20 dB. Also, to reduce the need for gain changes and resulting discontinuities, a logarithmic IF amplifier, with its video output proportional to the logarithm of the input, was installed in each channel. The dynamic range of these log-amps was 80 dB with a linearity of ±0.5 dB. The link operates at three coherent frequencies: 9.6, 28.8, and 57.6 GHz. The beamwidths of all the transmitting antennas are 10°, and the receiver beamwidths are 4.8° at the 9.6 GHz frequency and 1.2° at 28.8 and 57.6 GHz. With this modified configuration, an rf level of -132 dBm at the output of the receiving antenna was detectable at all frequency channels.

Instrumentation Description

A functional diagram of the transmitting terminal is shown in Figure 1. All three rf frequencies are derived from a 100 MHz, temperature-compensated crystal oscillator. A phased-locked, cavity-tuned (X96) multiplier is used to generate 20 mW at 9.6 GHz. An identical (X96) multiplier drives a varactor tripler that injection locks an 85 mW Gunn source at 28.8 GHz through a ferrite circulator. Part of the Gunn power is fed to a directional coupler providing 20 mW to a 25 dB-gain horn antenna, and the remaining power drives a varactor doubler. The output of the doubler provides about 12 mW of power at 57.6 GHz to a 25 dB gain-horn antenna. An IMPATT source previously used to provide 120 mW of power has been removed because of poor power and spectrum stability. The entire transmitter is mounted in a temperature-controlled enclosure that is held at 45°C ±1°C to reduce power variation to less than ±0.5 dB at 57.6 GHz in the worst case. Pointing of the transmitting antennas is accomplished either by an adjustable head on a tripod, since the unit is small, or by a manual positioner when mounted on the back of a vehicle for portability.

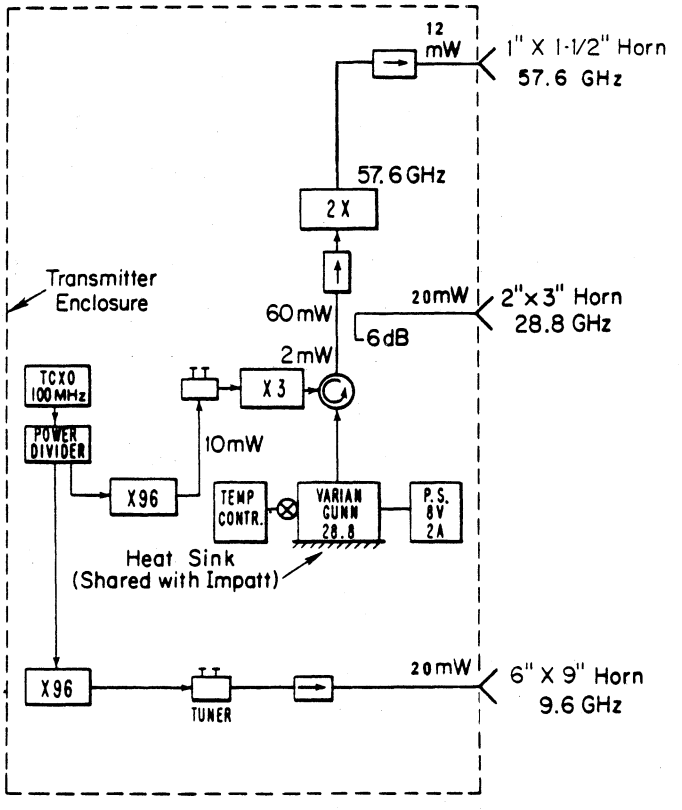

Figure 1. A functional diagram of the transmitting terminal.

A functional diagram of the receiving terminal is shown in Figure 2. All of the receiving rf components and the low noise IF preamplifiers are contained in a 45° ± 1°C temperature-controlled enclosure. Three parabolic reflectors (18, 24, and 12 inch, in order of ascending frequency) are mounted on the enclosure with low-noise downconverters coupled directly to the antenna feeds. This total assembly is mounted on the remote-controlled positioner. The receiver noise figure is determined by the input downconverter, which is a double-balanced mixer at 9.6 GHz with a 7.5 dB double sideband noise figure. The 28.8 and 57.6 GHz input mixers are of the stripline-waveguide-junction balanced type with double sideband noise figures of 5.5 and 6.0 dB, respectively. All local oscillator (LO) signals are generated from a voltage controlled crystal oscillator which is phase-locked to the 9.6 GHz received signal with a 5 MHz reference offset frequency. The multipliers for the voltage controlled 100 MHz reference to derive the LO injection signals are identical to the scheme used for the transmitter sources. Long-term (weeks) gain stability for each receiver is better than ±0.1 dB.

In the data acquisition system, the three IF frequencies of 5, 15, and 30 MHz are brought to the receiving van via coaxial cables, filtered, and amplified before entering an ac-to-dc log converter. At the log converter, the IF signals are converted to a dc level that is logarithmically related to the rf signal amplitude. These dc levels appear at the input of a digital scanner, which is capable of switching between each receiver level at rates of up to 30 times per second determined by the data-logging desk computer. The desk computer is also interfaced with a 5-1/2-digit voltmeter and is programmed to perform data collecting, data processing, tape storage, and data plotting functions. The receiving terminal and recording system are mounted on a mobile van. All antennas can be readily set for vertical and horizontal polarization, allowing linear and cross-polarized measurements. A remote-controlled antenna positioner allows for antenna pointing as a path is changed or permits a scanning of angles-of-arrival of signals for a complex path.

2.2 Measurements and Results

2.2.1 Common Materials as Path Obstructions

Comparative measurements of signal level on an LOS path to signal level on the same path when obstructed by sheets of common building materials were made on a 370-m path. The sheets of material (4' x 8') were large enough to cover the area immediately in front of the receiving antennas. However, there

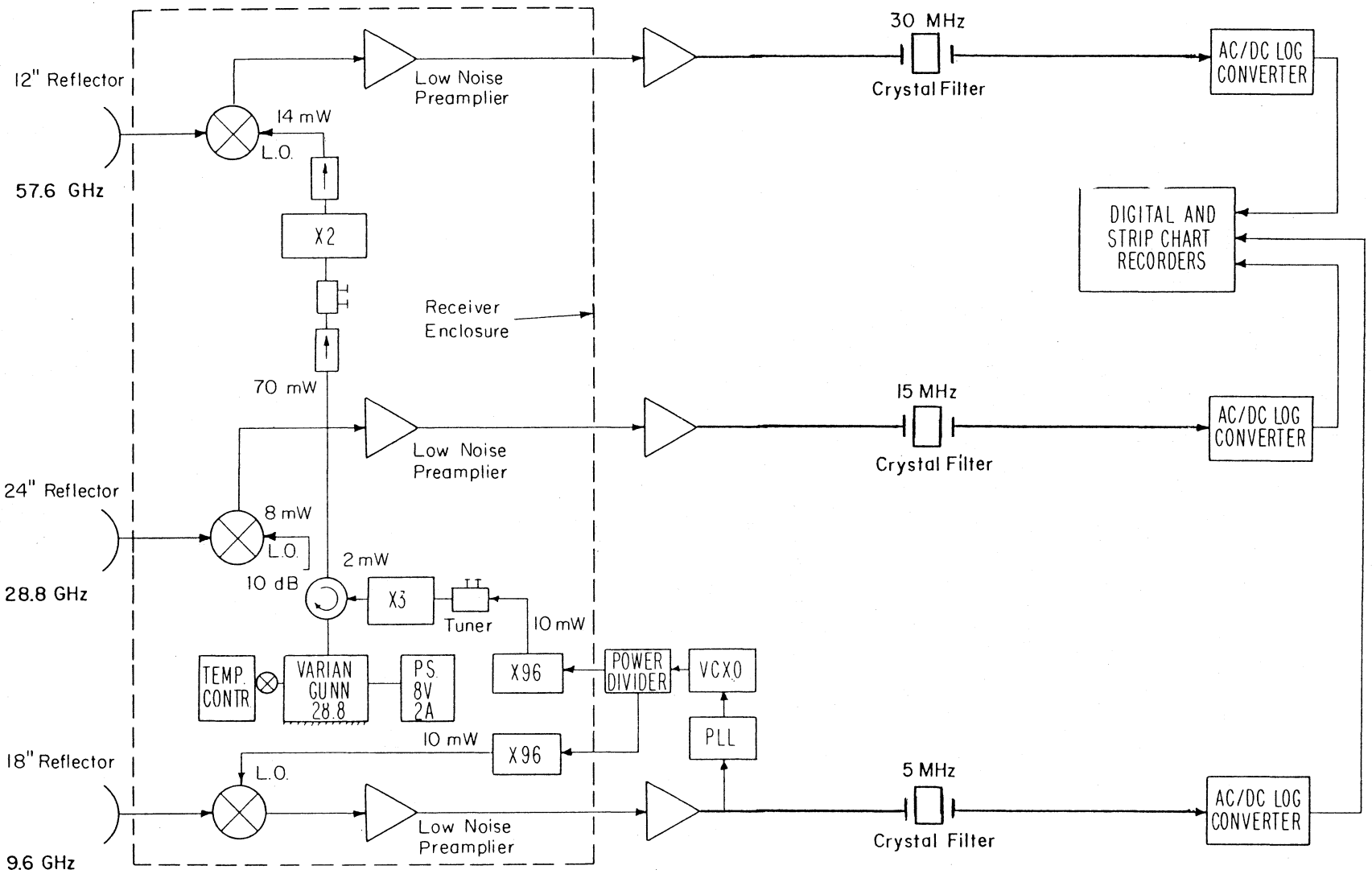

Figure 2. A functional diagram of the receiving terminal.

were edge diffraction components that contribute to the measured signal level but do not pass through the obstructing materials. This contribution becomes important only when the signal passing through the obstructions is very small. For example, in the case of an aluminum sheet, no signal should penetrate, but values of only 45 to 50 dB below the LOS path were measured. This signal level is, therefore, assumed to approach the limit of the loss measurement; however, because of edge sharpness of the 1/8" thick sheet of aluminum, a larger diffraction field would be produced than for the other materials measured.

Table 1 lists the results of the loss (plus diffraction) for the materials measured. In most cases, several readings were recorded with a slight change in the distance in front of the receiving antenna (roughly between 1 to 2 m). In the table, the average signal loss compared to the LOS path is indicated in addition to the highest and lowest values for the multiple readings. In general, the data for 9.6 GHz have the greatest deviation, which is probably due to its larger antenna beamwidth which allows a higher level of diffracted and perhaps reflected signals to bypass the obstruction.

A commercial absorbing material (Ecco Sorb CV-4)* had a specified loss of >40 dB at 10 GHz, >50 dB at 30 GHz, and >55 dB at 60 GHz, and as seen from the table, the measured values were reasonably near the quoted values. Both sheetrock (plasterboard) and dry fir plywood resulted in small signal losses. Surprisingly, wet plywood sheets stored outside and with an obviously high moisture content showed higher losses and somewhat greater frequency variations.

2.2.2 Buildings as Path Obstructions

Four buildings were used as path obstructions in these measurements. Each building was different in terms of construction materials, architectural design, and size. In each data set, the measurements were performed as a function of the distance the transmitter and receiver are from the building and of the pointing angles of the transmitter and receiver antennas.

For each data set, the path geometry is shown, and results are listed as a function of frequency. These collective data are useful in determining the

*The trade name is indicated because it is a common material used for rf shielding and does not imply a product endorsement by the U.S. Government.

Table 1. Signal Loss on Path Obstructed with Common Materials

Type of Obstructing Material	Signal Loss (dB)		
	9.6 GHz Maximum Minimum	28.8 GHz Maximum Minimum	57.6 GHz Maximum Minimum
Commercial Absorber (ECCOSORB CV-4)(*See previous page) 5 readings	38 +6 -2	51 +3 -5	59 +1 -4
Sheetrock 3/8 in - 2 sheets 5 readings	2 +1 -0	2 +1 -1	5 +1 -1
Plywood 3/4 in (dry) - 1 sheet 4 readings	1 +1 -1	4 +0 -1	8 +2 -3
Plywood 3/4 in (dry) - 2 sheets 1 reading	4	6	14
Plywood 3/4 in (wet) - 1 sheet 3 readings	19 +8 -13	32 +9 -8	59 +2 -2
Plywood 3/4 in (wet) - 2 sheets 3 readings	39 +2 -2	46 +2 -1	57 +2 -3
Aluminum 1/8 in - 1 sheet 1 reading	47	46	53

probability of a pair of terminals establishing a nonline-of-sight communications link given the performance parameters of the communications equipment.

Building #1:

This building, shown in Figure 3(A) and (B), has solid outside walls (20 cm thick), constructed of cement block with a 10 cm rock aggregate outside surface (total thickness is 30 cm). Figure 3(A) shows the transmitter (mounted on the pickup truck) at one of the locations relative to the building, and the picture in Figure 3(B) is of the receiver and the building. Inside the building there is a center hallway with offices constructed of glass and metal partitions on either side. The width of the building (that portion in the path) is 15 m, and it is 9 m in height.

The path and antenna pointing (as indicated by arrows) for the propagation measurements relative to this building are shown in Figures 4 and 5. The measured values as a function of frequency are given in dBm and are also shown in dB relative to the channel sensitivity (minimum measurable value), which

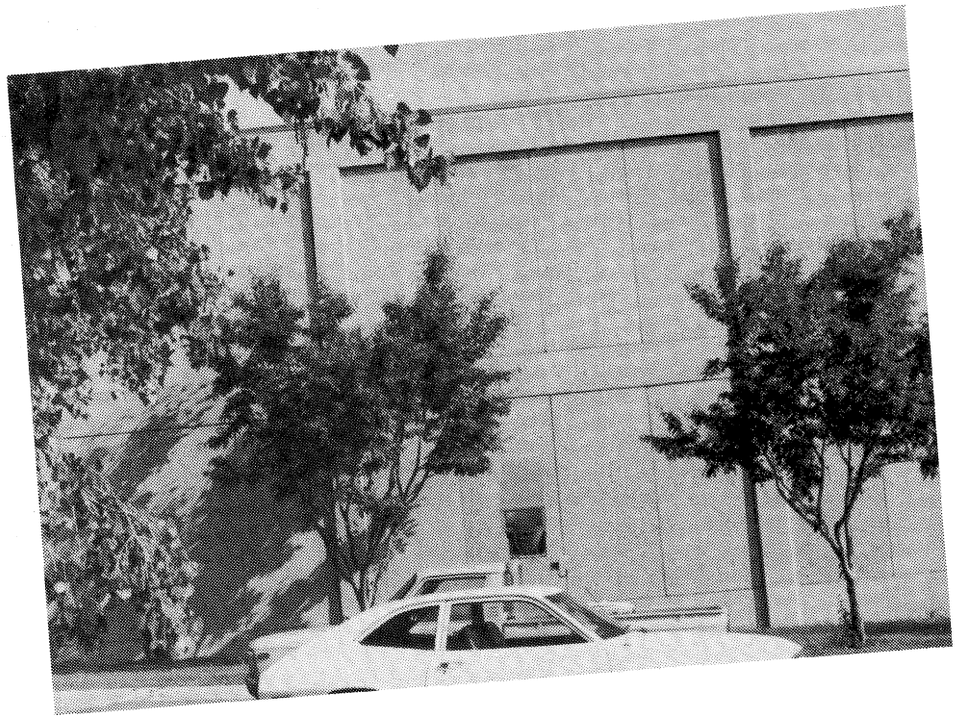

(A) Transmitter side.

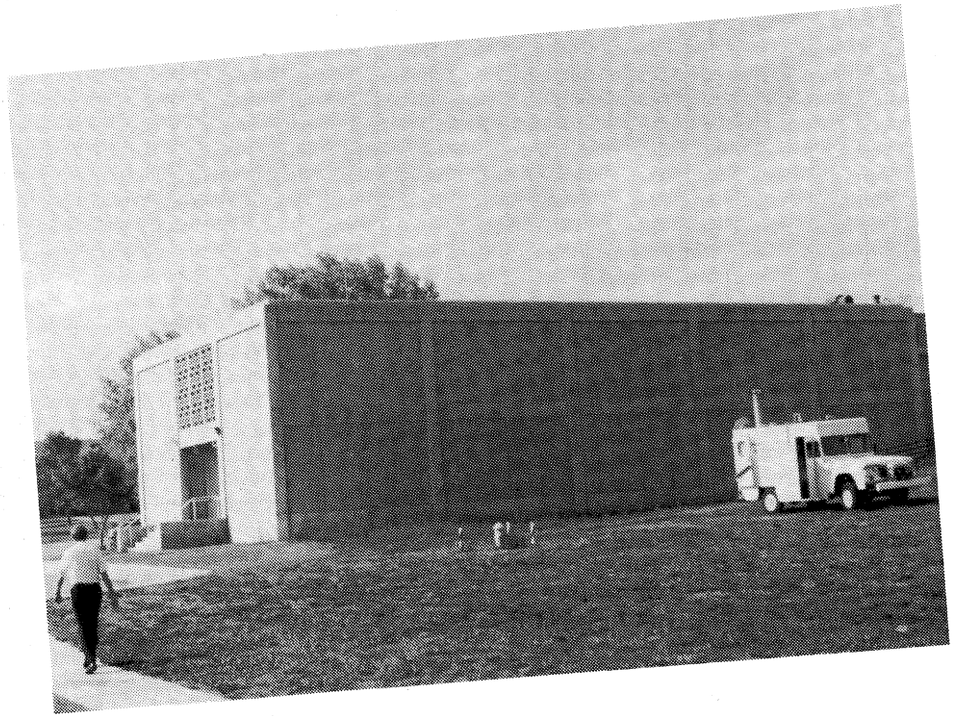

(B) Receiver side.

Figure 3. Photographs of building #1.

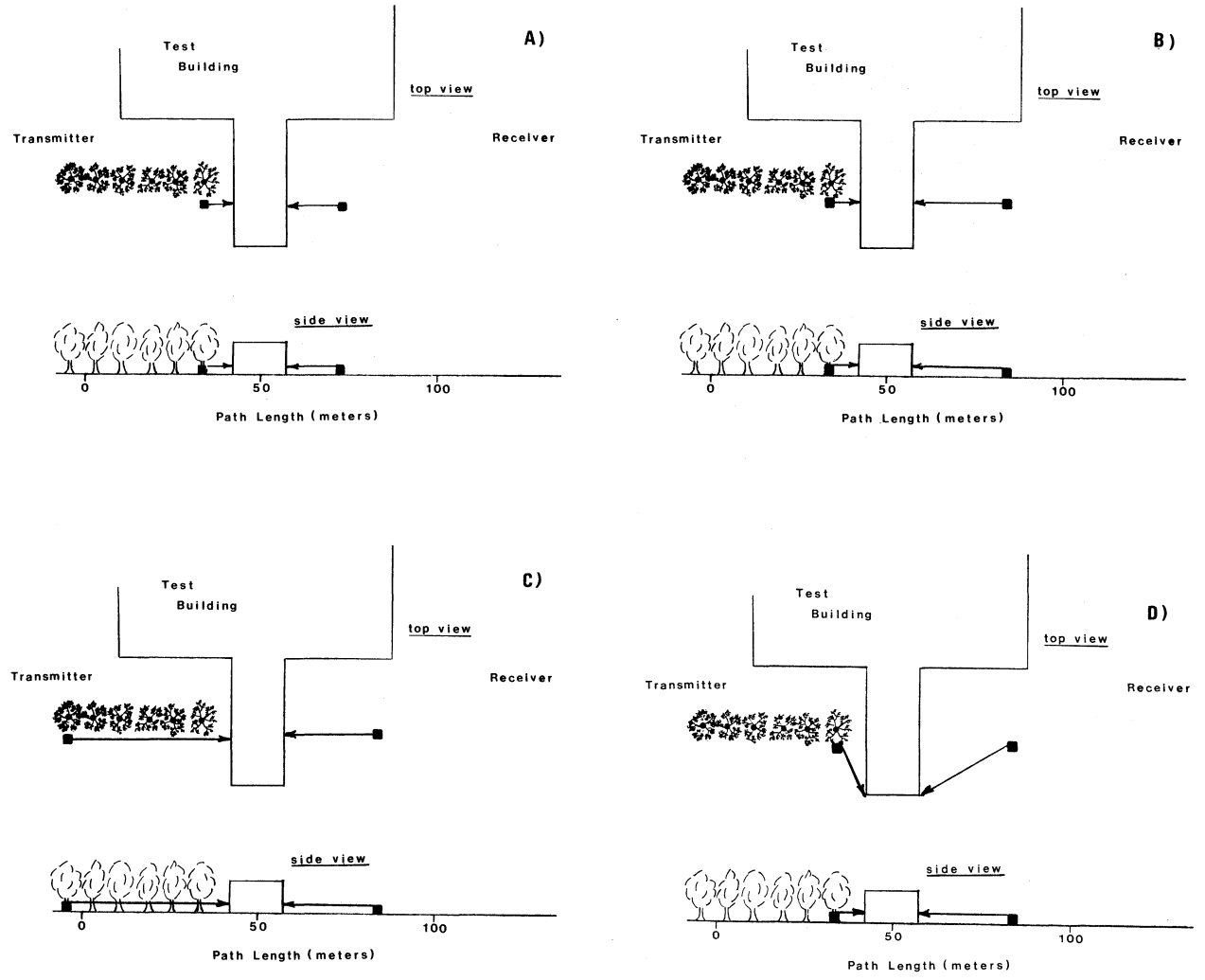

Frequency (GHz)

	9.6		28.8		57.6	
	dBm	dB*	dBm	dB*	dBm	dB*
A. Signal Level	-107	(25)	-132	(0)	-132	(0)
B. " "	- 87	(45)	-130	(2)	-132	(0)
C. " "	- 92	(40)	- 98	(34)	-113	(19)
D. " "	- 90	(42)	-102	(30)	-120	(12)

*Indicates level above system noise.

Figure 4. Path geometries and measured signal levels for building #1.

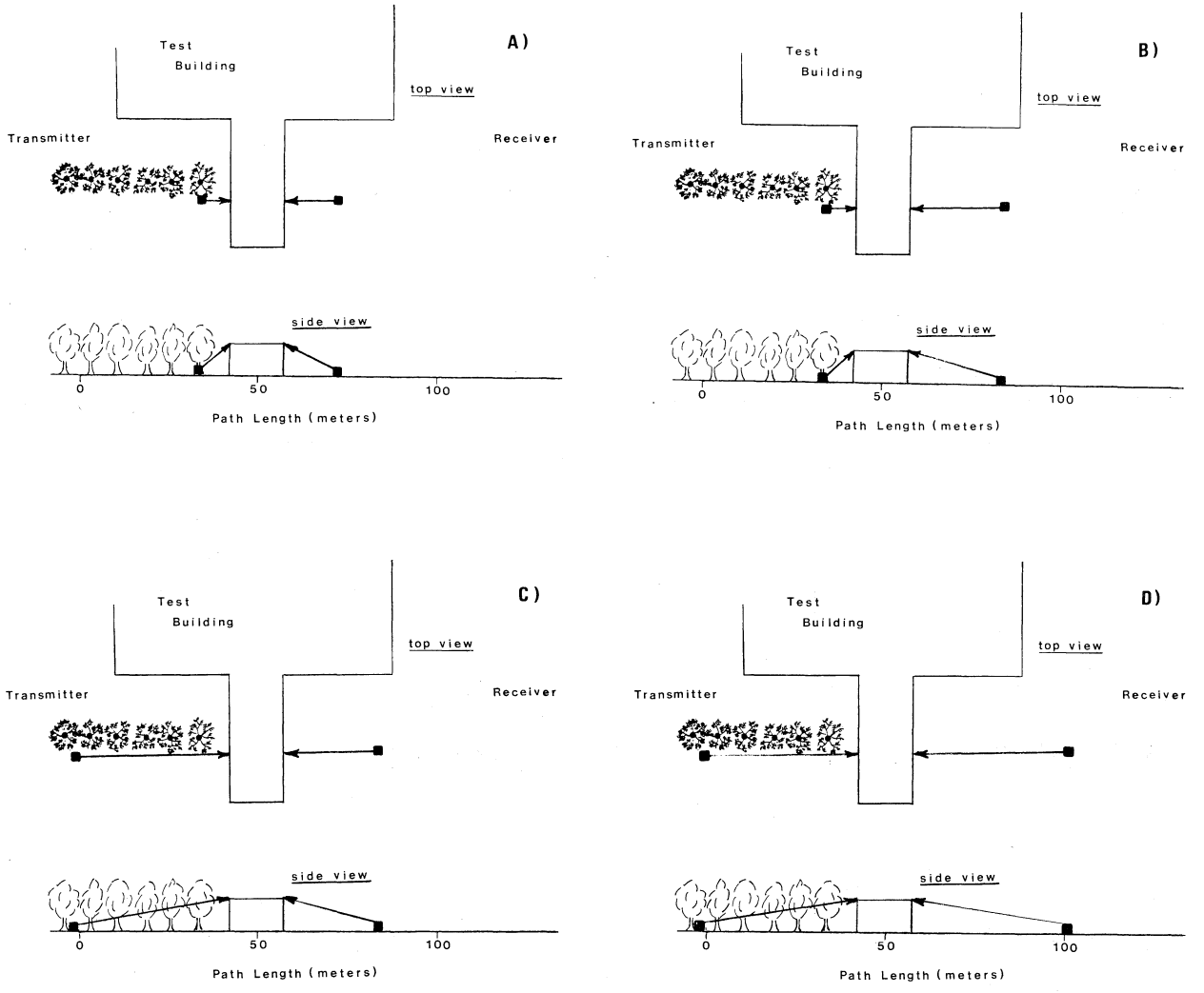

Frequency (GHz)

	9.6		28.8		57.6	
	dBm	dB*	dBm	dB*	dBm	dB*
A. Signal Level	-102	(30)	-110	(22)	-132	(0)
B. " "	- 80	(52)	- 80	(52)	- 93	(39)
C. " "	- 87	(45)	- 85	(47)	- 98	(34)
D. " "	- 72	(60)	- 77	(55)	- 92	(40)

*Indicates level above system noise.

Figure 5. Additional path geometries and measured signal levels for building #1.

for these channels was measured at -132 dBm. The total path lengths varied from 36 m to 100 m; however, the effect of path length on the received signal for these types of measurements is small (in most cases) compared to the loss due to the obstruction.

Sketches A, B, and C in Figure 4 show direct or (on path) pointing of both the transmitting and receiving antennas. Only the position of the terminals are changed, which changes the total path length and the area illuminated by the respective antennas at the building surfaces and the common volume of illumination above and to the side of the building as the path lengths increase. With direct pointing and a short path (36 m), as shown in Figure 4(A), no signal was detected above the noise threshold (-132 dBm) on the 28.8 and 57.6 GHz channels. The signal measured on the 9.6 GHz channel was -107 dBm or 25 dB above the system noise level. As the path from the receiver to the building is increased from 14 m to 25 m, as shown in Figure 4(B), the 9.6 GHz channel signal increases to a margin of 45 dB, the 28.8 GHz channel to a margin of 2 dB, and the 57.6 GHz channel remained at the noise level. In Figure 4(C), the transmitter-to-building path is increased from 7 m to 45 m. This change caused the 9.6 GHz channel level to decrease by 5 dB, the 28.8 GHz channel level to increase by 32 dB, and the 57.6 GHz channel level to increase by 19 dB. The results of these first three tests indicate that with this building as a path obstruction, little or no signal reaches the receiver by penetration at the two higher frequencies. The propagation mode is by "over and down" or "around and back" diffraction. This is supported by the fact that as the path-to-building lengths are increased, the received signal levels increase because of greater antenna illumination of the exterior edges of the building. In effect, the propagation mode appears to be by double-edge diffraction. In order to observe this mode, data were recorded for another double edge case as shown in Figure 4(D), where both the transmitter and receiving antennas are off-pointed horizontally to illuminate the building's vertical edges. The terminal locations are the same for this test as in Figure 4(B). The 28.8 and 57.6 GHz channels increased significantly from the geometry shown in Figure 4(B), again indicating that the propagation mode is mainly by diffraction except for some penetration at 9.6 GHz.

To further investigate the double-edge mode, the path geometries in sketches A, B, and C of Figure 5 were selected. These are respectively the

same as A, B, and C of Figure 4 with the antenna pointing on path in the horizontal plane, but the elevation angle was set to point at the top of the wall. Comparing respectively the results from the geometries in A, B, and C of Figure 4 to A, B, and C of Figure 5, all levels are increased with the exception that the 57.6 GHz levels in Figure 5(A) remained below the detectable threshold. In Figure 5(D), the receiver-to-building path was increased from 25 m to 42 m. With this change, the received signals were again increased.

To confirm the source of propagated energy, antenna scans were used for the geometries of Figure 5. In all cases shown, the maximum signal levels were obtained with the antenna mainbeams pointed directly at the roof edge and normal to the edge. This pointing (normal to the edge) was also in line with the direct path between terminals; therefore, it was not possible to determine the relative dependence of antenna pointing geometry (off-path angles).

A common volume of the atmosphere was illuminated by both transmitting and receiving antennas at a point 5 deg above this building, and detectable signals were seen. This signal was greater than at a pointing 5 deg below the edge; thus it is assumed to be a radiated source above the level of the antenna side lobes. At the time of this measurement, the ambient air temperature was near 90°F, and it is possible atmospheric convective turbulance could produce some side scatter components. An estimate is possible only at the higher frequencies (1° beamwidth), and although the components are difficult to separate, the level recorded was about 10 to 15 dB above the side lobe level at 5 deg from the mainbeam.

These measurements demonstrate that if a link using directive antennas is operated with an "unpenetratable" building as a path obstruction, it may be possible to establish a usable nonline-of-sight communications link by pointing the antennas to enhance the edge diffraction mode of propagation.

Building #2:

This building, like building #1, also had solid outside walls. The outer surface of this building was made of precast concrete panels. The picture of building #2 in Figure 6(A) was taken from near the transmitter location, and the picture taken from the receiver location is shown in Figure 6(B). The on-path width of this building measured 100 m, and it is 8 m high. The path configurations for this building are shown in Figure 7. The measured signals

(A) Transmitter Side.

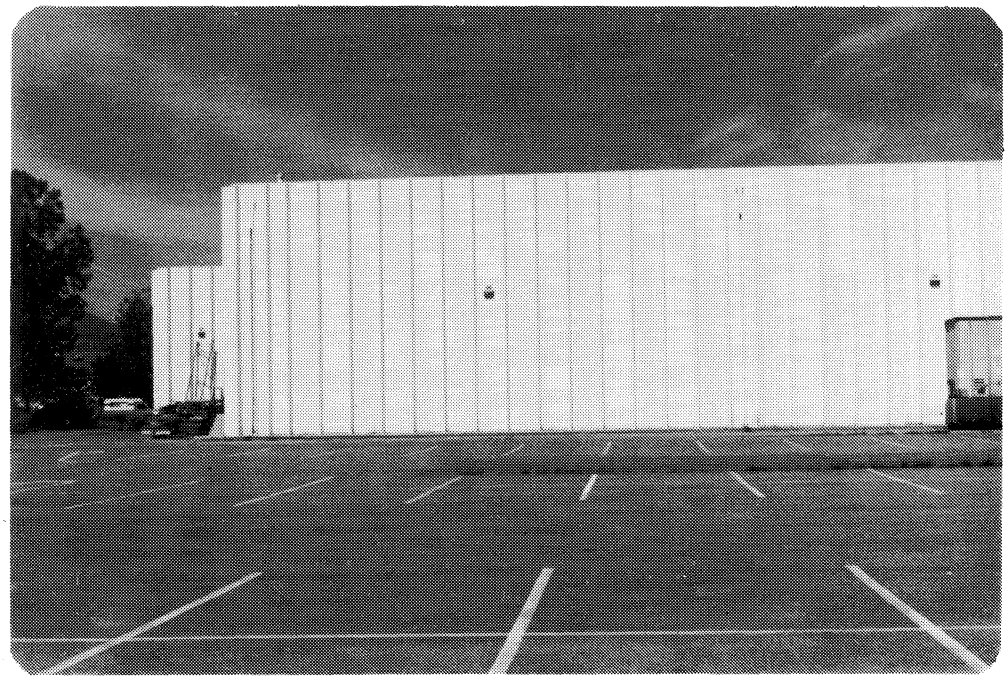

(B) Receiver Side.

Figure 6. Photographs of building #2.

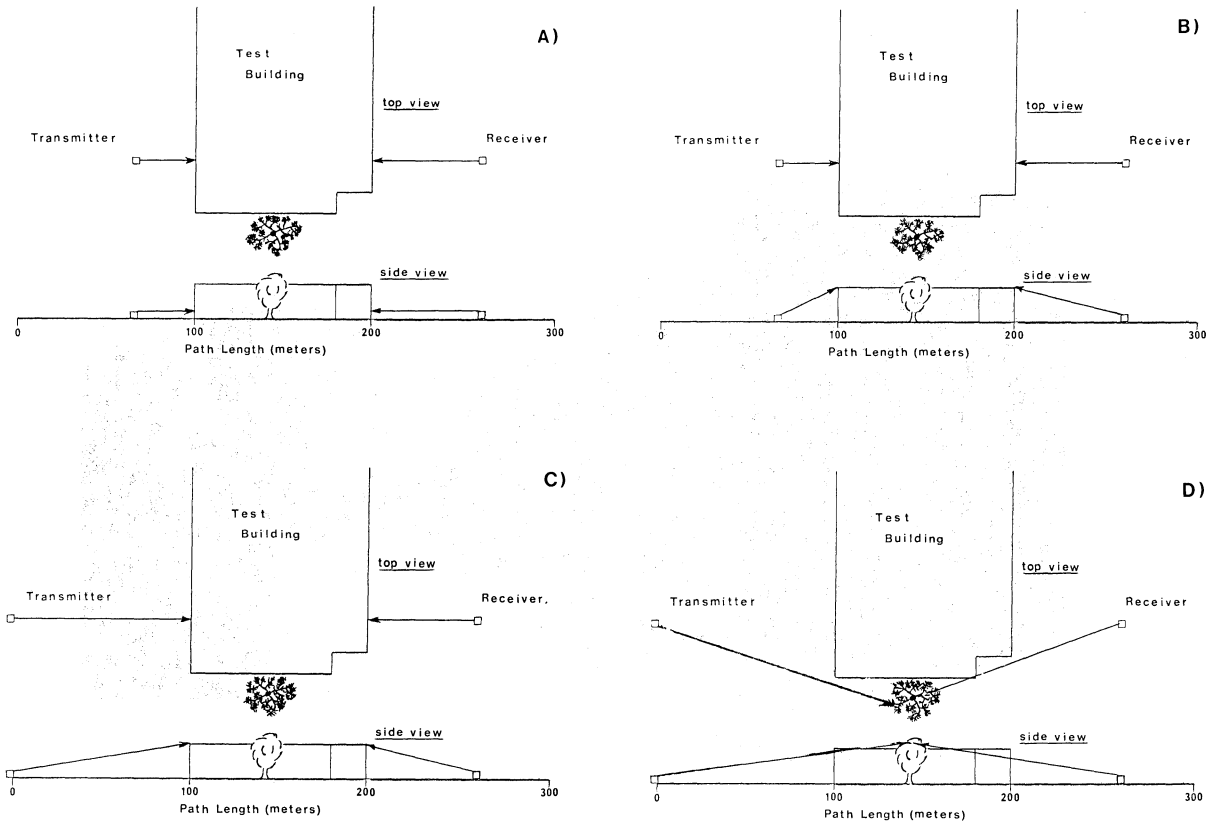

Frequency (GHz)

	9.6		28.8		57.6	
	dBm	dB*	dBm	dB*	dBm	dB*
A. Signal Level	-132	(0)	-132	(0)	-132	(0)
B. " "	-113	(19)	-117	(15)	-132	(0)
C. " "	-104	(28)	-104	(28)	-130	(2)
D. " "	- 83	(49)	- 84	(48)	-104	(28)

*Indicates level above system noise.

Figure 7. Path geometries and measured signal levels for building #2.

for Figure 7(A) did not exceed the -132 dBm system noise level. Thus no measurable signal penetrated this building with a transmitter-to-building path length of 32 m and a receiver-to-building path length of 60 m, with direct pointing between transmitting and receiving antennas. In Figure 7(B), the path lengths are unchanged; the horizontal pointing is on path, and both the transmitting and receiving antennas are vertically pointed toward the top of the walls. This change produced a signal increase of 19 dB at 9.6 GHz, 15 dB at 28.8 GHz, and no detectable signal at 57.6 GHz. In Figure 7(C), the transmitter-to-building path length was increased from 32 m to 100 m. In the horizontal plane, the antennas are still on path, and in the elevation plane, the antennas are pointing at the top of the wall. This increased path length produced an increase in all channels.

The results of measurements at this building are basically the same as for building #1. There was no detectable penetration with direct pointing, but an increase in levels with edge diffraction.

In Figure 7(D), the path lengths remain the same as for Figure 7(C), and the elevation angles are essentially unchanged. However, the antenna pointing in the horizontal plane was adjusted so that both the transmitting and receiving antennas illuminated a volume that included a tall cottonwood tree. This tree is to the right of the building in Figure 6(A) and partly visible at the left edge of the photograph in Figure 6(B). This change again increased all signal levels above previous readings. In this case, the branches and leaves of the tree serve as a scattering surface to propagate signals from the transmitters to the receivers.

Building #3:

This building has exterior walls surfaced with brick. The building on-path width is 53 m, and it is 14 m high. It is an office building with exterior windows, as seen in Figure 8. The geometries for these measurements are shown in Figure 9. The total path length of 118 m and the transmitter-to-building and receiver-to-building lengths are the same for all tests. The data in Figure 9(A) are with direct on-path pointing for both the transmitting and receiving antennas. As stated above, the width of the building is 53 m. However, for tests A and B, because of a courtyard in the path, the effective width is 38 m. Also, because of the courtyard, there are four outside walls in the path. The results are not much different from building #1, with penetration signals of 19 dB at 9.6 GHz, 2 dB at 28.8 GHz, and 0 dB at 57.6 GHz

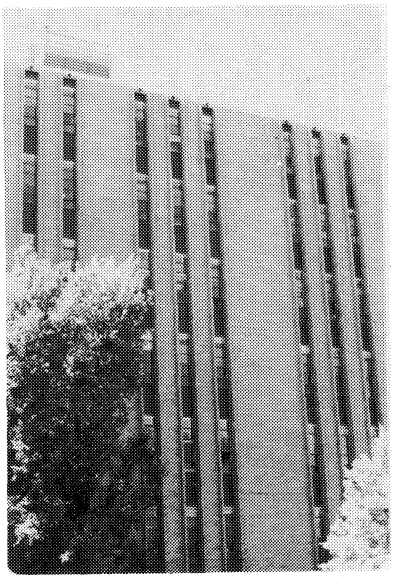

(A) Transmitter Side.

(B) Receiver Side.

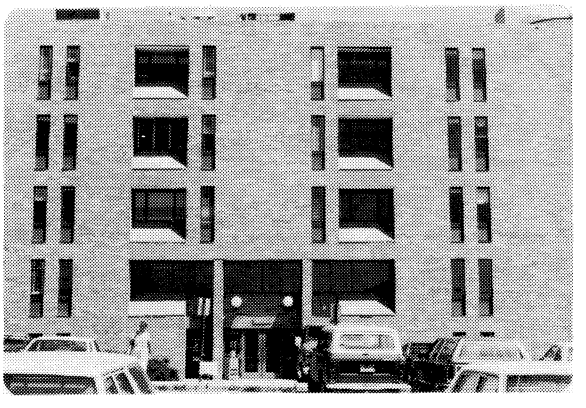

(C) Receiver Side.

Figure 8. Photographs of building #3.

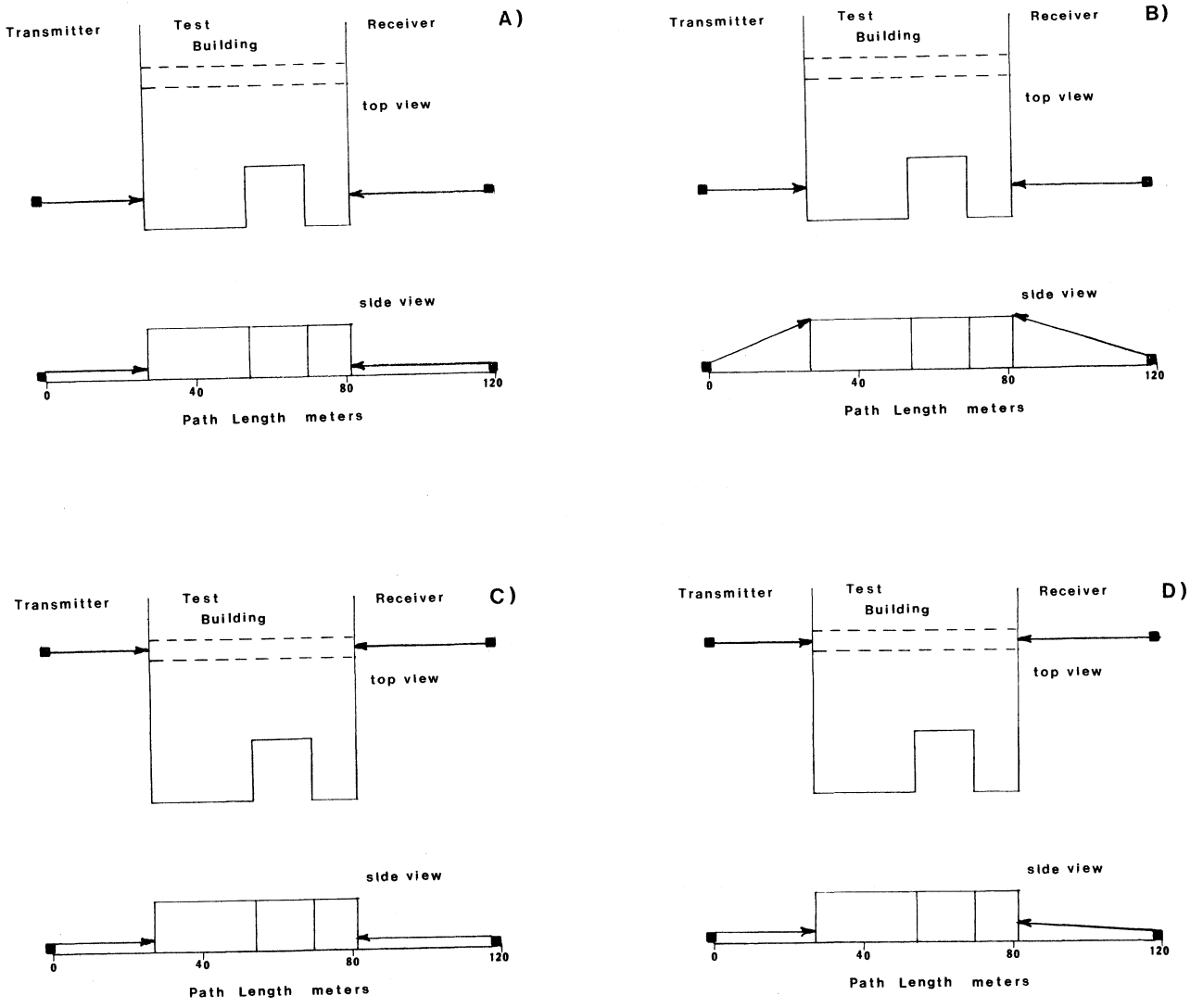

Frequency (GHz)

	9.6		28.8		57.6	
	dBm	dB*	dBm	dB*	dBm	dB*
A. Signal Level	-113	(19)	-130	(2)	-132	(0)
B. " "	-104	(28)	-114	(18)	-127	(5)
C. " "	- 89	(43)	-100	(32)	-117	(15)
D. " "	- 83	(49)	- 80	(52)	-113	(19)

*Indicates level above system noise.

Figure 9. Path geometries and measured signal levels for building #3.

relative to the -132 dBm noise threshold. In Figure 9(B), the effect of edge diffraction again becomes apparent as all signals increase to respective values of 28 dB, 18 dB, and 5 dB for frequencies of 9.6, 28.8, and 57.6 GHz.

In Figures 9(C) and 9(D), the location of the transmitting and receiving terminals was moved toward the center of the building and aligned with the hallway. This hallway extends through the building, but is not line-of-sight, being partly on the first floor level and partly on the second floor. The signal levels at all frequencies again increase with all antennas at on-path pointing. The new readings are 43 dB at 9.6 GHz, 32 dB at 28.8 GHz, and 15 dB at 57.6 GHz. In Figure 9(D), the receiving antenna was elevated by 5°, which further increased the received signals. The change in receiver antenna pointing more effectively used the propagation path created by the hallway.

Building #4:

This is an office building with predominantly glass walls. The photographs in Figure 10 show views of the building. These walls (windows) are chromatic coated glass, which exhibited a surprisingly high signal loss. The path geometries and antenna pointing angles for the measurements at this building are shown in Figure 11. The drawing in Figure 11(A) shows the transmitter and receiver terminals on a 72 m path. The building was unoccupied at the time the measurements were made, so that only the two glass exterior walls were in the path. The configuration in Figure 11(B) is a similar path, except in this case the path was through the exterior glass doors of a hallway. These doors were tinted, but not coated. Comparing the results of these data sets show that the coated glass attenuated the received signals of all channels by 50 dB or more compared to the attenuation of the tinted glass. Also, by comparison, these attenuations are approximately equal to the measured signal losses using a commercial absorbing material (see Section 2.2.1). The loss through the tinted glass was estimated at from 5 to 7 dB at 9.6 GHz, 8 to 9 dB at 28.8 GHz, and 9 to 11 dB at 57.6 GHz greater than a free space (LOS) path of the same length.

2.2.3 Measurements in Residential Areas

The measurements in the residential areas were of three types: dense residential, sparse residential, and sparse residential with one terminal elevated. The houses in the dense residential area were mainly one-family, one-story frame dwellings. The pictures in Figure 12 show typical houses of wood

(A) Transmitter Side.

(B) Receiver Side.

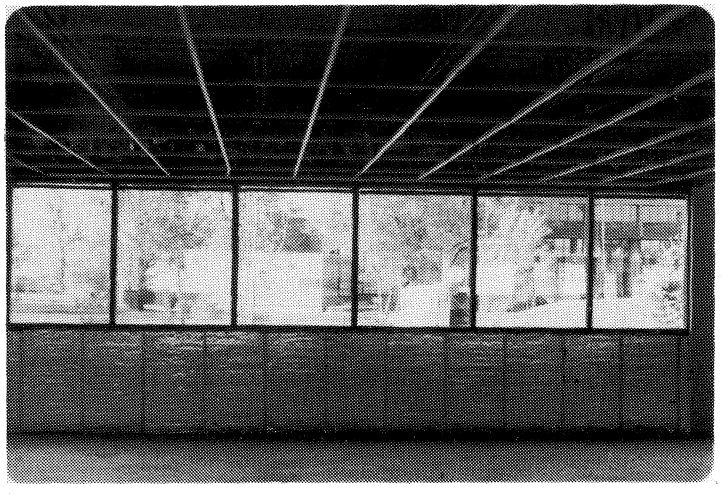

(C) View from inside the building toward the receiver side.

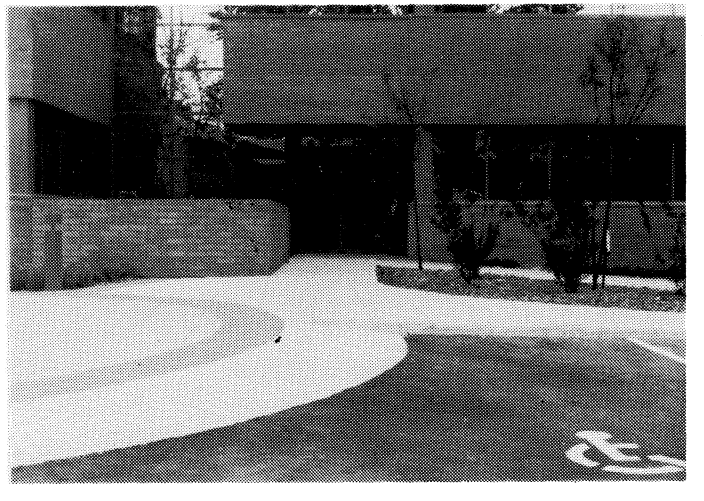

(D) Receiver side at the hallway.

Figure 10. Photographs of building #4.

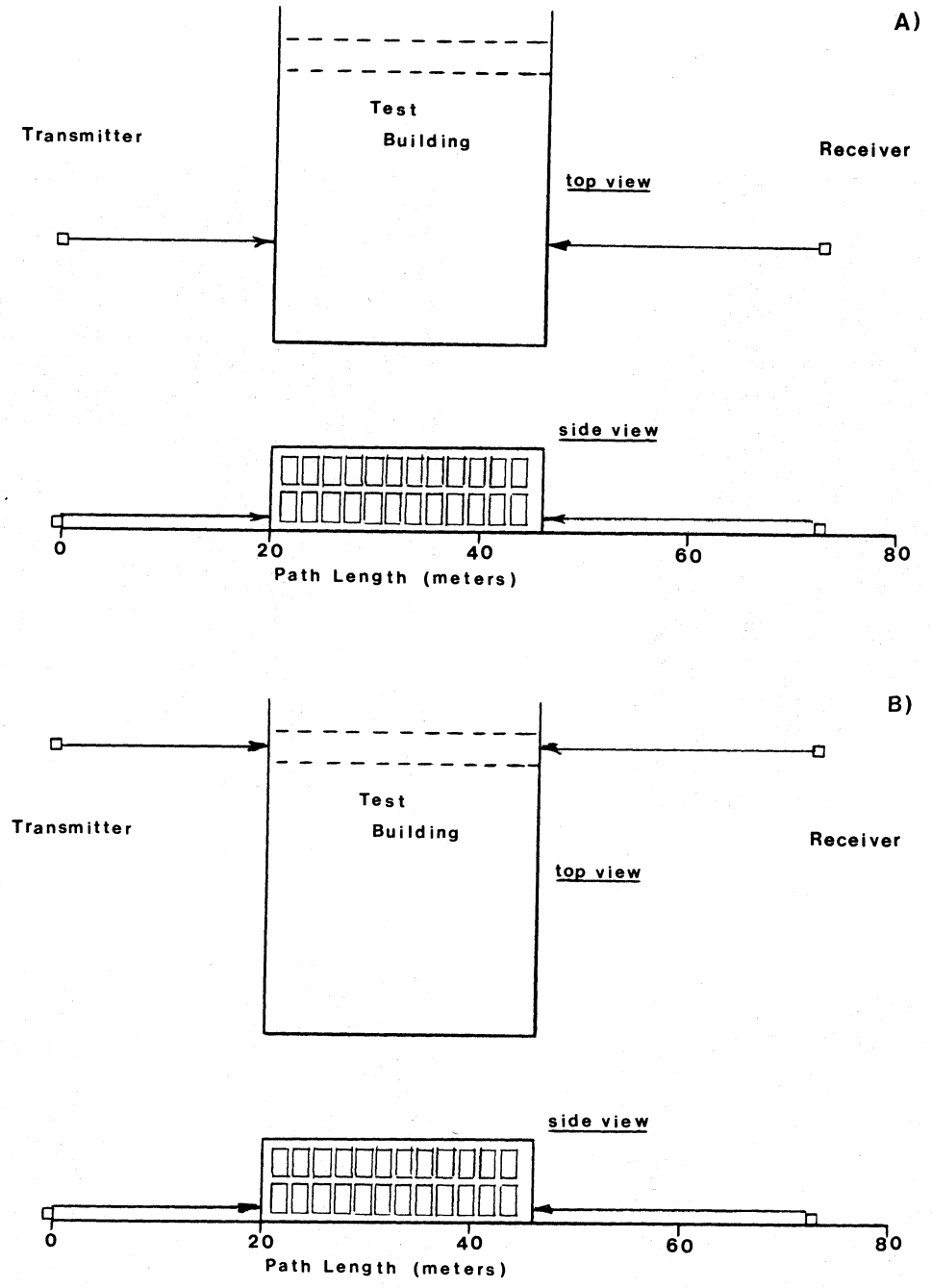

Frequency (GHz)

	9.6		28.8		57.6	
	dBm	dB*	dBm	dB*	dBm	dB*
A. Signal Level	-88	(44)	-90	(42)	-107	(25)
B. " "	-35	(97)	-32	(100)	- 57	(75)

*Indicates level above system noise.

Figure 11. Path geometries and measured signal levels for building #4.

(A) Transmitter at location #1.

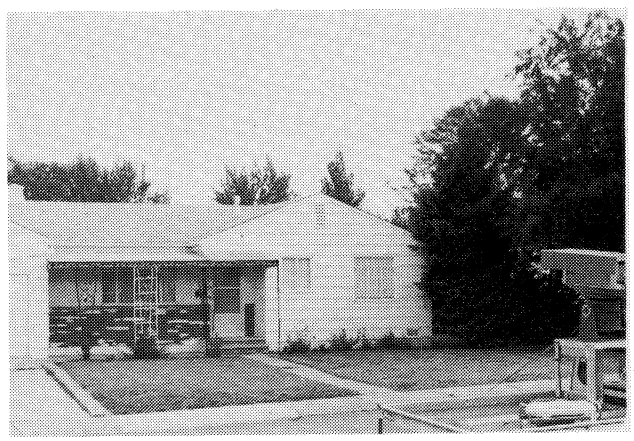

(B) Transmitter at location #3.

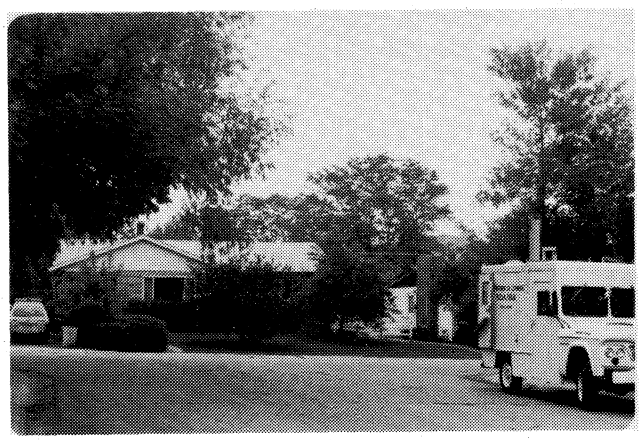

(C) Receiver location.

Figure 12. Transmitter and receiver locations in the dense residential area.

construction for this dense area with many trees and bushes in the yards. In the street map in Figure 13, three separate transmitter locations are identified as is the single receiver location. The dwellings in this area faced the streets, with backyard property lines adjacent and no alleys.

Table 2 lists the received signal level (RSL) calculated from space loss, the measured RSL, the loss due to the obstructions, and the signal margins (dB above the system noise levels). The first seven sets of data were recorded with the transmitter at location #1. Variations in these data resulted primarily from changes in the elevation angle of the receiving antennas. Set #7 also included changes in the receiver azimuthal angle and in the transmitter elevation angle.

The path, approximately 100 m from the transmitter at location #1 on 29th Street to the receiver just off 30th Street, was obstructed by at least two houses and by several trees as shown in Figures 12A and 12C. Starting with observation #1 in the table, both antennas were oriented for direct path pointing. Successive observations, #2 through #6, were made with the receiving antennas progressively elevated to 2.5°, 5.0°, 7.5°, 10.0°, and 15.0° An azimuthal scan between ±15° of direct path was performed, and the peak value was recorded. The measured results show an increase in level at all three frequencies, as the elevation angle is increased, reaching a peak at the 5.0° and 7.5° observations. These results are similar to the observations experienced in the previous section using buildings as path obstructors. As before, the propagation mechanism is some combination of diffraction, reflection, and/or scattering from the leaves of the trees. Observation #7 was made on the same path, but with transmitter and receiver antenna pointed for the maximum RSL found for this path. Observation #8 was made with the transmitter located at position #2 in Figure 13. The path length is still about 100 m, and the antennas are adjusted (pointed) for maximum signal level. The received signals are less on this path than on the previous path, presumably due to a lower effective scattering cross section. The final data set (#9) is with the transmitter moved to location #3 as seen in Figure 12B. Again, the antennas were pointed for maximum levels. On this path (180 m), the received levels are still well above the system noise levels, but lower than the maximized levels from the other two paths. In general, the loss increased with frequency; however, the differences for the higher two frequencies were small.

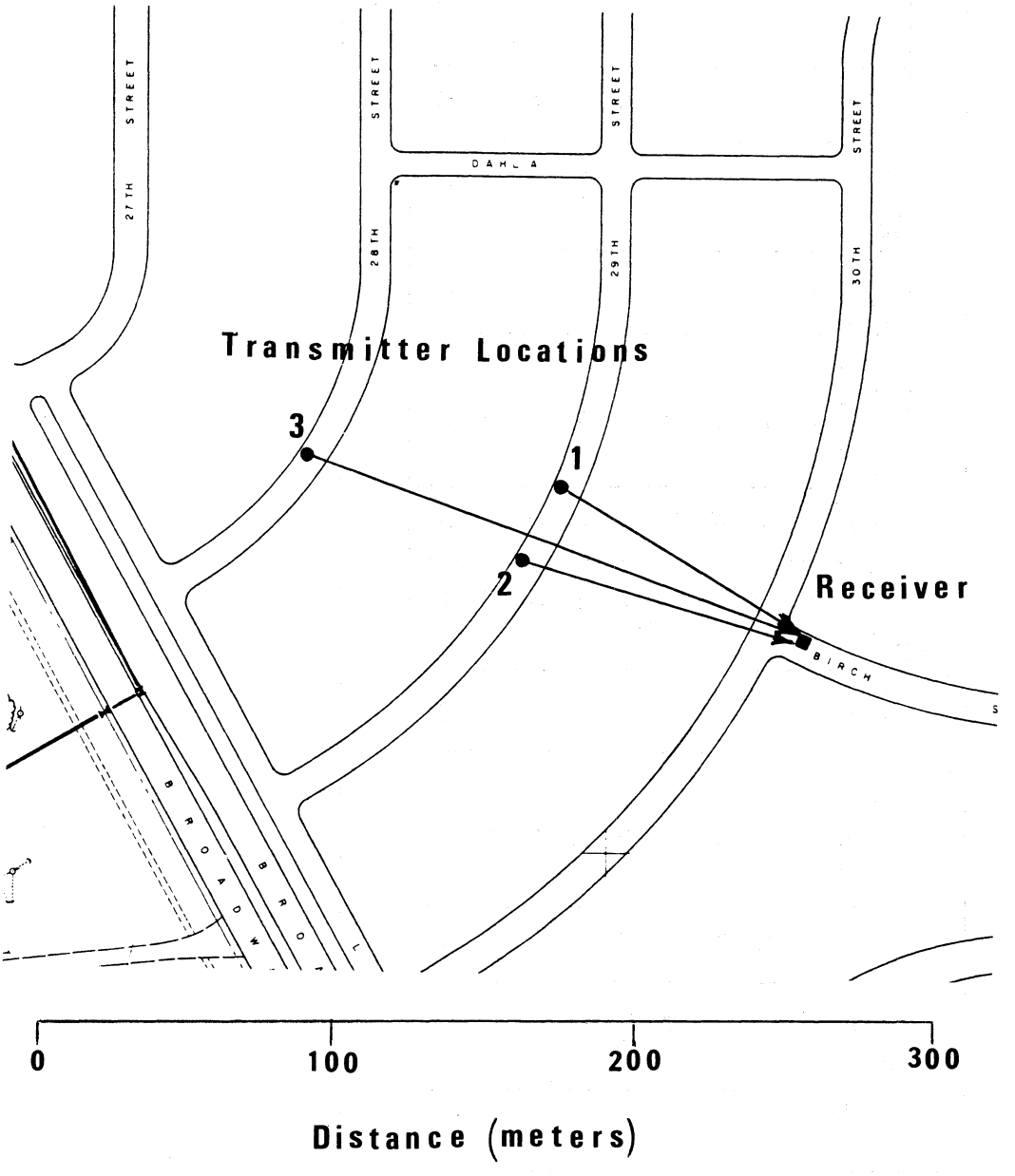

Figure 13. A street map of the dense residential area.

Table 2. Measured Data in the Dense Residential Area

Test #	Tx Location	Antenna Angle (degrees) TX AZ	TX EL	RX AZ	RX EL	Frequency (GHz) 9.6 dBm RSL if LOS	9.6 dBm Measured RSL	9.6 Loss dB	9.6 Above Noise dB	28.8 dBm RSL if LOS	28.8 dBm Measured RSL	28.8 Loss dB	28.8 Above Noise dB	57.6 dBm RSL if LOS	57.6 dBm Measured RSL	57.6 Loss dB	57.6 Above Noise dB
1	1	0	0	0	0	-29	-73	44	59	-26	-95	69	37	-44	-114	70	18
2	1	0	0	SC	2.5		-71	42	61		-92	66	40		-114	70	18
3	1	0	0	SC	5		-65	36	67		-78	52	54		-92	48	40
4	1	0	0	SC	7.5		-62	33	70		-75	49	57		-93	49	39
5	1	0	0	SC	10		-64	35	68		-80	54	52		-99	55	33
6	1	0	0	SC	15		-78	49	54		-98	72	34		-118	74	14
7	1	0	10	+7	+5		-62	33	70		-66	40	66		-81	37	51*
8	2	-7	+7	-3	+7		-73	44	59		-76	50	56		-97	53	35*
9	3	-8	+7	-5	+6	-35	-88	53	44	-32	-92	60	40	-51	-119	68	13*

*Maximized pointing.

An additional set of data was recorded with the transmitter at location #1. The results in the form of recorded signal levels for an 8 minute period are shown in Figure 14. The antenna pointing was the same as observation #3 in Table 2. The received signal level for each channel is indicated on the abscissa (dBm) and 1-min time marks are shown on the ordinate. The interesting feature of these data is the effect of the wind. The first half of the figure shows a data segment approximately 4.5 min in duration. At the onset, a light breeze was blowing at the site. A little over a minute into the record, the wind intensity increased sharply, and both a change in the average level and variation in level occurred on all channels. These changes result from changes in the path-related orientation of the leaves and branches and movement of the leaves in the path. These measurements support the premise that one of the propagation mechanisms is scattering from the leaves in the path. Data features similar to these were observed in earlier measurements of propagation loss through trees (Violette et al., 1981). The changes in average level are estimated at 2-4 dB in this sample, and the variations (scintillations) range from 15 to 20 dB. The second half of the figure shows a continuation of the time series with the wind still blowing and two short (approximately one-half minute) periods during which the transmitters at all frequencies were shut off. During the off periods, the system noise levels are recorded. From these records, the received signal levels (above the system noise levels) are easily determined as the difference between the on and off periods. For this path, the respective margins for 9.6, 28.8, and 57.6 GHz were 67, 54, and 40 dB.

The second residential area was chosen for its low housing density. However, the area was covered with many trees. A map of the test area is shown in Figure 15, and the resulting data are shown in the table at the bottom. The pictures in Figure 16 show the receiver and transmitter locations for these tests. The top two pictures show the receiver site. The left-hand picture shows the 950 m LOS calibration path, and the picture of the transmitter terminal #1 shows the same path as seen from the transmitter. The arrow in this picture locates the receiver terminal. The receiver terminal picture on the right-hand side shows the foreground of path Nos. 2, 3, and 4 as viewed from the receiver. The remaining pictures show, respectively, the foreground of path Nos. 2, 3, and 4 as seen from the transmitter.

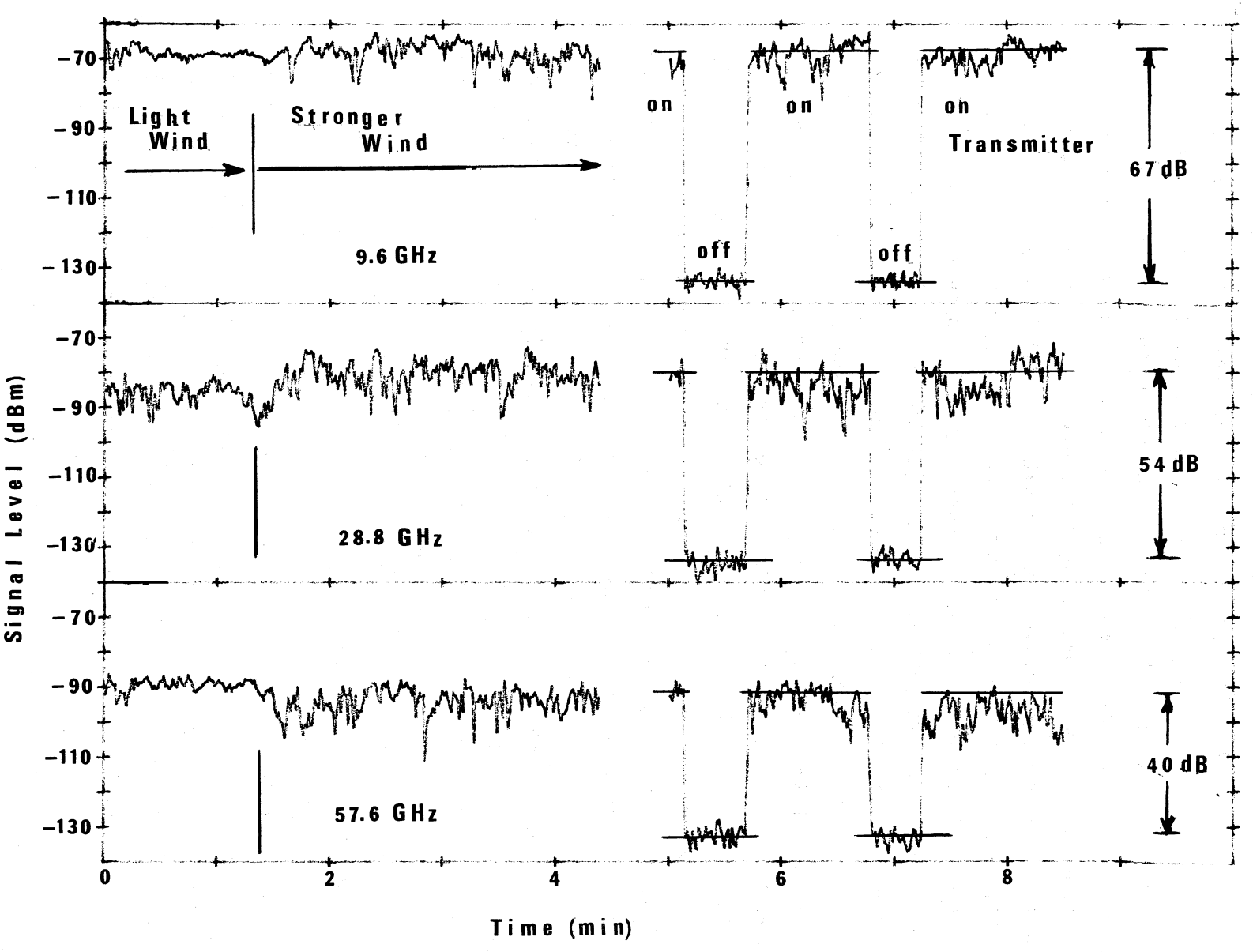

Figure 14. Received signals in the dense residential area. Transmitter antennas were AZ = 0°, EL = 0°. Receiving antennas were AZ = 0°, EL = 5°.

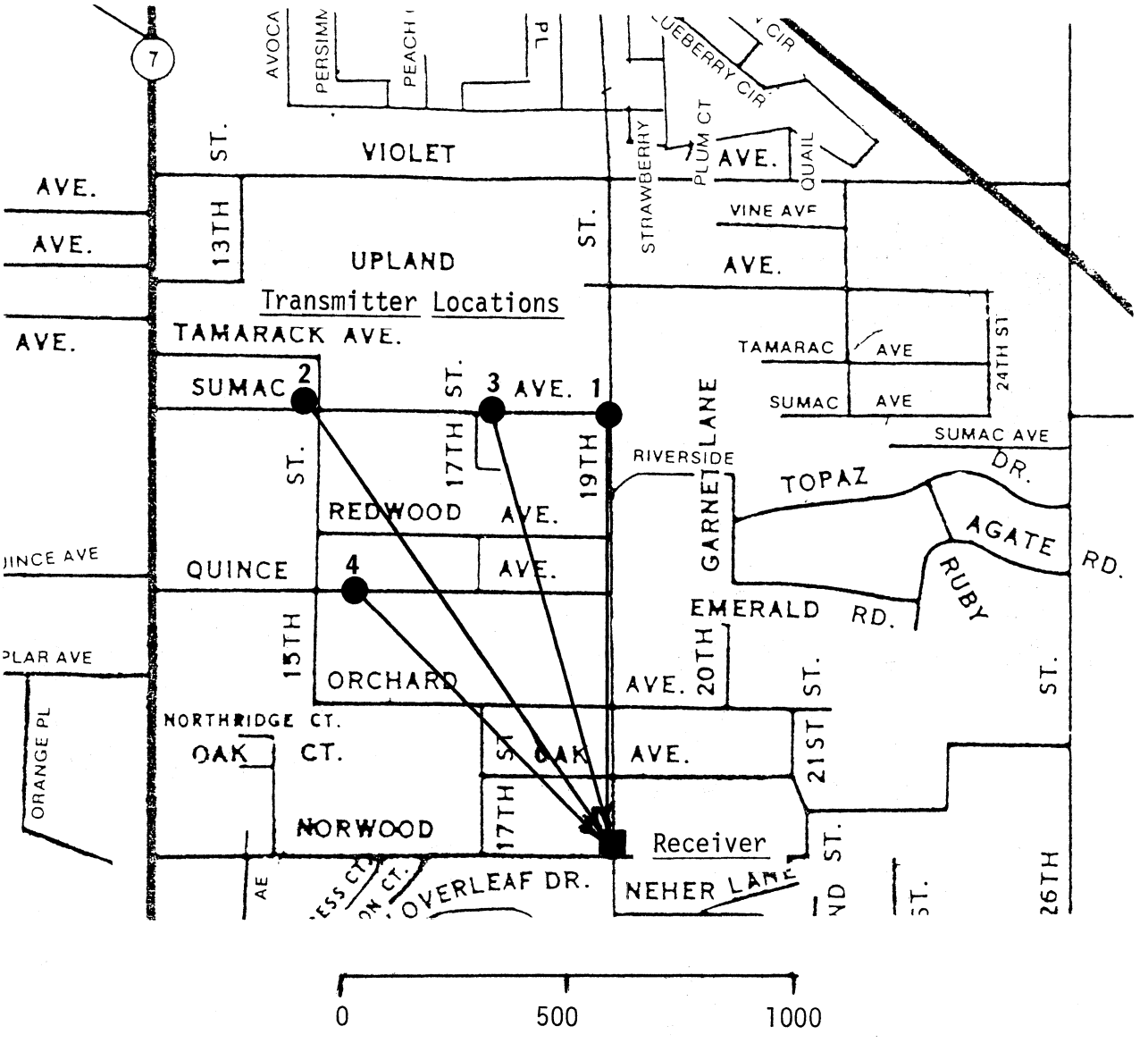

File	Distance	Location	9.6	28.8	57.6
1	950 m	Sumac - 19th	- 48 (84)	- 37 (95)	- 67 (65)
2	1200 m	Sumac - 15th	-132 (0)	-132 (0)	-132 (0)
3	1000 m	Sumac - 17th	-106 (26)	-114 (18)	-132 (0)
4	900 m	Quincy - 15th	-104 (28)	-112 (20)	-132 (0)

Figure 15. A street map and results from measurements in the less-densely populated urban area.

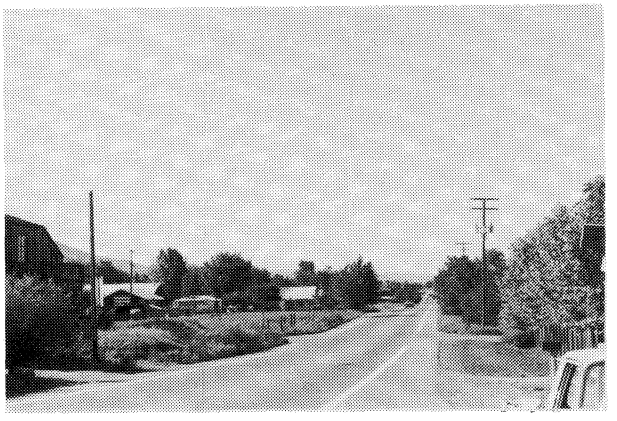

Receiver terminal looking toward transmitter position #1.

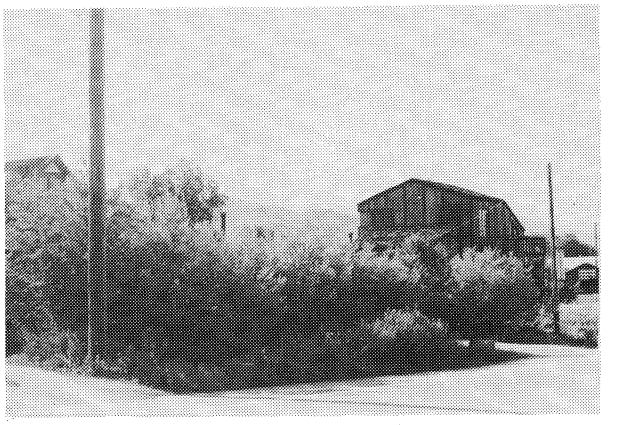

Receiver terminal looking toward transmitter positions #2, #3, and #4.

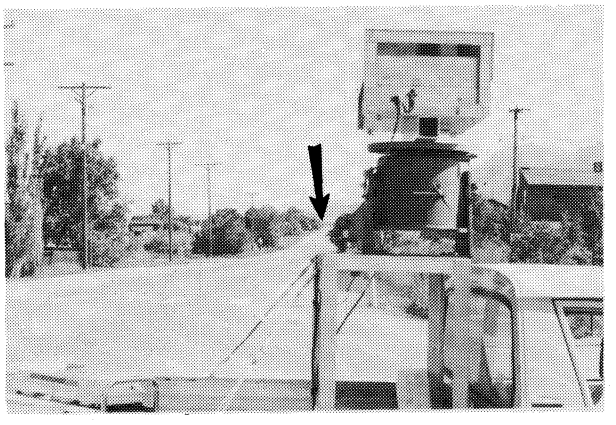

Transmitter location #1.

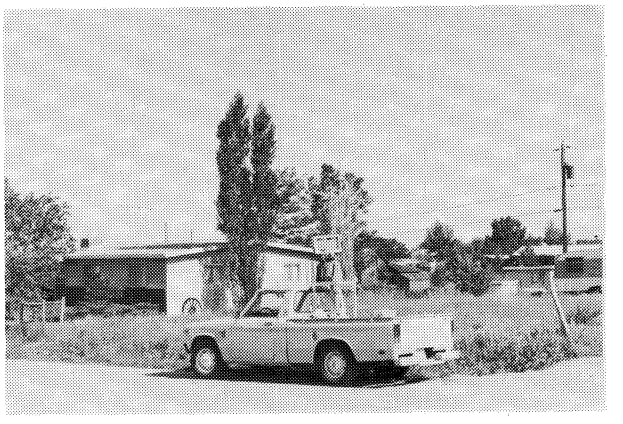

Transmitter location #2.

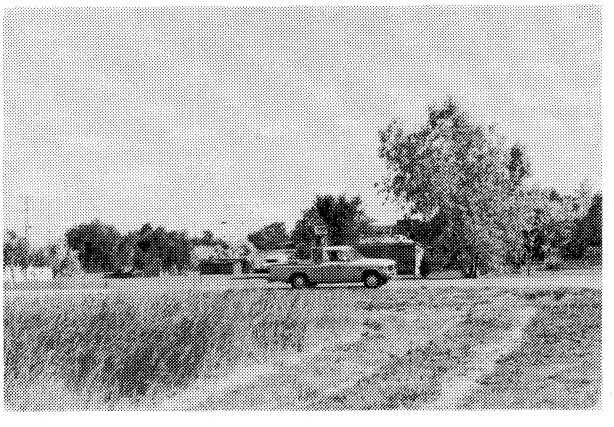

Transmitter location #3.

Transmitter location #4.

Figure 16. Pictures of residential path terminal locations for the less-densely populated urban area.

The data in the table in Figure 15 show the measured results from the four paths. Path No. 1, an LOS, 950 m path, produced very high signal levels on all channels, as expected. Path No. 2 is 1200 m and nonline-of-sight, obstructed by trees and houses and, in addition, the elevation of the terrain between terminals is higher than either terminal. The signals received on all channels for this path were equal to or less than the system noise level (-132 dBm). On path Nos. 3 and 4, levels above the system noise were received on the 9.6 and 28.8 GHz channels, but not on the 57.6 GHz channel. Levels of 26 and 28 dB above the noise threshold were recorded at 9.6 GHz and 18 and 20 dB at 28.8 GHz. These data show that, except for the line-of-sight calibration site, only marginal reception was achieved on these approximately 1-km paths.

The third set of measurements was in an area of intermediate housing density, and the receiving terminal was located on a hilltop site where the terrain was approximately 30 to 40 m above the terrain surrounding the transmitter locations. The map in Figure 17 shows the terminal locations for these tests, and the table gives the results. The pictures in Figure 18 show the path foreground of the receiver and three transmitter locations and the obstructions that extended 1 to 3 deg above the direct path. The results in the table of Figure 17 show much higher received signal levels for the three nonline-of-sight paths of length comparable to the previous data set. Two differences in this configuration, compared to the previous configuration that affect propagation are: (1) the receiving terminal is in a clearing, not subject to attenuation from dwellings and trees and (2) the path beyond the immediate foreground at each transmitter location is clear, such that signals diffracted by the buildings and trees in the foreground would propagate to the receiver with only the free-space loss.

3. CHANNEL CHARACTERISTICS FOR PATHS ALONG AN URBAN STREET USING IMPULSE RESPONSE MEASUREMENTS AT 30.3 GHZ

Line-of-sight links along an urban street encounter a common problem, deep signal fading, and possible channel distortion as the position of terminals are changed. The obvious reason for this fading is the presence of multipath signals reflecting from street and building surfaces that mix with the direct signal. The degree of distortion is a function of the excess time delay and amplitude of these multipath signals relative to the direct signal. Multipath signals are responsible for frequency selective fades, which

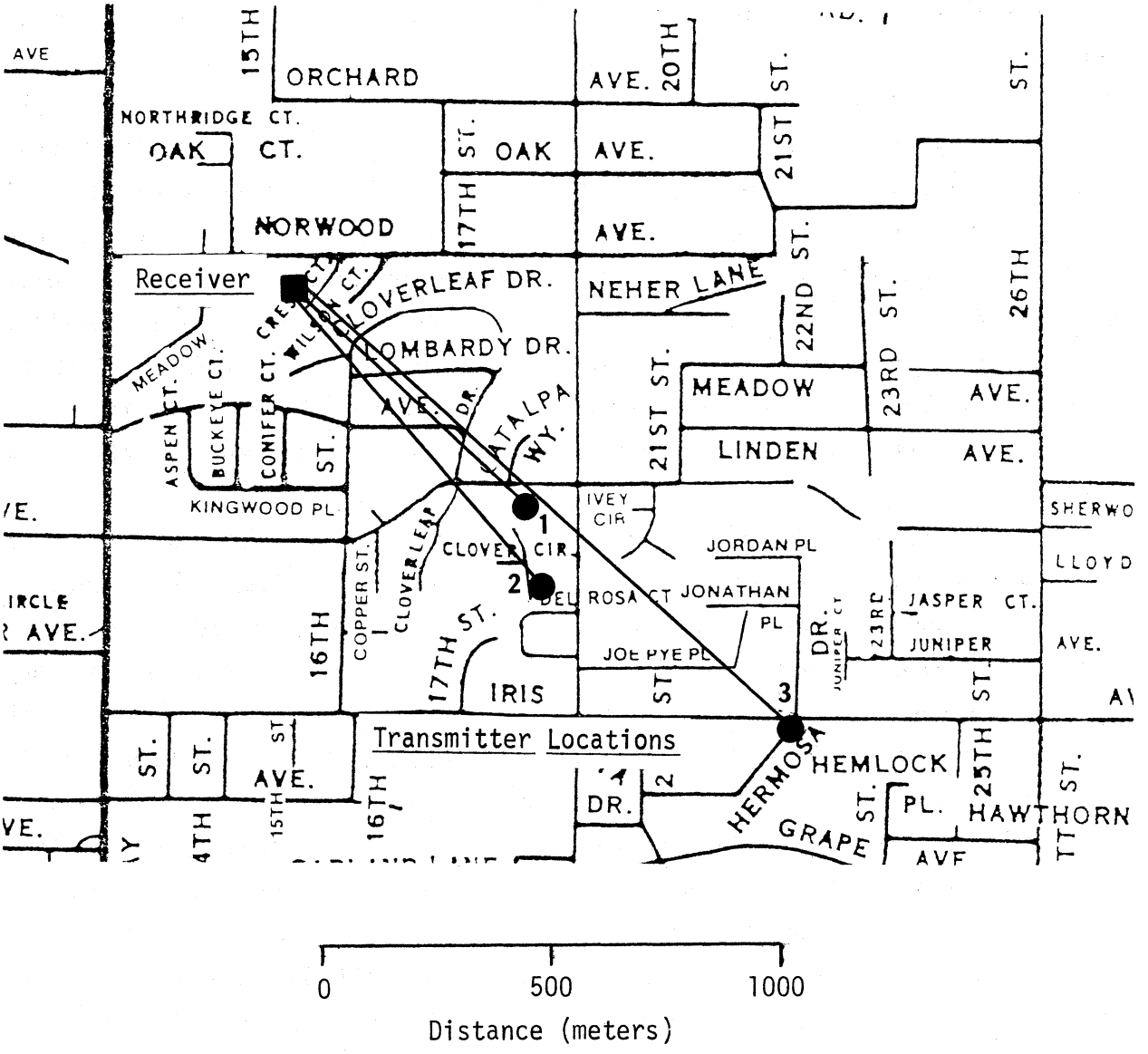

Distance	Location	9.6	28.8	57.6
0.65 km	#1	-90 (42)	-106 (26)	-113 (19)
0.80 km	#2	-51 (81)	- 68 (64)	- 81 (51)
1.45 km	#3	-84 (48)	- 82 (50)	- 97 (35)

Figure 17. A street map and results from measurements in a suburban area with the receiver terminal at an elevated position.

Receiver location.

Transmitter location #1.

Transmitter location #2.

Transmitter location #3.

Figure 18. Pictures of the terminal sites for the measurements in the suburban area with the receiver terminal at an elevated position.

means the received signal level changes pronouncedly as the propagated rf signal is varied in frequency. Therefore, if a wideband channel is used, fades will occur within the channel and produce amplitude distortion.

For certain types of modulation, the delayed signals interfere with the primary modulation of the direct signals. One common example is in digital modulation. In this case, a given time duration at one of two frequency or phase states (FSK or PSK) represents the bit characters, and if the multipath time delay is one-half or more of this duration, then intersymbol interference causes errors in the data (Violette et al., 1983b).

Attempts were made to measure the strengths of multipath signals in an urban environment to determine reflection coefficients of surfaces at the micro/millimeter wave bands (Violette et al., 1983a). Only single position measurements were accomplished, and the process was tedious and not precise as it involved using antenna scans to separate multipath signals. Instrumentation has been developed to record the impulse response of a channel. With this impulse instrumentation, individual multipath amplitude and time delays can be recorded within 50 ms, which permits a terminal to travel down a street while obtaining as much resolution as required to describe the channel in the street environment. A rigorous discussion of the impulse response technique is found in Hufford et al. (1982) and Linfield et al. (1976).

3.1 Description of Impulse Instrumentation and Related Diagnostic System

The micro/millimeter wave system was developed to operate as a diagnostic probe to investigate propagation at millimeter wavelength (Violette et al., 1983b). An important part of this system is the impulse probe. A 30.3 GHz carrier accommodates a subcarrier and baseband modulation in a fully coherent network. In addition to the 30.3 GHz wideband channel, two coherent cw channels (11.4 and 28.8 GHz) were recorded in order to obtain high resolution (20 samples/sec) fade data as well as an indication of frequency dependence. Bit error rate (BER) measurements at a 500 Mb/s rate are available to evaluate channel performance. Bit error rates were not recorded for this report, but will be included in the next series.

The impulse response of the channel is accomplished by phase modulating (phase shift keying) the 30.3 GHz carrier with a pseudorandom binary sequence at a rate of 500 Mb/s. The 30.3 GHz signal is transmitted through the channel (the atmosphere) to a receiver where the signal is demodulated to reproduce the 500 Mb/s pseudorandom sequence degraded by any distortion that may have

occurred in the propagation between transmitter and receiver. At the receiver terminal, a replica of the transmitted pseudorandom binary sequence is generated. A cross-correlation is performed between the received demodulated bit stream and the replica of the transmitted bit stream by allowing one bit stream to slide by the other in time as a result of a slight offset between the bit-clock rates. At the interval in time when the bit sequences are identically aligned, an impulse is generated at the correlation output with a base duration equivalent to two bit times. With no distortion in either the hardware or the channel, the impulse shape would appear as a triangle with a base duration of 4 ns for the 500 Mb/s rate and a height that is a function of the received signal level (RSL) because the received demodulated signal is compared before limiting occurs. Channel amplitude and phase dispersion during propagation of the signal appears as amplitude and time changes in the impulse shape. A choice of two pseudorandom word lengths is selectable, 2^7 and 2^{15}, but usually, due to the need for time resolution, the short word is used. With the short word, a 12-bit analog-to-digital converter (ADC) (2.5 mV resolution and a 10 V peak correlation voltage) provides a 36-dB dynamic range when the processing noise is less than the -36 dB level. Noise sources other than the signal-to-noise ratio created by the rf circuitry that can raise the impulse measurement minimum detection level are data clock leakage, data generator nonsymmetries, and the sum-of-the-squares circuitry employing high-gain dc amplifiers. Without limiting rf noise, the dynamic range of the impulse circuitry is about 40 dB; therefore, the 36 dB range available with the 2.5 mV resolution of the ADC is both reasonable and adequate for the contemplated applications. The purpose of the sum-of-the-squares circuitry is to combine the in-phase and quadrature-phase baseband signals so that impulse waveforms are independent of delay time or phase changes on the rf path (Violette et al., 1983b).

A dedicated, multitasking, real-time microprogrammable computer system with a 1 megabyte memory, a 20-megabyte hard disk, and a 65 megabyte tape permits flexibility in hardware control, data processing, and data storage. One of the major advantages in changing to this new computer system is that the measuring system control and all data handling can occur at a sufficient rate to resolve the channel characteristics even for a worst case where a terminal is in motion in an urban environment. For example, an impulse response can be processed and stored at 2-s intervals, and if all signal

channels are sampled at a 20-per-second rate, impulse responses can be taken at 5-s intervals. At present, two 8-channel ADC cards are used, with each channel sampled at up to a 55-kHz rate.

3.2 Impulse Measurement Calibration

In order to be assured that the impulse measurements accurately depict the response of the channel, a controlled test with known parameters was required. To accomplish this, physically measurable multipath signals for a realistic range of amplitudes and delay times were generated. Using waveguide lengths to create delayed paths is mechanically difficult, and since 70 dB or more of isolation was necessary, both flange leakage and attenuator inaccuracies were found to present problems. A more manageable scheme used the 1.5 GHz subcarrier to create controlled multipath to provide a test of the data generation and correlation processing.

Figure 19 shows the test setup for the impulse circuitry calibration. All components, except the network between the dc to 18 GHz divider and combiner, are part of the channel probe system. Even at 1.5 GHz, ± 500 MHz (the modulation bandwidth), adjustable-length UHF coaxial air lines produced perturbations that generated standing waves and dispersive components, which reduced power levels by 6 or 7 dB from the straight-through signal level. The best method found to perform calibration measurements was to construct a set of coaxial cables cut in 1/4 ns steps, to produce the actual propagation delays. The reason for such fine steps is that the summed output of the co- and quad-phase squaring circuits ($E_i^2 + E_j^2$, Figure 19) must be carefully balanced to produce an impulse curve that remains constant for all possible phase delays of the received carrier. Measuring a "direct" signal in the presence of delayed signals is the most critical test, because the phase of the 1.5 GHz reconstructed carrier is determined by the combined vector phase of all signals to be measured.

Several adjustments are required to obtain the best compromise in maintaining a proper power level ratio between the "direct" and delayed signals with phase shifts in the modulated carriers. Note that the combined sum-of-the-squared signals ($E_i^2 + E_j^2$) is recorded in the impulse measurement and represents signal <u>power</u>. The phase of the reconstructed carrier injected into the co- and quad-phase demodulators must be finely adjusted to produce nulls in the quad-phase channel when the input carrier has a phase difference of 0° or 180° and nulls in the co-phase channel for phase differences of ±90°. To

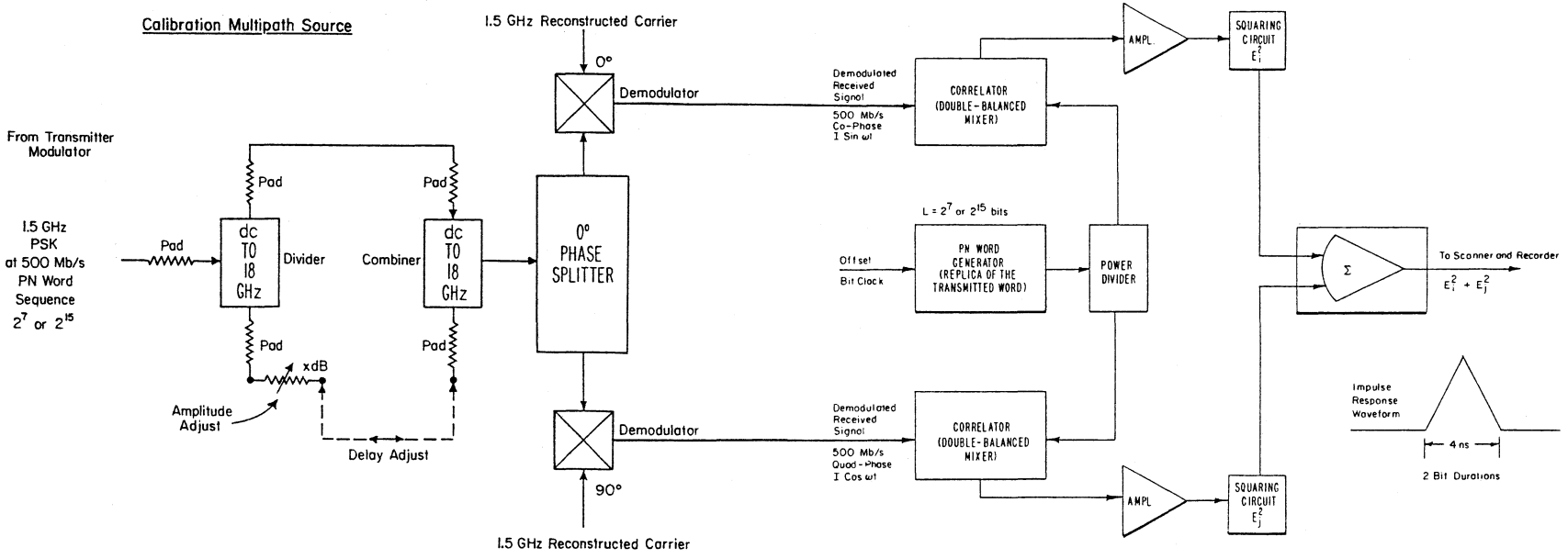

Figure 19. Test setup for the impulse circuitry calibration.

maintain these relationships, line lengths were adjusted to compensate for differences in time delays between the co- and quad-phase branches containing the demodulator, correlator, amplifier, and squaring circuits. By performing these adjustments carefully for all combinations of rf phase, agreement in power levels measured via the impulse response compared to within ±1 dB of the values of attenuators for two signals delayed by more than 2 ns and for amplitude differences of less than 18 dB. Because of a nonlinear interaction of stages to the 1.5 GHz subcarrier in the divider and/or combiner depicted in Figure 19, interference patterns sometimes occurred for impulse times that overlapped. To test the overlapping case, a folded path or radar-type measurement was required using a fixed and a movable corner reflector (Violette et al., 1983b). Since this radar-type measurement was performed with an rf carrier at 30.3 GHz (wavelength = 1 cm), an adjustable head for a milling machine was used for positioning to within one-eighth of a wavelength (λ). With signal delay time differences between 1 and 2 ns, the amplitude variations were observed not to exceed ±1.5 dB. For delay time differences of less than 1 ns, it was difficult to determine the precise point of signal separation. It had been hoped that relative amplitude measurements could also be performed to calibrate the probe in the more realistic radar-type mode. The intent was to use a fixed and a movable reflector and adjust the amplitude of the movable reflector by placing it toward the edge of the antenna beamwidth (0.74°), but the high background clutter made relative amplitude measurements impossible in the surroundings and for the geometry readily available. After the link is instrumented for portability, a better site can be selected to perform this calibration.

An example of impulse measurements for each type of controlled multipath test is shown in Figure 20. In this figure, the upper impulse curve resulted from the test setup of Figure 19 with only a single branch (no multipath). The lower curve was recorded by the full rf probe at 30.3 GHz operated in a radar or folded path mode of about 320 m in length using a 27 dBsm corner reflector of side (a) = 32 cm, where dBsm = 10 log $4 \pi a^4/3\lambda^2$. In the upper curve, a 1.5 GHz (0.67 ns) interference pattern is seen, which interacts with the controlled multipath and "direct" signals when they overlap in time. Also, on the trailing edge, the effects of the coaxial fittings (SMA type), which connect pads, divider, and combiner together, are apparent when compared to the response of the lower curve where the link is coupled through antennas

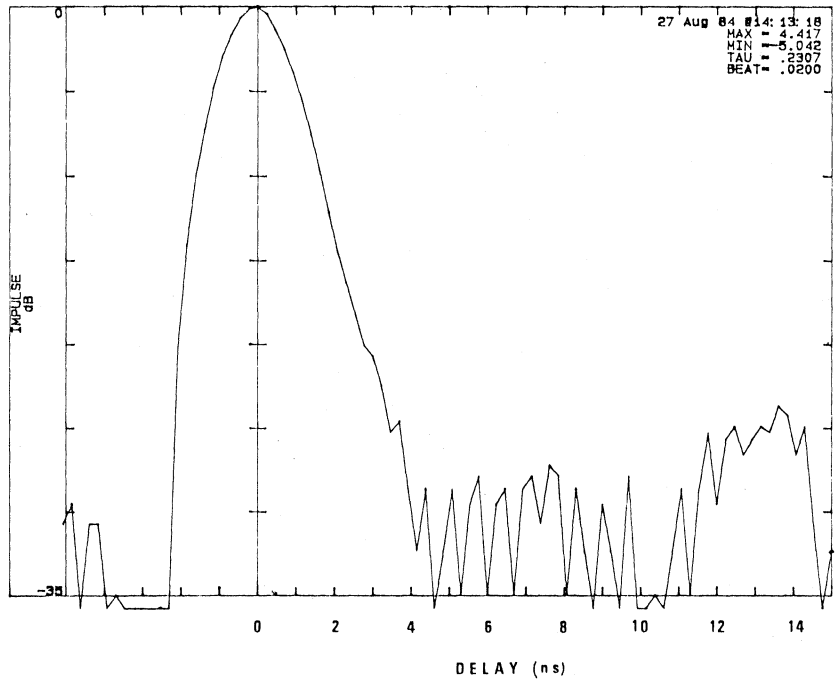

From the delay line calibration test setup at subcarrier (1.5 GHz).

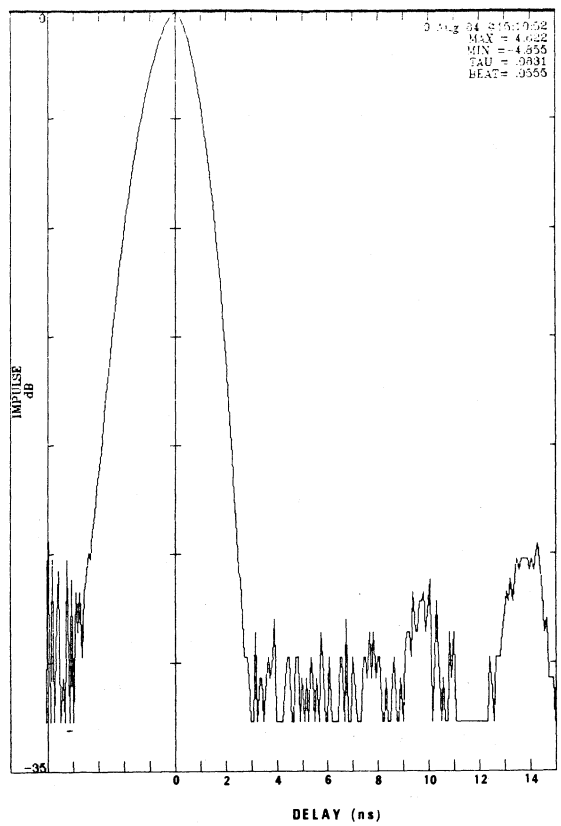

From the radar mode using 27 dBsm reflector at 30.3 GHz.

Figure 20. Examples of impulse calibration measurements.

and wide bandwidth rf converter stage. In the lower curve, a typical rf channel with no multipath is shown except that since the reflector was placed at a rooftop, some leading edge reflections from the building surface were in evidence. Note also for the lower curve, the baseline level has a random or noise-like appearance in contrast to the 0.67 ns period beating. Figures 21 and 22 show two sets of multipath signal amplitudes with electrically delayed paths of approximately 3 and 4.5 ns, using coaxial cables. The impulse curve marked reference is for a no multipath condition. Unfortunately, reflections are seen from coax connectors at a relatively high power level beginning at -15 dB. When a connector is loosened, the corresponding power level increases at that particular delay time, which identifies the source of the perturbation. These connector reflections interact with signals of similar delays and show as fluctuations in the trailing edges of the impulse curve. The break (knee) of the impulse curve of Figure 21 occurs very near the indicated decibel level inserted in the delayed branch. The time delay indicated by the knee varies slightly from that indicated on the curve at 3 ns, but this is due to limitations in measuring electrical delay accurately. In calculating delay lines, it was not possible to determine electrical delays of attenuators other than their physical length. Some variation is seen in the position of the leading edge which is derived by the computer in mathematically centering on the peak level of the signal. Also, some reshaping occurred about the peak area depending on the relative amplitude and phase of the multipath signals. As seen, these variations can cause up to 1/3 ns variation in determining the center of the impulse curve. A similar situation exists in Figure 22 where the amplitudes are quite close to the inserted attenuations, but some variation in delay times at 4.5 ns of the extended branch is seen due to the makeup of the pads.

As the multipath delay is reduced, the knee of the curve begins to disappear as seen in Figure 23 (1.5 ns) and Figure 24 (0.9 ns). It is apparent that the multipath is present and creating channel distortion, except for the condition of the -10 dB multipath at 0.9 ns delay in Figure 24. In this case, the delayed signal combined within the period of the impulse envelope of the "direct" signal in such a manner that the 1.5 GHz interference beat affected the trailing edge of the -10 dB impulse response. Obtaining values for amplitudes at delay times less than 2 ns was not reliable because of the 1.5 GHz interference inherent in the test procedure. However, the majority of the

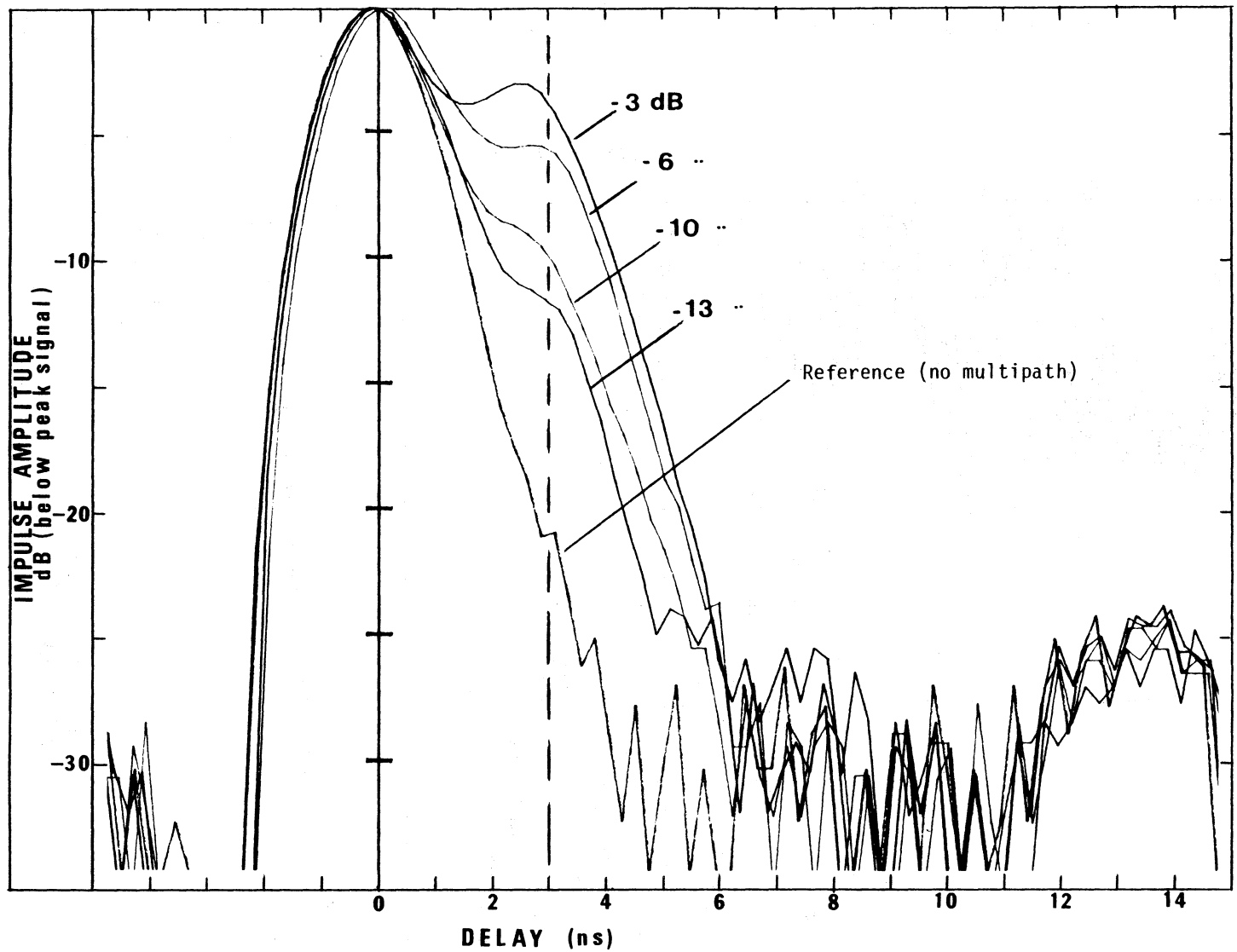

Figure 21. A set of multipath delay amplitudes with an electrically delayed path of 3 ns.

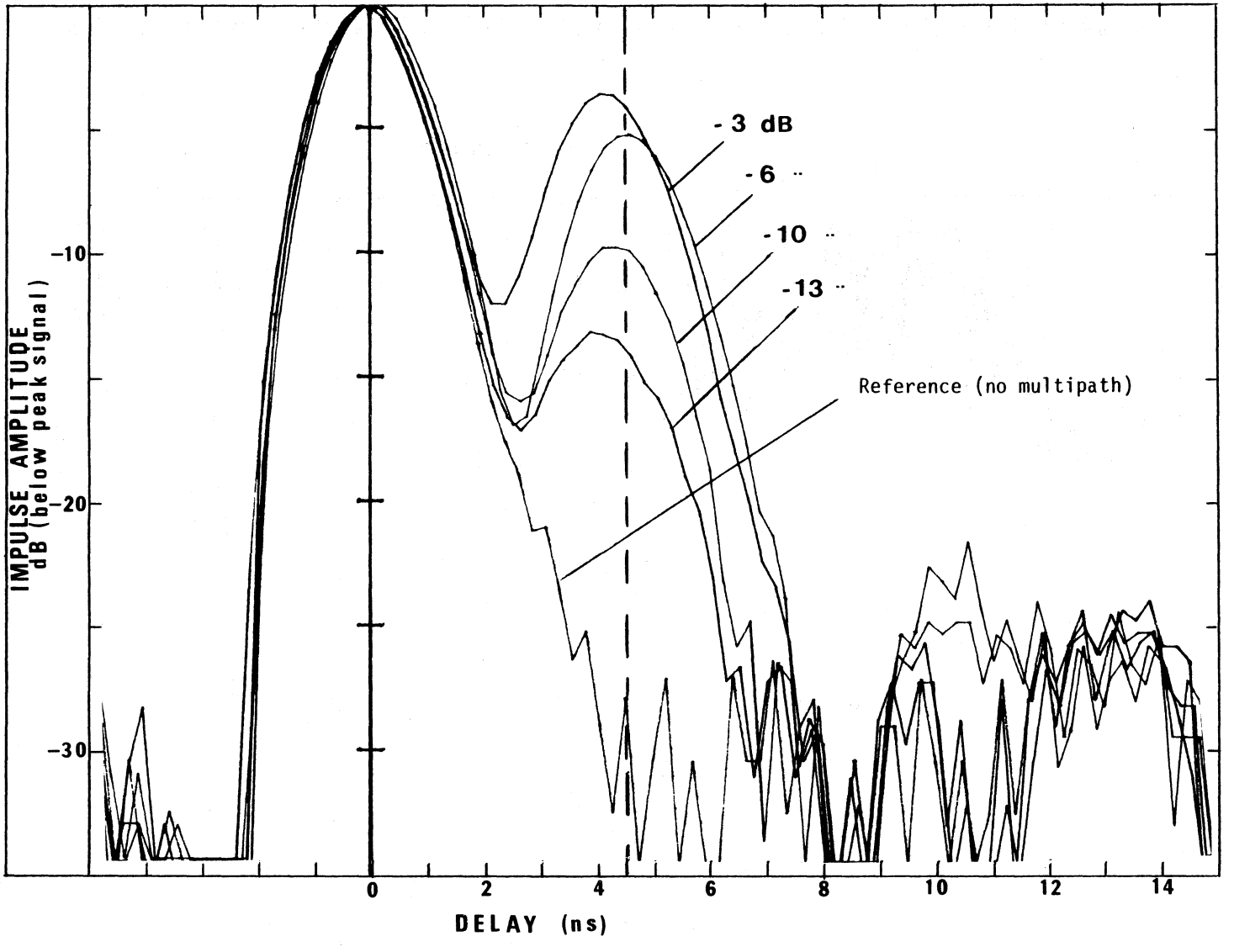

Figure 22. A set of multipath delay amplitudes with an electrically delayed path of 4.5 ns.

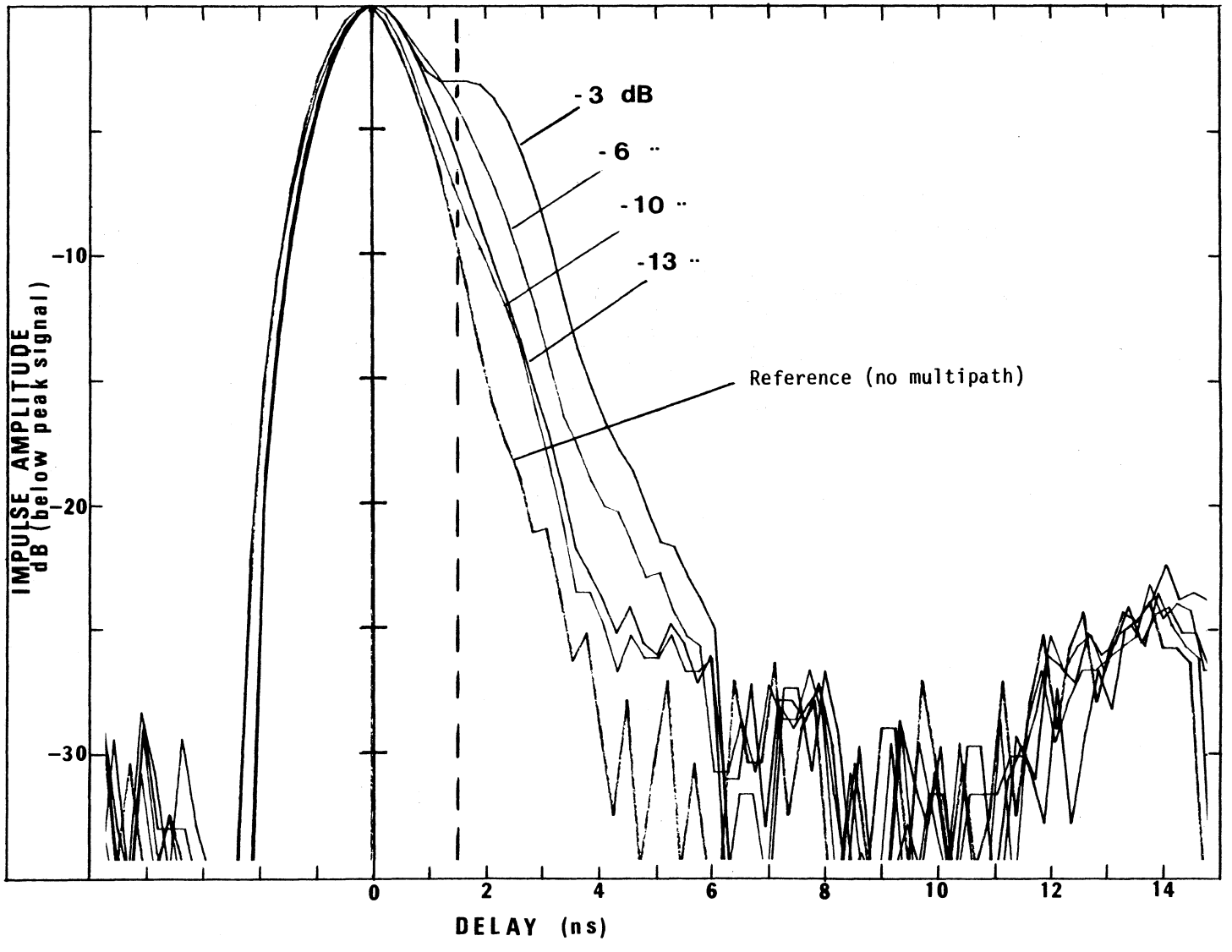

Figure 23. A set of multipath delay amplitudes with an electrically delayed path of 1.5 ns.

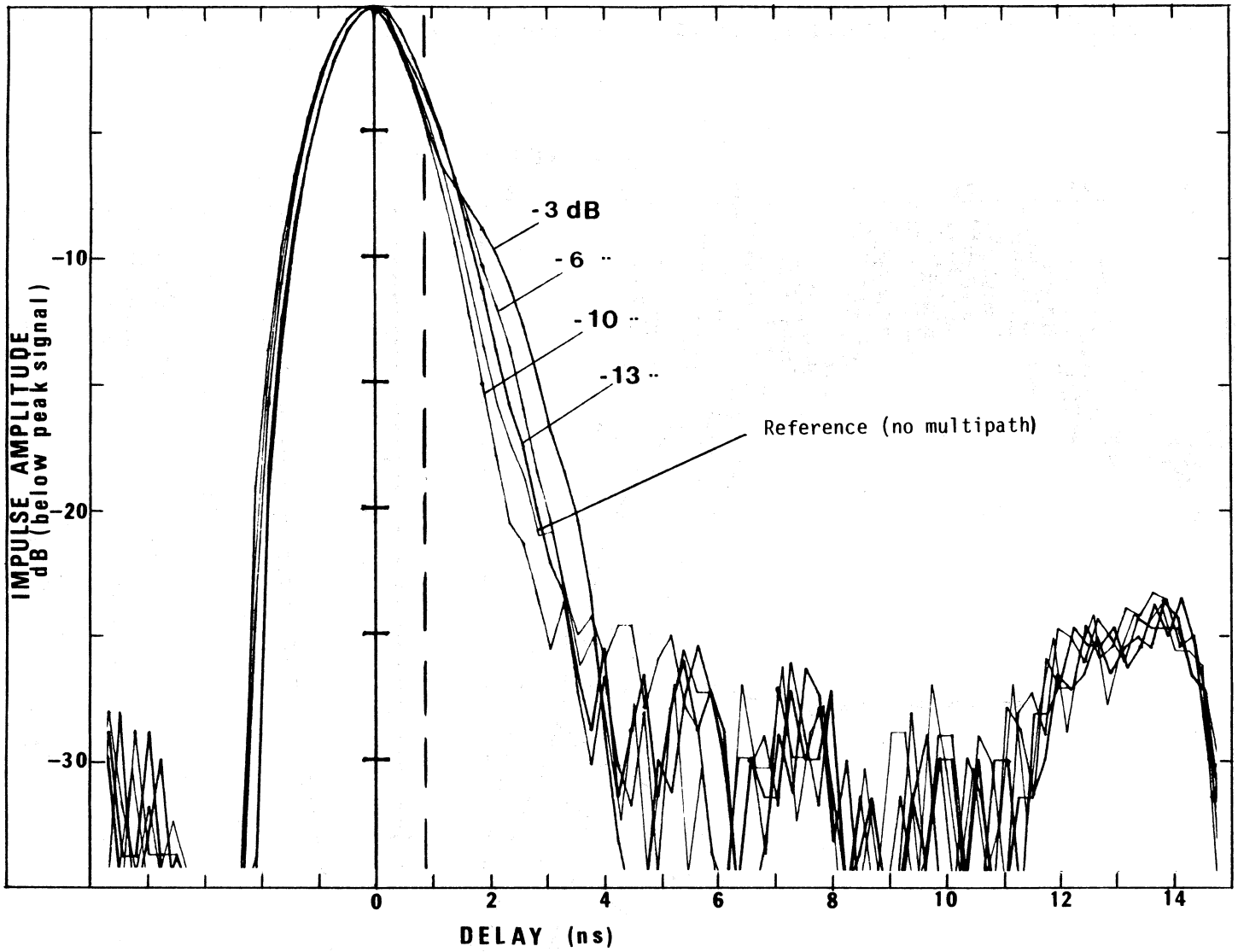

Figure 24. A set of multipath delay amplitudes with an electrically delayed path of 0.9 ns.

measurements under 2 ns delay displayed the proper impulse response. At a future time, on a radar-type range, selected responses at delay times less than 1 ns can be stored in computer memory and used to fit data taken on unknown paths to derive discrete multipath amplitude and delay values using a best fit method. If several multipath rays occur within 1 or 2 ns of the direct ray, it would be unlikely the components could be identified, but the resulting distortion can still be measured.

Another example is Figure 25, where the delayed branch was varied in four steps between 0.9 to 1.5 ns at a level approximately 3 dB below the reference level. Note the envelope for the 1.2 ns delay curve falls more rapidly than the reference envelope and rises again across the reference curve. The period of these interference intervals is one-half the 1.5 GHz carrier period. This 1.5 GHz interference beat is seen as noise or clutter as the impulse envelope decays toward the -35 dB baseline. The amplitude of the interference beat is a function of the subcarrier that leaks through the test network and eventually modulates the bit stream that is compared in the correlator. Since the interference does not appear when the rf system is used, it is not of concern in the application of the impulse probe. All of the other delay times in Figure 25 were logically represented by the impulse response curves.

In Figure 26, a -10 dB multipath level was used with delay times of nominally 2.5, 3, 7, and 8 ns. The 2.5 ns delay curve shows about a 1/2 nanosecond discrepancy which again seems to be a small 1.5 GHz interference beat. For the 7 ns curve, a power split occurred, no doubt due to a faulty connector at the combiner port. The multipath branch shows a -13 dB peak power at 7 ns and an apparent -20 dB reflected peak power at approximately 9 ns as indicated on the figure.

Figure 27 displays a 6.8 ns time delay branch with impulse recordings for attenuator values of 3, 6, 10, and 13 dB. The delay for this measurement was produced by a 55-in length of RG 58 coaxial cable which has a loss of 0.3 dB/ft at 1.5 GHz. Each delayed path peak power level recorded an attenuation of between 1 and 1.2 dB greater than the indicated value of the attenuator. In other long delay measurements, the delay cables were of RG 174 which has an extrapolated loss of about 0.06 dB/ft at 1.5 GHz.

While many difficulties were encountered in the above calibration process, it is believed that the compensation and balancing adjustment were performed so that the accuracy in measuring discrete multipath time delay and

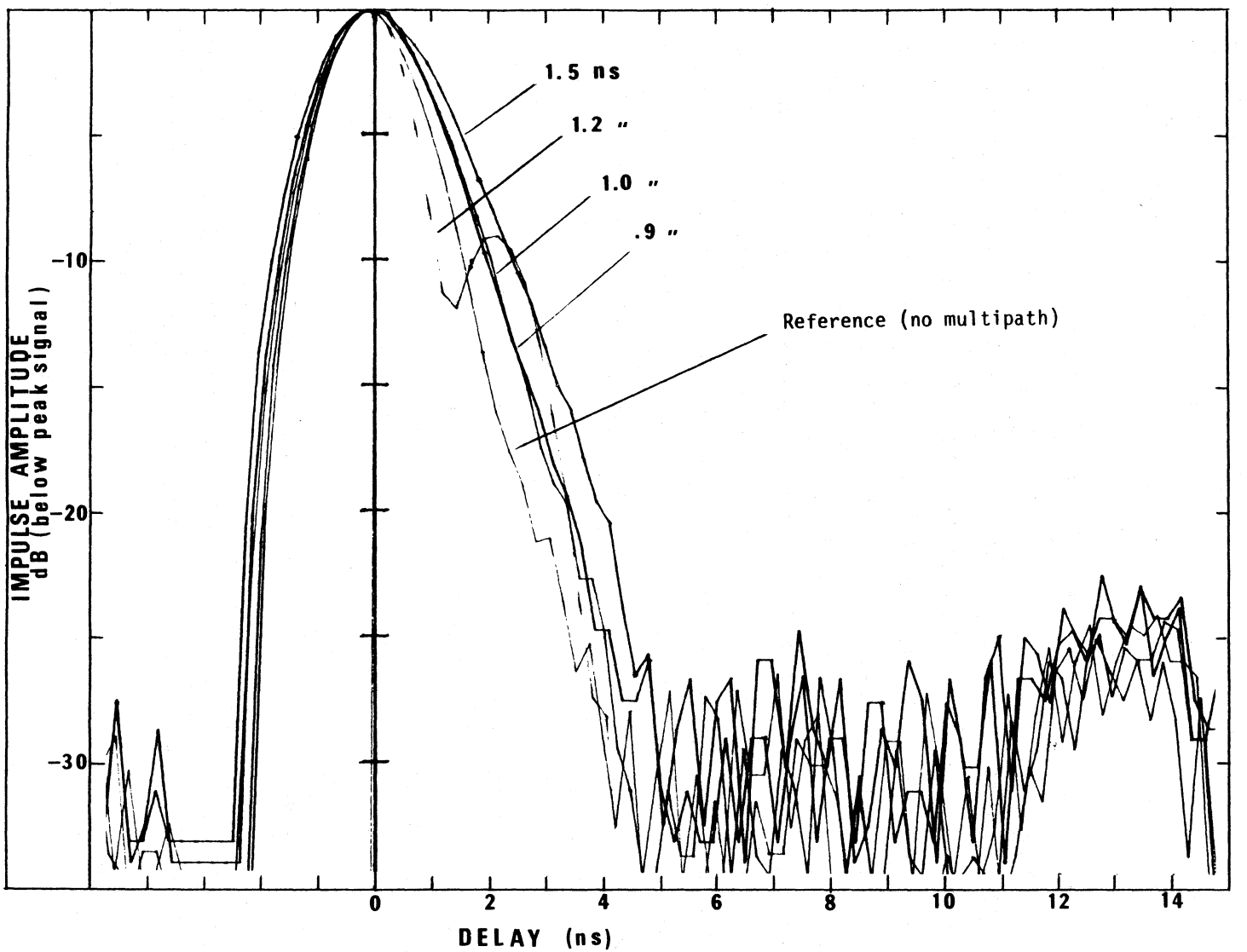

Figure 25. A set of impulses with delayed components between 0.9 and 1.5 ns. The delayed component amplitude is -3 dB.

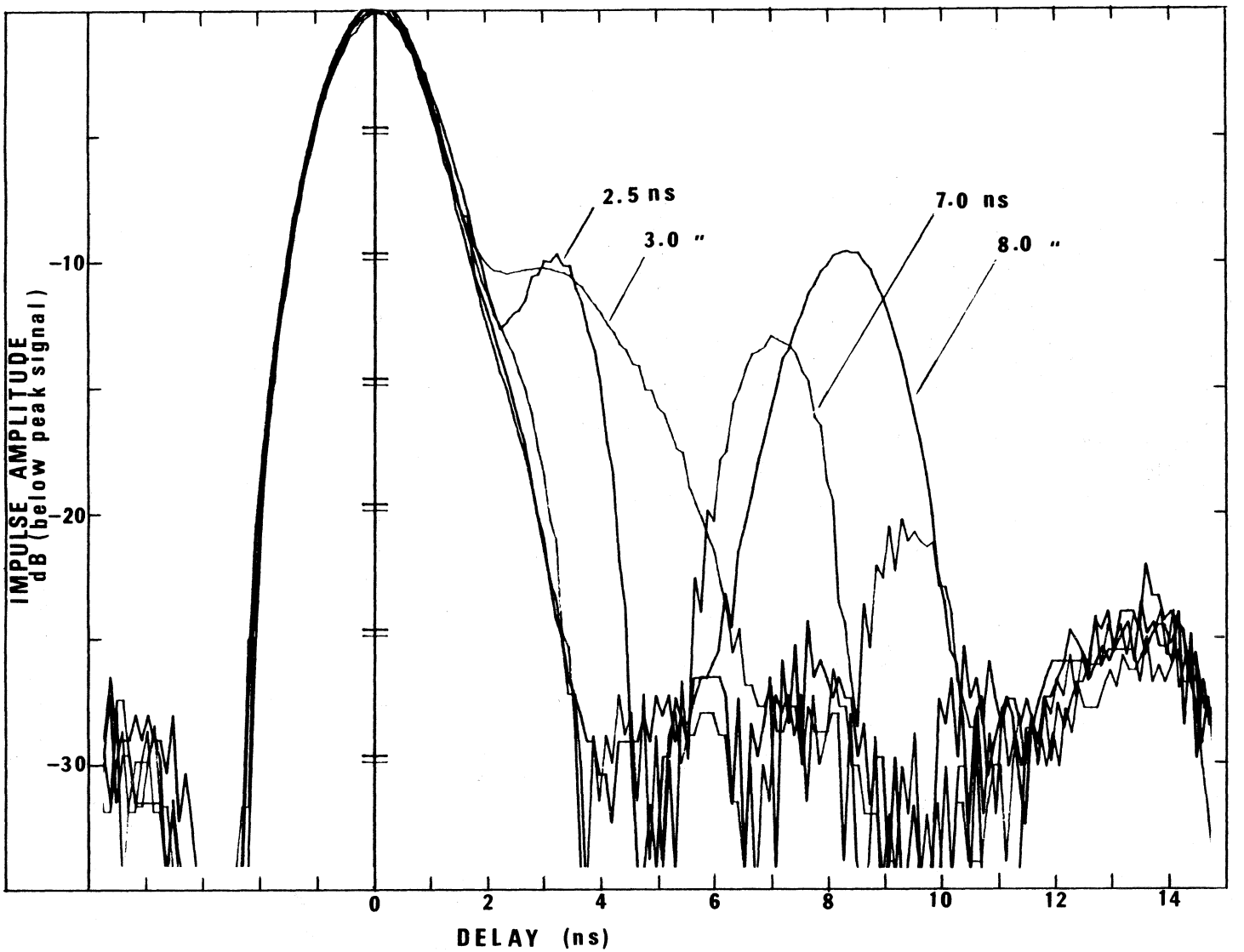

Figure 26. A set of impulses with delayed components between 2.5 and 8.0 ns. The delayed component amplitude is -10 dB.

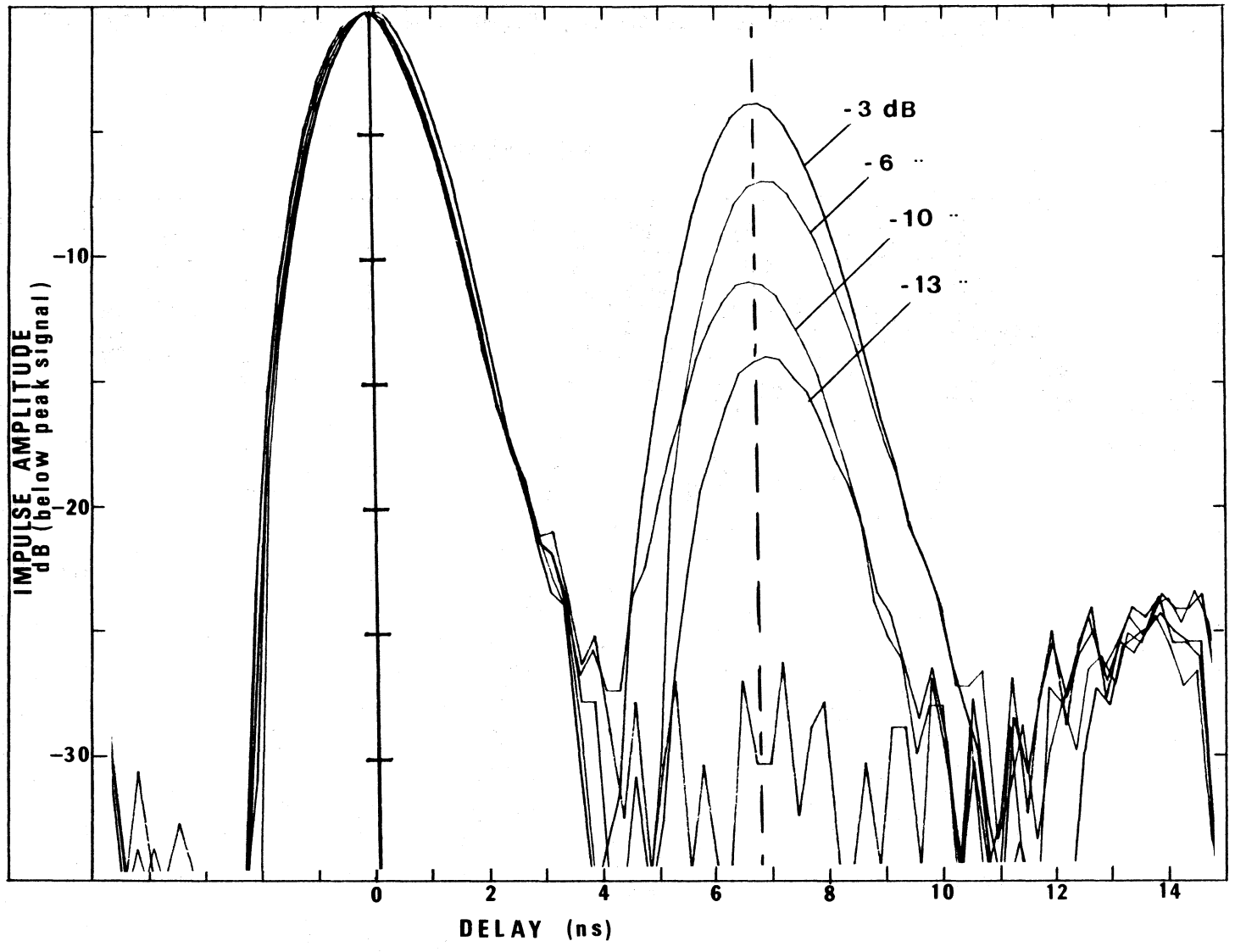

Figure 27. A set of multipath delay amplitudes with an electrically delayed path of 6.8 ns.

relative power is well within 1 ns and 2 dB, respectively, where signal components show a separation within the impulse response curve. A full system calibration may be conducted when the instrumentation is mobile.

3.3 Urban Street Measurements

The primary objective of this effort is to become sufficiently familiar with the impulse probe to determine if propagation characteristics can be measured at millimeter-wave frequencies for paths in a complex environment such as an urban street. Measurements of signal fading resulting from multipath signals of unknown strength, delay time, and numbers were reported in April 1983 (Violette et al., 1983a), and with considerable effort an attempt was made to identify the main reflecting surfaces producing the fading for a single position of the terminals along the path.

Instrumentaion has since been developed so that a channel probe can be mounted on vehicles and moved along a street to record impulse responses at 3 to 5 s intervals. These time intervals are short enough for vehicle speeds of 5 to 15 mph to record the complete signal dynamics of the path along the street. In other words, the use of the impulse probe hopefully will sufficiently describe signals resulting from reflections off street surfaces, buildings, cars, etc. in terms of their amplitudes and delay times, so that channel performance can be evaluated for any terminal location along a path. The performance of a channel is not only determined by signal fades that affect the signal-to-noise ratios but also by distortion caused by multipath signals that act as an interfering signal to the signal propagated along the direct path. The severity of this distortion is a function of multipath amplitude and the amount of delay in arrival after the direct signal. These parameters are directly related to the usable bandwidth of a channel.

Data taken in this first series of measurements using the new probe van are intended to provide an initial comparison of fading characteristics as a function of several system parameters and, in particular, provide detailed propagation characteristics (amplitude and phase dispersion) in the urban environment by use of the impulse measurements. Frequency dependence is shown between a "microwave" (11.4 GHz) and a "millimeter-wave" (28.8 GHz) channel. Antenna polarization dependence was examined for each linearly polarized component. Signal amplitude fading characteristics for a narrow bandwidth channel (5 kHz) are compared to a wide bandwidth channel (700 MHz for signal level branch, 1000 MHz for impulse branch). Also, channel characteristics

were recorded using narrow beamwidth antennas (2.5°) for comparison to characteristics recorded using wide beamwidth antennas (30°). Detailed impulse response measurements accompanied the antenna polarization and beamwidth comparisons.

The antenna used at the 11.4 GHz transmitter terminal was a 28° beamwidth (±3 dB) standard gain horn. A 30° beamwidth conical horn was shared by the 28.8 GHz and 30.3 GHz (wideband) channels by means of an orthomode transducer that coupled the two orthogonal linearly polarized signals simultaneously. At the receiving terminal, the 11.4 GHz channel used a 10° rectangular horn. Through another orthomode transducer, the 28.8 and 30.3 GHz receivers shared a 12-in scalar horn lens antenna which has approximately a 2.5° beamwidth. For the widebeam antenna measurements, the 28.8 and 30.3 GHz channels shared a 30° scaler feed horn. Both scalar horn antennas have sidelobe peaks that are at least 26 dB below the mainbeam. To change polarization on 28.8 and 30.3 GHz, a manual waveguide transfer switch was provided.

3.3.1 Measurement Scenario

This series of measurements was conducted along 17th Street in downtown Denver, Colorado. Measured data included the relative amplitude of the received signal as a function of transmitter-receiver separation in addition to the impulse responses sampled at about 3-m intervals along the path. The test path is the same as used for earlier millimeter-wave propagation studies reported by Violette et al. (1983a).

The drawing in Figure 28 shows street intersections along 17th Street. Also on the drawing is a height profile of the street relative to the transmitter location at the start of each run (usually the Larimer Street intersection). Two receiver locations are indicated near the intersections of Tremont and 17th and Glenarm and 17th.

Thirteen runs were made using the narrowbeam (2.5°) antennas for the 28.8 and 30.3 GHz links and 10° antennas on the 11.4 GHz link. Two runs were made using widebeam (30°) antennas for the 28.8 and 30.3 GHz links. The antennas for the 11.4 GHz link remained the same.

Two consecutive passes with the transmitter were made along 17th Street with the antenna polarization switched between the 28.8 and 30.3 GHz channels after the first pass.

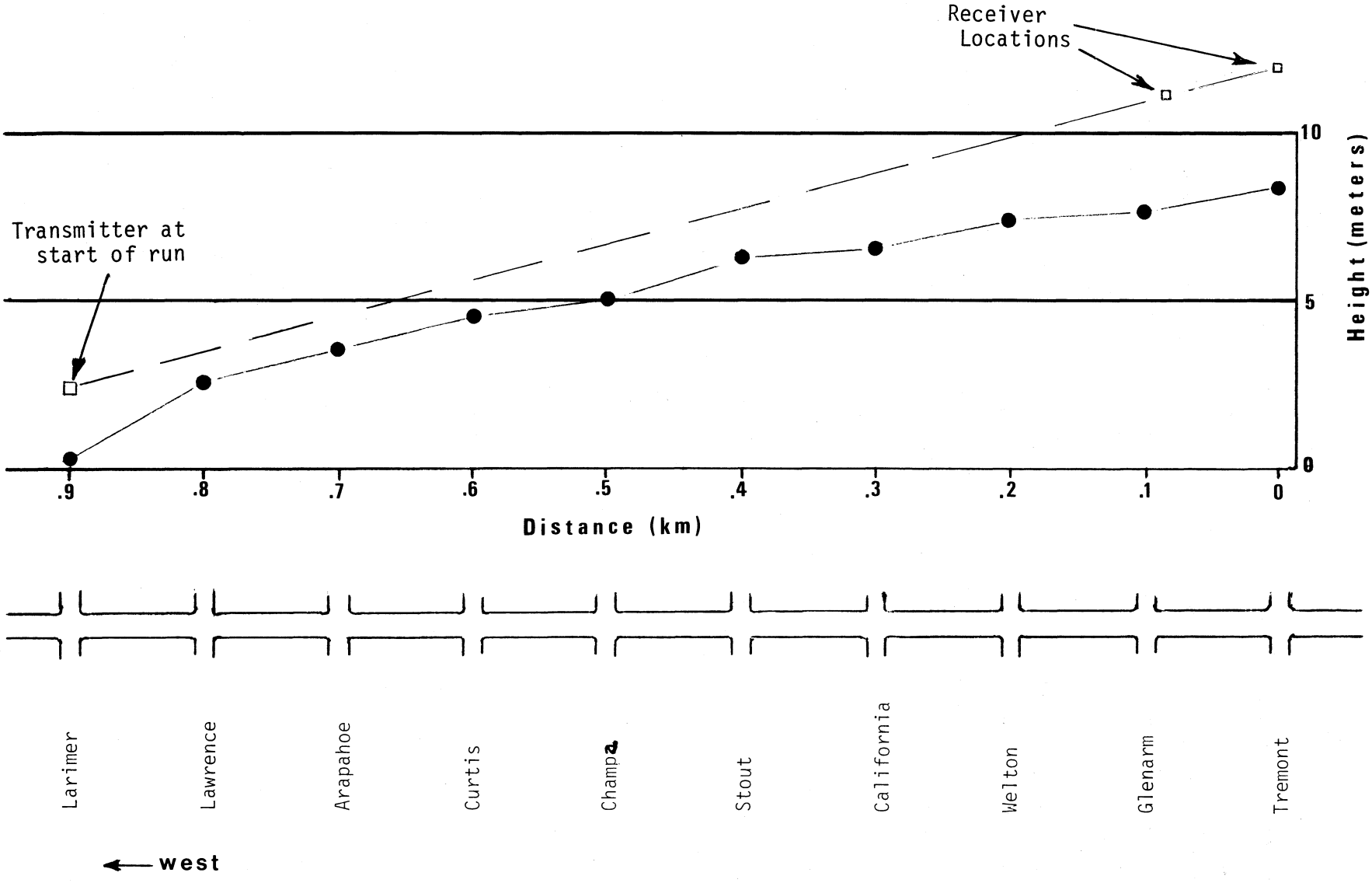

Figure 28. A drawing showing the street intersection elevation profile and the LOS path for the portion of 17th Street in Denver, CO, used to measure signal amplitude as a function of distance.

3.3.2 Discussion of Data

Figure 29 displays received signal level (RSL) plots for three separate trips of the transmitter terminal down 17th Street with the receiver terminal stationed just east of the Tremont Street intersection (runs 3, 4, and 6). The antenna beamwidths for these runs were approximately 2.5 deg for the 28.8 and 30.3 channels with vertical and horizontal polarization, respectively. Certain fading signatures repeated for each channel for every run, but there are differences in fading depth and general features. Measurements reported by Violette et al. (1983a) (rural area) showed that signal fading rates and amplitudes repeated very closely, if not precisely, for all terminal separations starting from 1.6 km, provided the position of objects along the path remained fixed. This suggests the stability of the instrumentation and slight variation in the moving terminal's speed and course are not a significant influence on signal fading for this case.

In the case of the 17th Street path, even though these runs were made on a Sunday evening and into Monday morning, numerous cars, vans, trucks, and busses were moving along the nearly 1 km portion of the street. Occasionally a vehicle would park along the street for extended periods. All of these occurrences changed the propagation environment, but did not dominate the signal characteristics. The antennas generally maintained LOS over cars except for the portion of the path near Lawrence, Arapahoe, and Curtis Streets, where the path was near grazing when the transmitter was near Larimer Street. Vans, busses, and trucks may block the LOS view, but this occurrence is detectable because all channels produce simultaneous fades and can be identified in most instances.

A signal limiting is seen on the 11.4 GHz channel about halfway between Welton and Glenarm due to saturation at the output of the IF log amplifier. The signal drop-off of the two higher frequency channels, which occurs near the end of the runs between Glenarm and Tremont, is a result of the inability to maintain optimum antenna pointing as the transmitting vehicle passes the receiving van. Run #3 of Figure 29 differs from runs #4 and #6 because the transmitter terminal traveled along the third (from the left side) traffic lane where the fourth (out of four) lane was used for all other recorded runs.

Many short-duration (in distance traveled) fades occurred that exceeded 30 dB on the narrow bandwidth channels (11.4 and 28.8 GHz), but only rarely on the wide bandwidth channel (30.3 GHz). Since multipath fading is a frequency

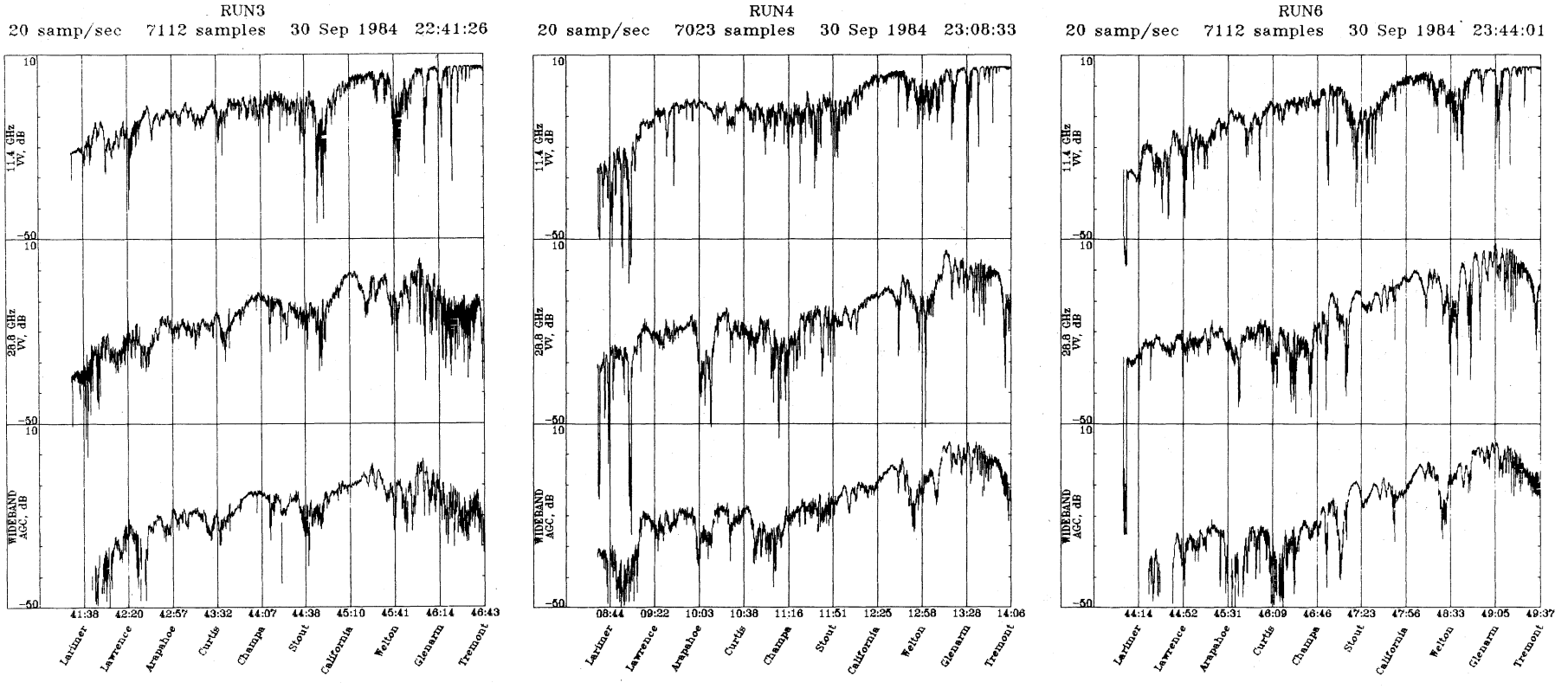

Figure 29. Received signal levels from runs 3, 4, and 6 along 17th Street (Larimer to Tremont) in Denver, CO.

selective fading, the total signal power would not be expected to decrease by the same ratio in the wideband channels as in a narrowband channel where the fade can occupy the total signal bandwidth. For example, if a single multipath signal was delayed 5 ns from the direct path, fade minimums occurred with 200 MHz spacing. Therefore, in the 700 MHz wide bandwidth channel, two fade minimums will always be present along with two enhanced peaks.

As indicated by Violette et al. (1983a), the multipath signal with the greatest amplitude was most likely reflected from the street surface and consequently would produce the deepest fades. Because the car traffic could screen the street surface on occasion and not necessarily the direct path, then probably not all deep fades are seen on each run.

A comparison of multipath fading according to antenna polarization is shown in Figure 30. Polarization for the higher two frequencies is reversed between runs as marked by a "VV" indicating both transmitter and receiver terminals use vertical antenna polarization or by "HH" indicating horizontal polarization at both terminals. As observed by Violette et al. (1983a), there is not an obvious difference in fading patterns as a function of antenna polarization. The only distinguishable difference is the possibility that deeper fades may exist for the VV mode at Welton Street and beyond, toward the receiver. If true, this might be explained by the fact that the Brewster angle, where the reflection coefficients are minimum, would occur at this distance because the grazing angles from building surfaces are in the proper vicinity, 5 to 15 deg. If in fact these reflections are lower in amplitude, it would allow the reflection from the street surface to dominate. A study of the impulse recordings should permit a more detailed view of Brewster angle effects.

For the last two runs in this series, using the narrow beamwidth receiving antennas, the receiving terminal was moved to a point about 25 m east of the Glenarm Street intersection. Figure 31 shows the RSL for two consecutive runs made less than 15 minutes apart and recorded at the new receiver location (between Tremont and Glenarm). As indicated, the LOS view was blocked in run #12 by a van around Champa Street and in run #13 by a truck near Curtis. Otherwise, the fading characteristics are quite similar between runs. The main difference between runs with the receiver near Glenarm and runs with the receiver at the Tremont intersection is that much more frequent deep fading occurs between Larimer to just beyond Curtis Street, and this region also

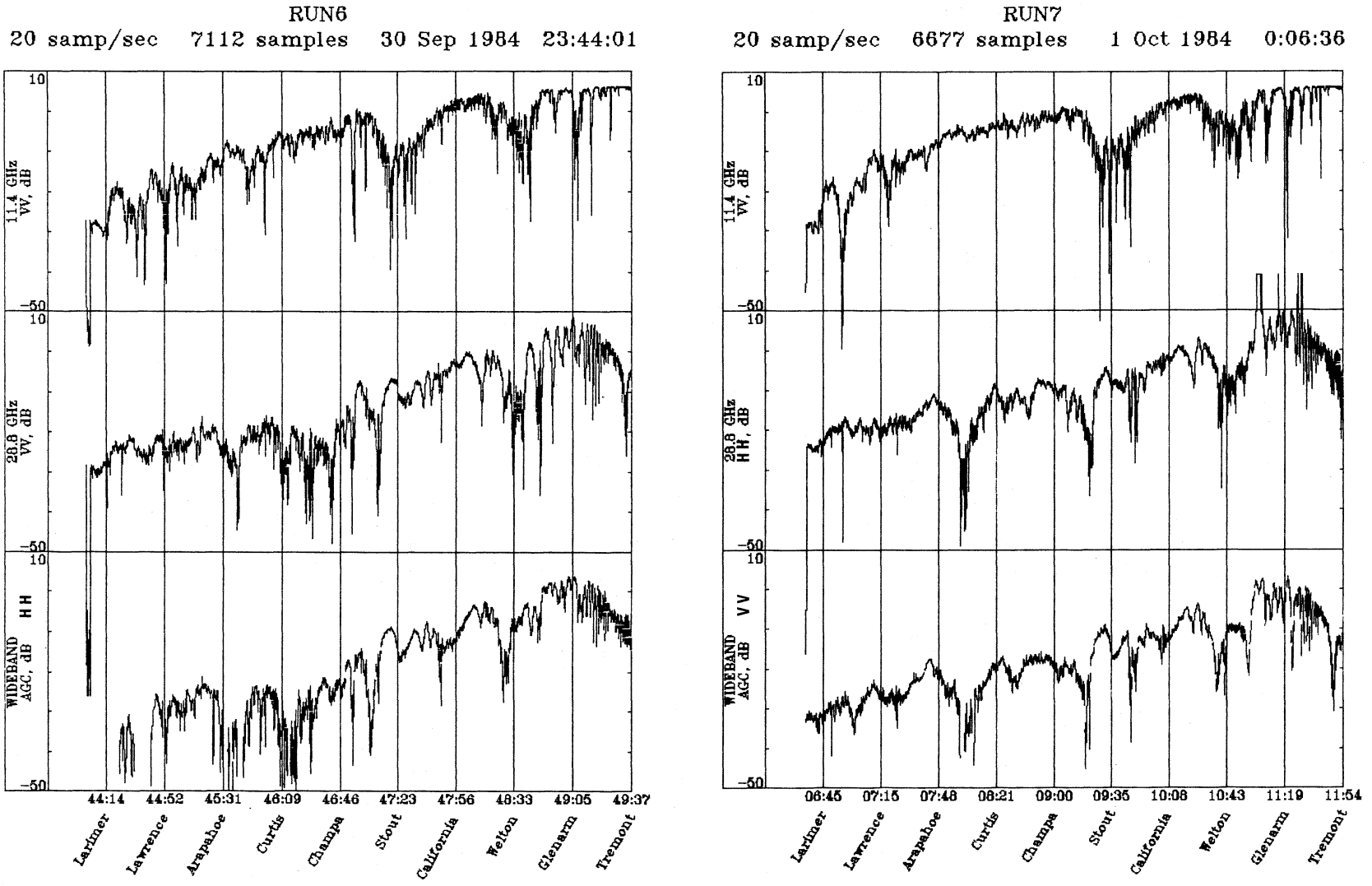

Figure 30. Received signal levels from runs 6 and 7 along 17th Street (Larimer to Tremont) in Denver, CO, for polarization comparisons at the 28.8 GHz and wideband (30.3 GHz) channels.

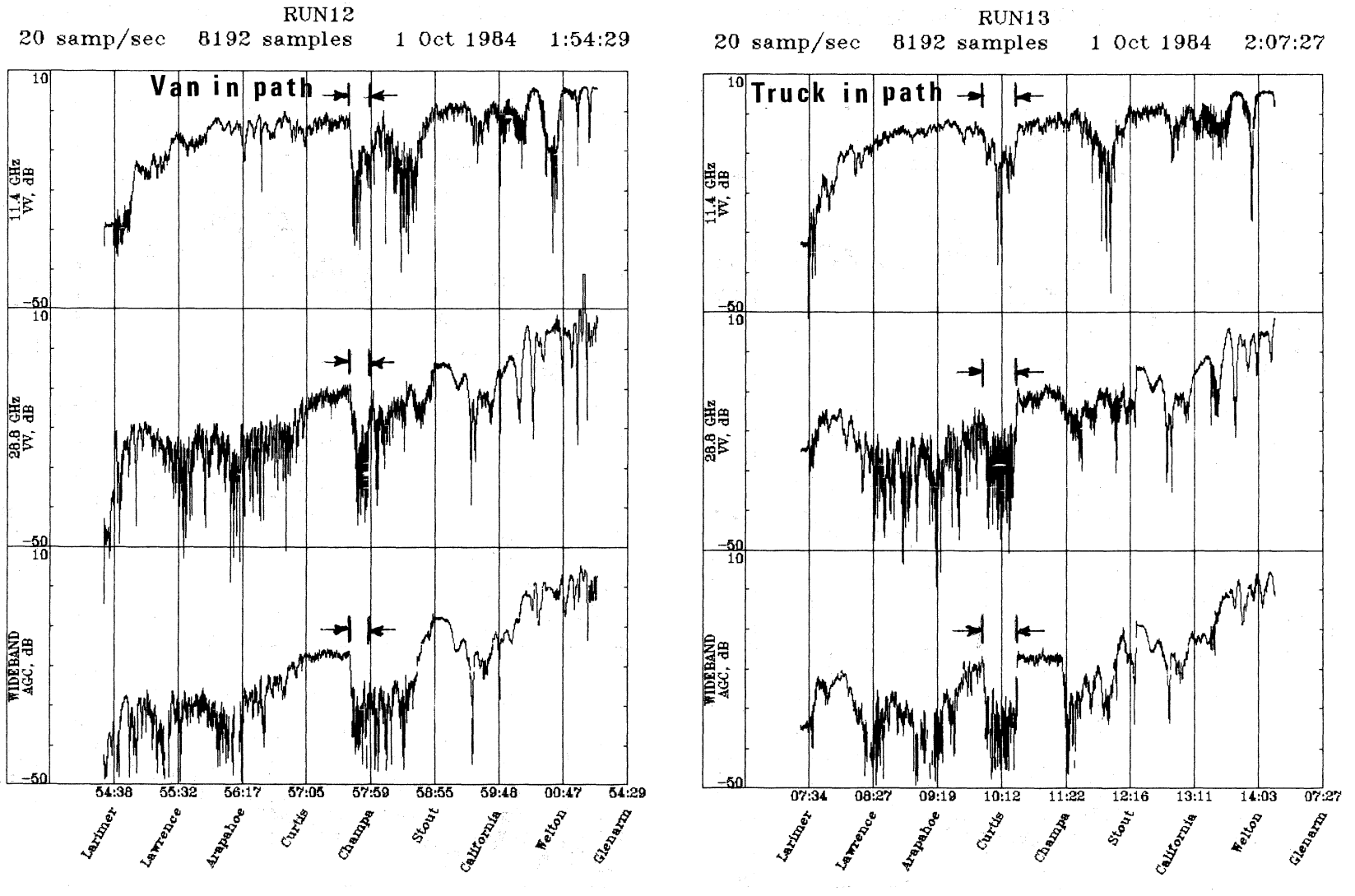

Figure 31. Received signal levels from runs 12 and 13 along 17th Street (Larimer to Welton) in Denver, CO.

showed a very dramatic difference on the impulse measurement displayed in the next section of this report.

Figure 32 shows a comparison of the RSL for narrow beamwidth antennas (2.5°) at 28.8 and 30.3 GHz and the RSL using a wide beamwidth antenna (30°) when the transmitter traveled the same path up 17th Street. It is logical that the wide beamwidth antennas will receive more multipath signals. But in the wide bandwidth channel, several fades and enhancements may exist simultaneously; therefore, the net signal level change would not be large. With the wide-beam antenna on the 28.8 GHz channel, an increased number of strong, discrete multipath signals is suggested by increased occurrence of fades of 20 dB or greater. This, unfortunately, was the extent of the wide antenna beam data because shortly after run #1 on October 10, equipment overheating occurred due to an air-conditioner failure, which produced erratic data and eventually resulted in permanent damage to data-generating hardware. This terminated these measurements, but intentions are to resume in 1985.

3.3.3 Impulse Response Measurements

The impulse probe compares a coded data stream transmitted through the propagation channel with a replica of the transmitted data stream generated at the receiver. If no distortion occurs in the propagation channel, a cross-correlation of the two data streams will produce an impulse curve that matches a known calibration impulse curve. Then, any deviation from the calibrated impulse curve represents the distortion generated by the propagation channel. In the case where the propagation channel is in an urban environment, multipath signals are the chief cause of distortion. If the multipath signal delay is less than about 2 ns from the direct path signal, then the impulse curve will display a broadening of the trailing edge. When the multipath signal delay exceeds 2 ns, a separate impulse curve will be seen with its peak indicating the amplitude relative to the direct signal and its horizontal displacement indicates the relative delay time.

An example of a calibration or low distortion impulse curve, which can be used as a reference to gauge channel performance, is shown in Figure 33. These reference curves were taken over a 120 m path with the 2.3 deg beamwidth receiving antenna. The location of the terminals was in the Commerce Department's Boulder Laboratories campus in the portion of the parking areas with convenient power drop, where the system is operated when not in a portable state. Impulse curves (1) through (9) were recorded at approximately 2-s

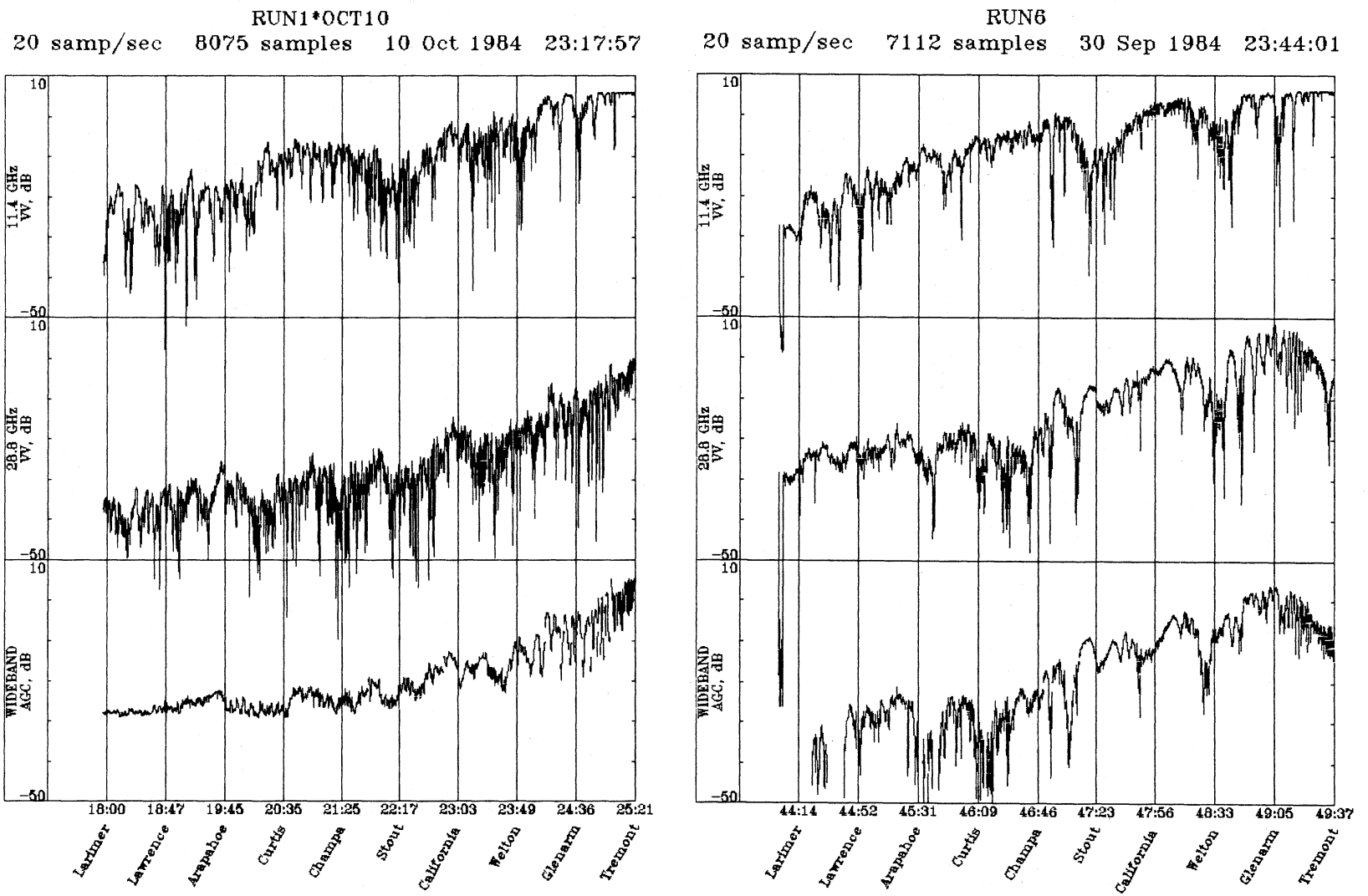

Figure 32. Received signal levels from run 1 (wide-beam antenna) and run 6 (narrow-beam antenna) along 17th Street (Larimer to Tremont) in Denver, CO.

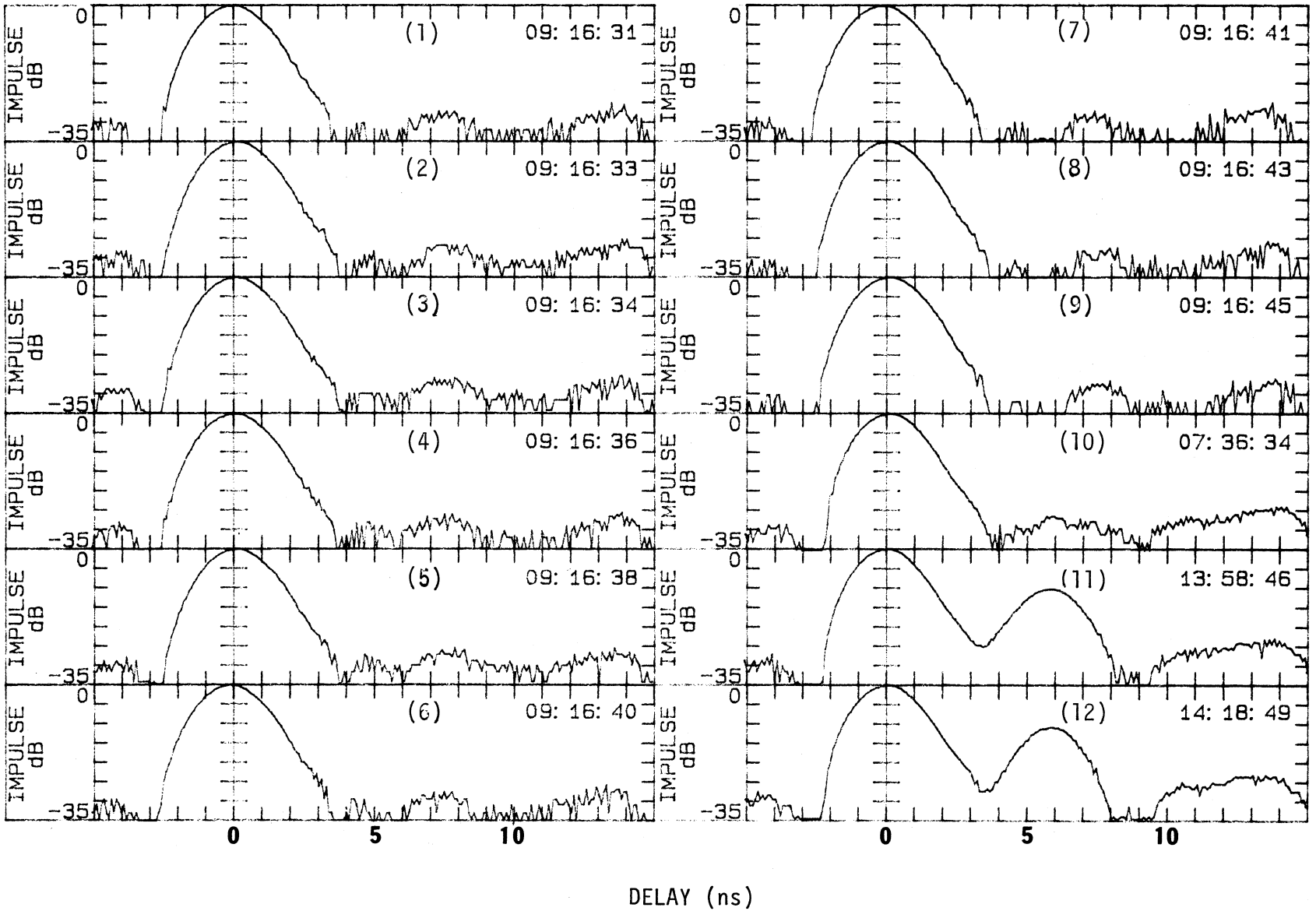

Figure 33. Reference and test impulse recordings over a 120 m path.

intervals to demonstrate the relative stability of the channel and hardware. There is a slight ground reflection broadening the trailing edge of the impulse curves, but these are more than 20 dB below the direct signal. The antenna height on the van-mounted receiving terminal does not provide sufficient clearance to benefit from the full -26 dB sidelobe suppression because the angle to ground falls on the skirt of the mainbeam for the 120 m path. The background clutter region beyond 4 ns from the direct path was observed to change in signature as vehicles moved around the parking areas. The beamwidth of the transmitting antenna was 30 deg. On a different day, curve (10) was taken with the receiving antenna pointed toward the transmitter and curves (11) and (12) were taken with the receiving antenna off-pointed about 2 deg toward a grassy bank at the edge of the parking area. In these last two impulse curves, the reflection from the bank is seen at a delay of about 6 ns.

Four sets of impulse measurements (sampled at 7-s intervals) were recorded on October 1, 1984, while the transmitting terminal traveled up 17th Street at an average speed of about 5 mph. The first two sets were recorded starting at Arapahoe Street and ending near the receiver terminal at Tremont Street, a total of about 0.7 km. Both terminals had antennas vertically polarized and used a beamwidth of 30° at the transmitter and 2.3° at the receiver. The last two sets were recorded with horizontally polarized antennas. The third set was also recorded between Arapahoe and Tremont, while for the fourth set, the transmitter traveled from Larimer (about 0.8 km) to a location 25 m east of Glenarm (the new receiving terminal location).

To best perceive the channel characteristics, the entire series (set) of impulse measurements for a given run is shown, so that they can be analyzed and compared to the reference impulse record of Figure 33. Figures 34, 35, 36, and 37 show the first set (run #8) beginning at 00:27:20 hrs MST on October 1. The transmitter terminal did not start traveling until after the 00:27:28 record. Occasionally, records are omitted because after a computer selected gain change, responding to signal fades, data word synchronization was not immediately achieved due to a select code error by the decoder on the interface bus. This resulted in an improper delay time scale because lock-up during the impulse measurement generates spurious peaks at the correlated output which interferes with the computer counting of impulse peaks. On an average, only about one record in 10 had to be omitted.

Table 3 lists the times the transmitter terminal passed the center of the indicated intersection for all the runs displayed. With this information, the

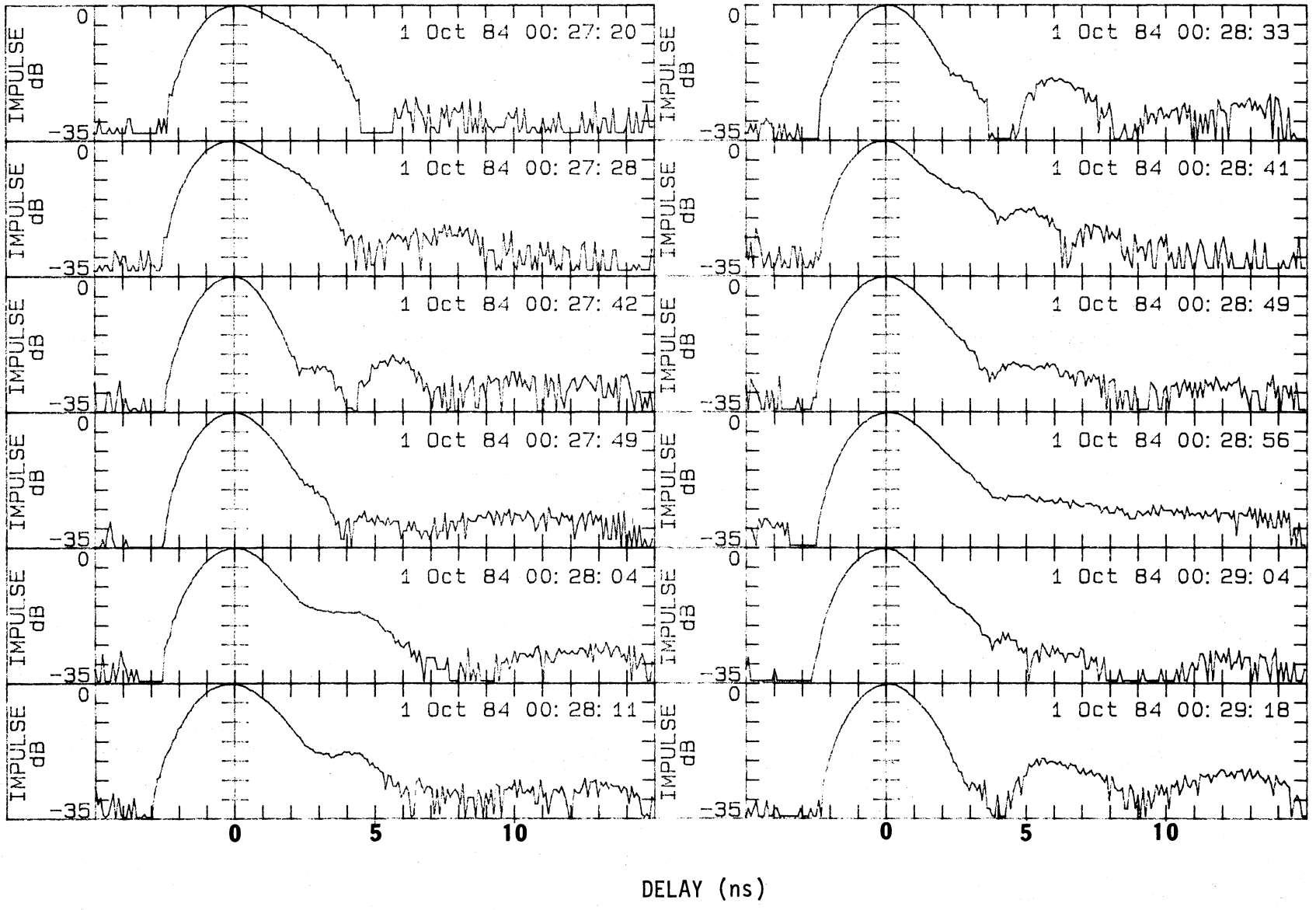

Figure 34. Impulse measurements on 17th Street (run #8) beginning at 00:27:20, October 1, 1984.

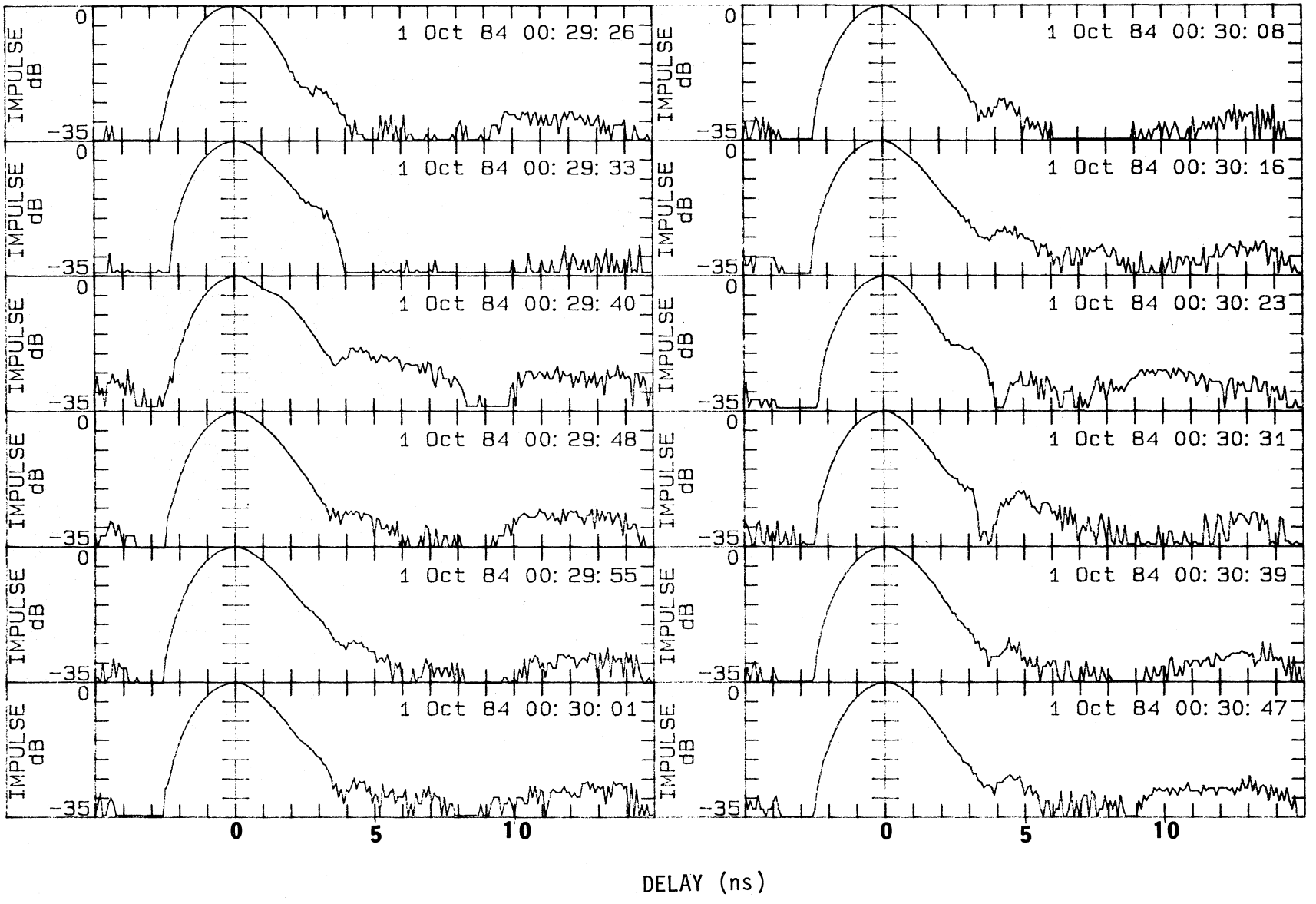

Figure 35. Impulse measurements on 17th Street (run #8) beginning at 00:29:26, October 1, 1984.

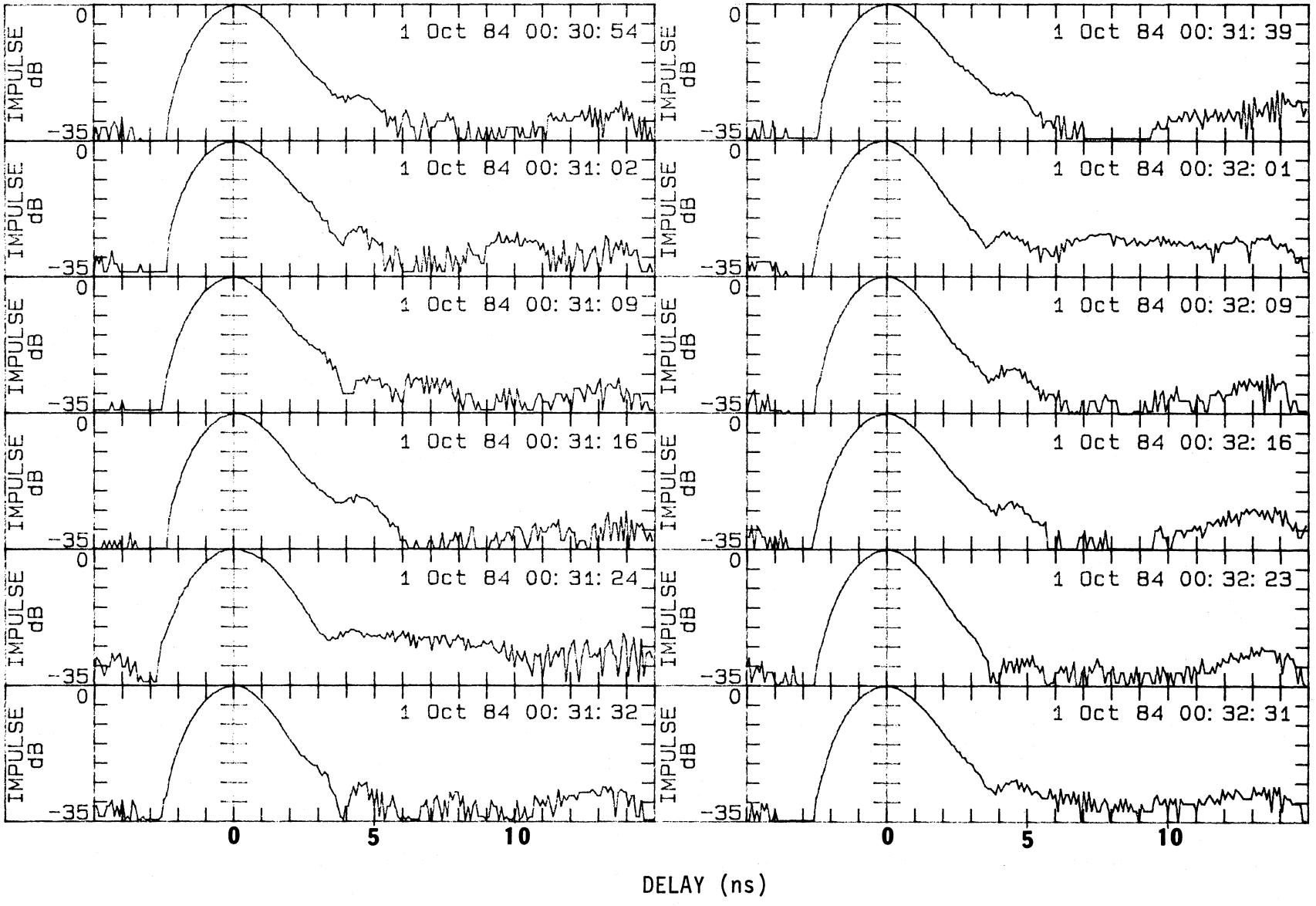

Figure 36. Impulse measurements on 17th Street (run #8) beginning at 00:30:54, October 1, 1984.

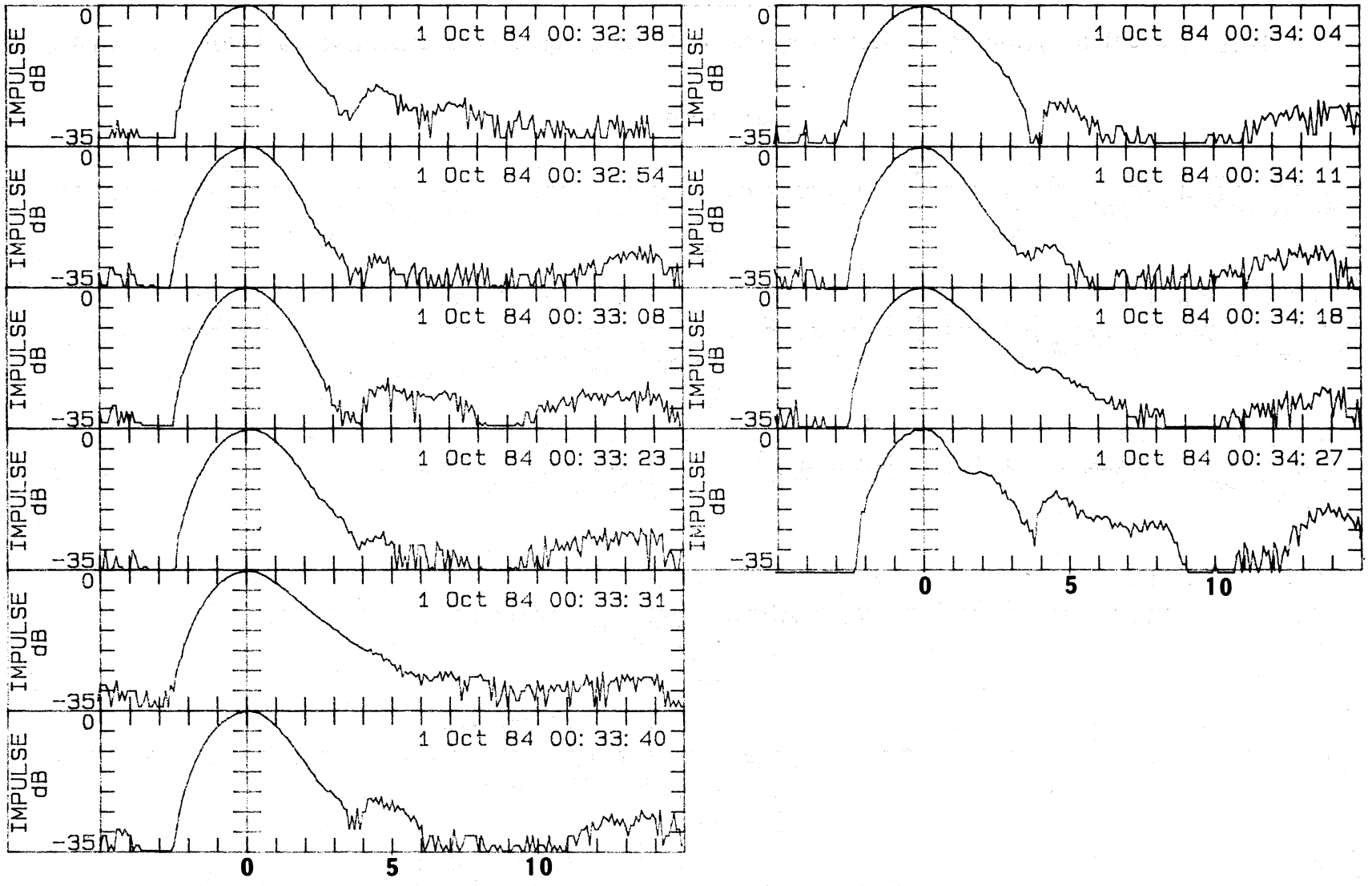

Figure 37. Impulse measurements on 17th Street (run #8) beginning at 00:32:38, October 1, 1984.

Table 3. Impulse Measurements on 17th Street in Denver, Colorado

A List of times when the transmitter arrived at the center of the intersections for the October 1, 1984, data (2.3 deg receiving antenna beamwidth).

Run #8, VV Polarization		Run #10, HH Polarization	
Arapahoe	00:28:00 hrs MST	Arapahoe	01:15:45 hrs MST
Curtis	00:28:50	Curtis	01:16:30
Champa	00:29:55	Champa	01:17:15
Stout	00:31:00	Stout	01:17:55
California	00:31:55	California	01:18:40
Welton	00:32:45	Welton	01:19:25
Glenarm	00:33:40	Glenarm	01:20:10
Tremont	00:34:30	Tremont	01:20:50
Run #11, HH Polarization			
Larimer	01:36:40 hrs MST		
Lawrence	01:37:45		
Arapahoe	01:38:35		
Curtis	01:39:15		
Champa	01:40:05		
Stout	01:40:50		
California	01:41:40		
Welton	01:42:25		
Glenarm	01:43:10		

A list of times when the transmitter arrived at each center of intersection for the October 10, 1984, data (30 deg receiving antenna beamwidth).

Run #1, HH Polarization			
Curtis	23:20:34 hrs MST		
Champa	23:21:22		
Stout	23:22:18		
California	23:23:04		
Welton	23:23:50		

particular street path that the record typifies can be identified. The channel distortion is quite evident, but most multipath signals with delays longer than 3 ns were no greater in amplitude than about 15 dB below the direct signal. Because of the fading shown in Figure 30, we know there are stronger multipath signals, such as reflections from the street surface, present at certain points along the path, but with short delays that do not separate from the direct path impulse curve. For example, the time delay between the direct path and a reflection from the street surface is less than 0.1 ns for the approximately 2 m antenna height at a terminal separation of 300 m or more. This short delay time for a street surface reflection is not distinguishable from the direct path signal; therefore, the resulting impulse response curve at a near zero time delay is effectively a composite of the direct path and any street surface multipath present for the above indicated conditions. A somewhat longer delay shows as an impulse broadening such as in the 00:29:40 record, which indicates a multipath of less than 2 ns and an amplitude of only about 3 dB below the "direct" path signal. The second set of impulse records is very similar to the first set so they are not shown.

Figures 38, 39, and 40 show impulse records for the Arapahoe to Tremont route (third set, run #10), but with linear horizontally polarized antennas. At 01:16:42, just past Curtis Street, the largest multipath of about 3 dB at slightly greater than 2 ns delay is seen. The impulse record on the first set (run #8) at 00:29:04 is approximately the same point past Curtis Street as is the 01:16:42 record (run #10). The record at 00:29:18 of the first set is comparable in location to 01:16:49 of the third set. As indicated above for grazing angles of reflection less than 20 deg, the horizontally polarized waves, in theory, experience a higher reflection coefficient. A horizontally polarized antenna is so described relative to a horizontal plane such as the street surface, but when compared to walls of buildings, the polarization behaves as a vertically polarized signal. Therefore, the Brewster angle effects reverses in these situations. An examination of the first impulse set (VV polarization) and the third impulse set (HH polarization) indicates very little difference due to polarization for those particular runs. More data will be collected at a later date, and some emphasis will be placed on determining if any Brewster angle effect can be found.

The fourth set (run #11) of impulse records differs from the third set only because the receiver terminal was moved about three-quarters of a block

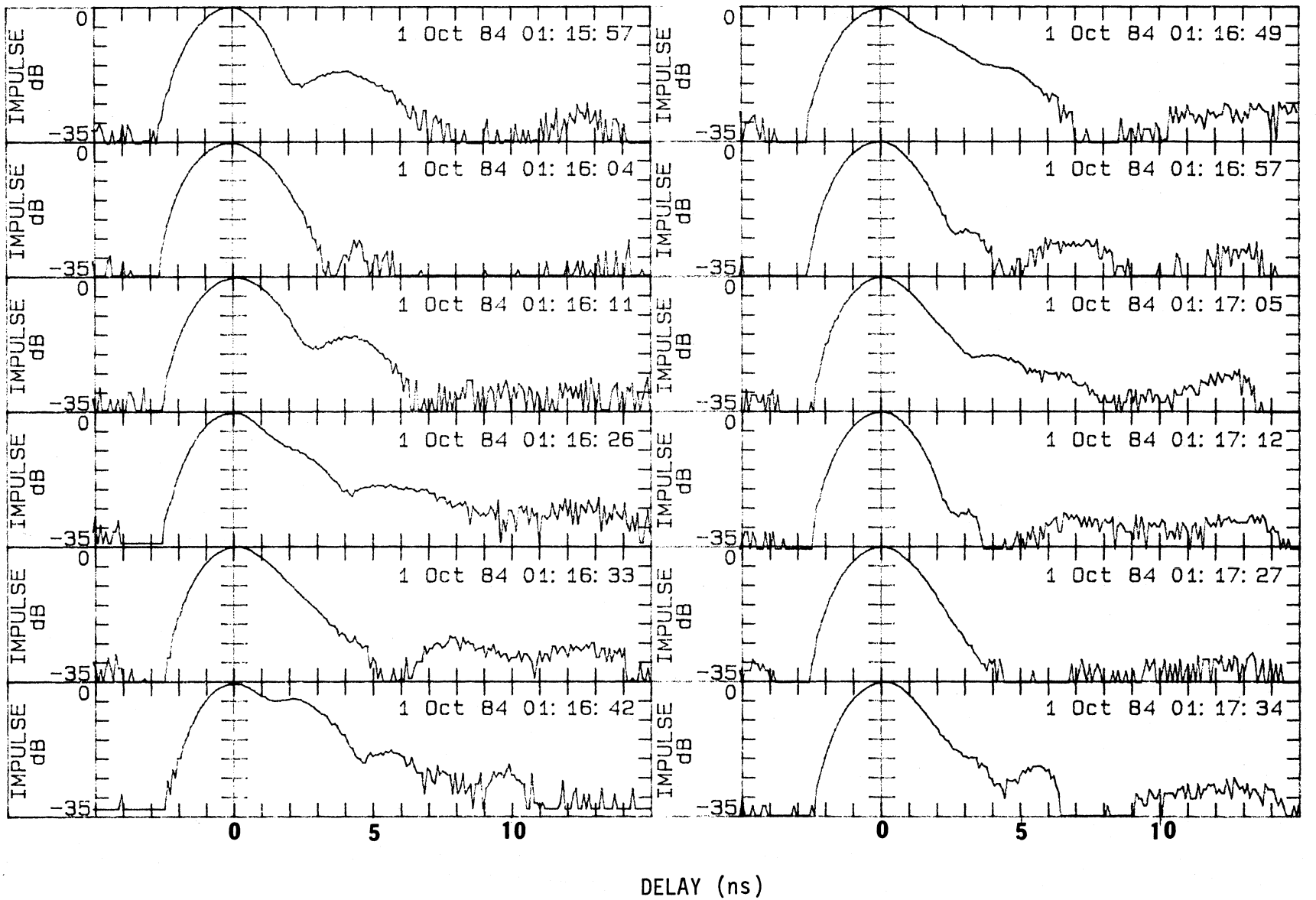

Figure 38. Impulse measurements on 17th Street (run #10) beginning at 01:15:57, October 1, 1984.

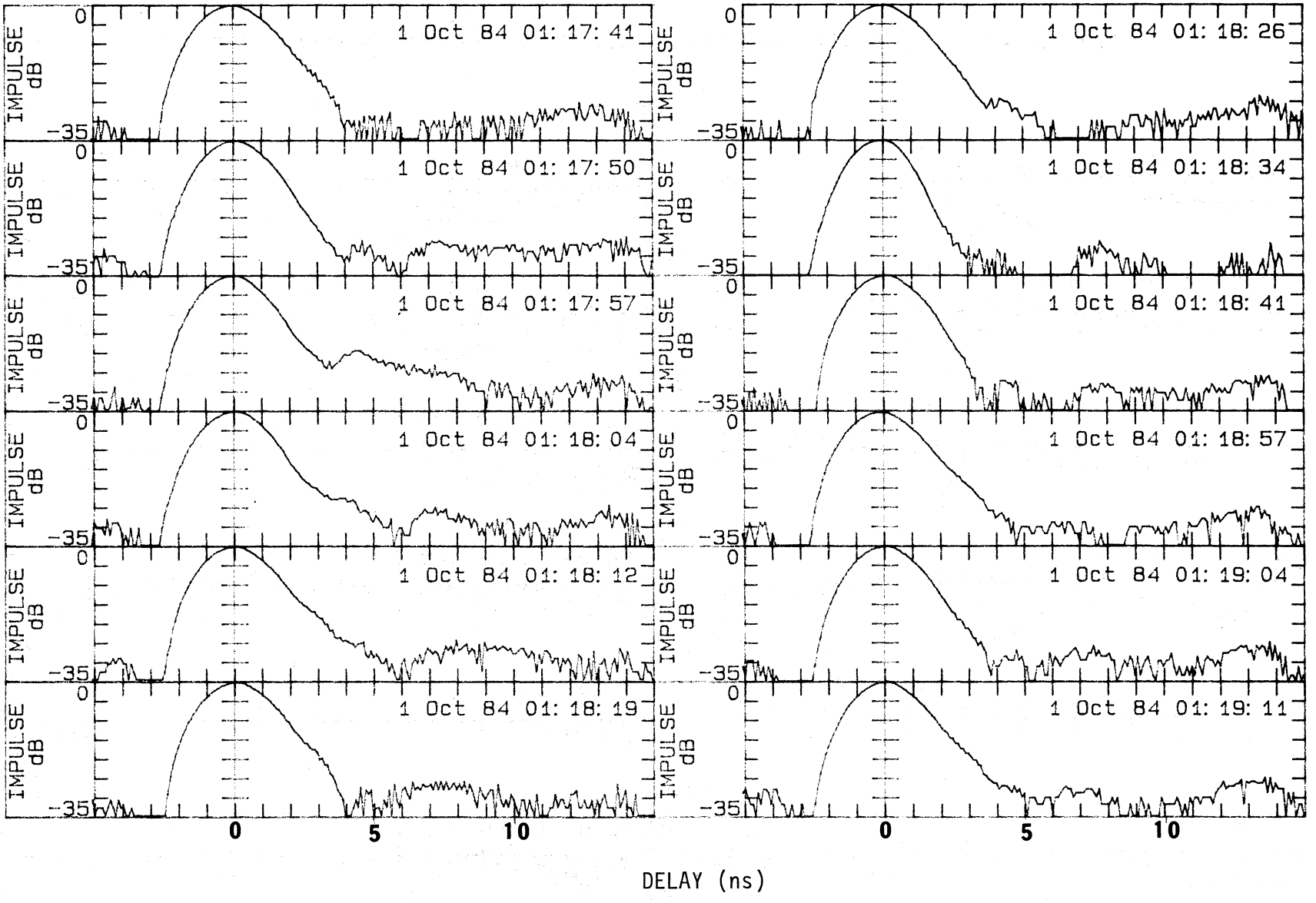

Figure 39. Impulse measurements on 17th Street (run #10) beginning at 01:17:41, October 1, 1984.

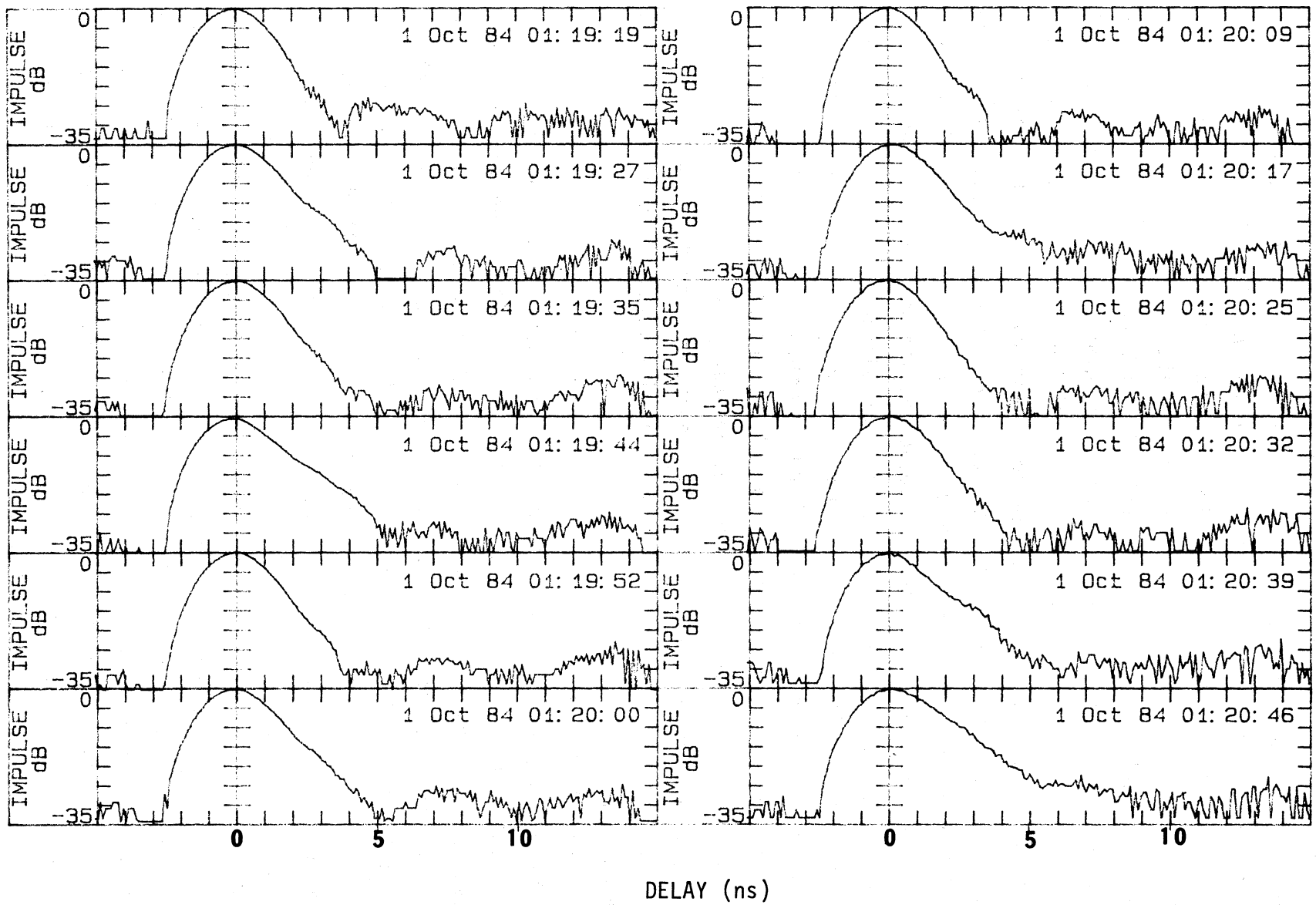

Figure 40. Impulse measurements on 17th Street (run #10) beginning at 01:19:19, October 1, 1984.

to the west, about 25 m east of Glenarm Street. This produced a dramatic increase in multipath signal strengths and time delay. Antenna polarization was again horizontal. For this set, the route was from Larimer Street to Glenarm Street with the time of arrival at the center of each intersection listed in Table 3. Figures 41, 42, 43, and 44 show the data taken at the new receiver terminal locations. At 01:37:53, just past the Lawrence Street intersection, a multipath signal exceeded the impulse amplitude at the time the "direct" signal reached the receiver, arriving with a delay of about 3.5 ns. It should be noted that the computer is programmed to label the signal with the greatest amplitude as the direct path signal. In the case of the 01:37:53 measurement, the first envelope peak is the direct signal, but the computer centered the time delay axis about the strongest signal, which was a reflected multipath component for this path situation. Very substantial multipath signal amplitudes occurred along the route from Larimer until just beyond Champa. The reason for the sizable increase in multipath activity at the new receiver location is not known. As discussed in Section 3.3.2, the RSL for this route, shown in Figure 31, indicated greater multipath activity. There may be considerable terminal position dependence when an urban path is used and only further measurements will determine the extent of this dependence.

For the 17th Street configuration and the 2.3 deg receiving antenna beamwidth, the impulse measurements for the two receiving locations showed the largest amplitude and longest delayed multipath signals when the terminals were separated by more than about 350 m. With respect to distortion, the channel quality would be sufficient to support bandwidths of up to 400 MHz or digital data rates of up to about 200 Mb/s (depending on type of modulation). However, deep frequency-dependent fading (up to 30 dB) occurred at frequent intervals which required an appropriate fade margin to prevent excessive channel outages.

For a second series of impulse measurements, the 2.3 deg beamwidth receiving antenna was replaced with a 30 deg beamwidth antenna which was identical to that used at the transmitting terminal. On October 10, two additional runs were attempted with the wide beamwidth, horizontally polarized, configuration. The route for these runs was from Larimer Street to Tremont Street where the receiving terminal was parked as in the earlier runs. By this time, overheating due to the air-conditioner problems had

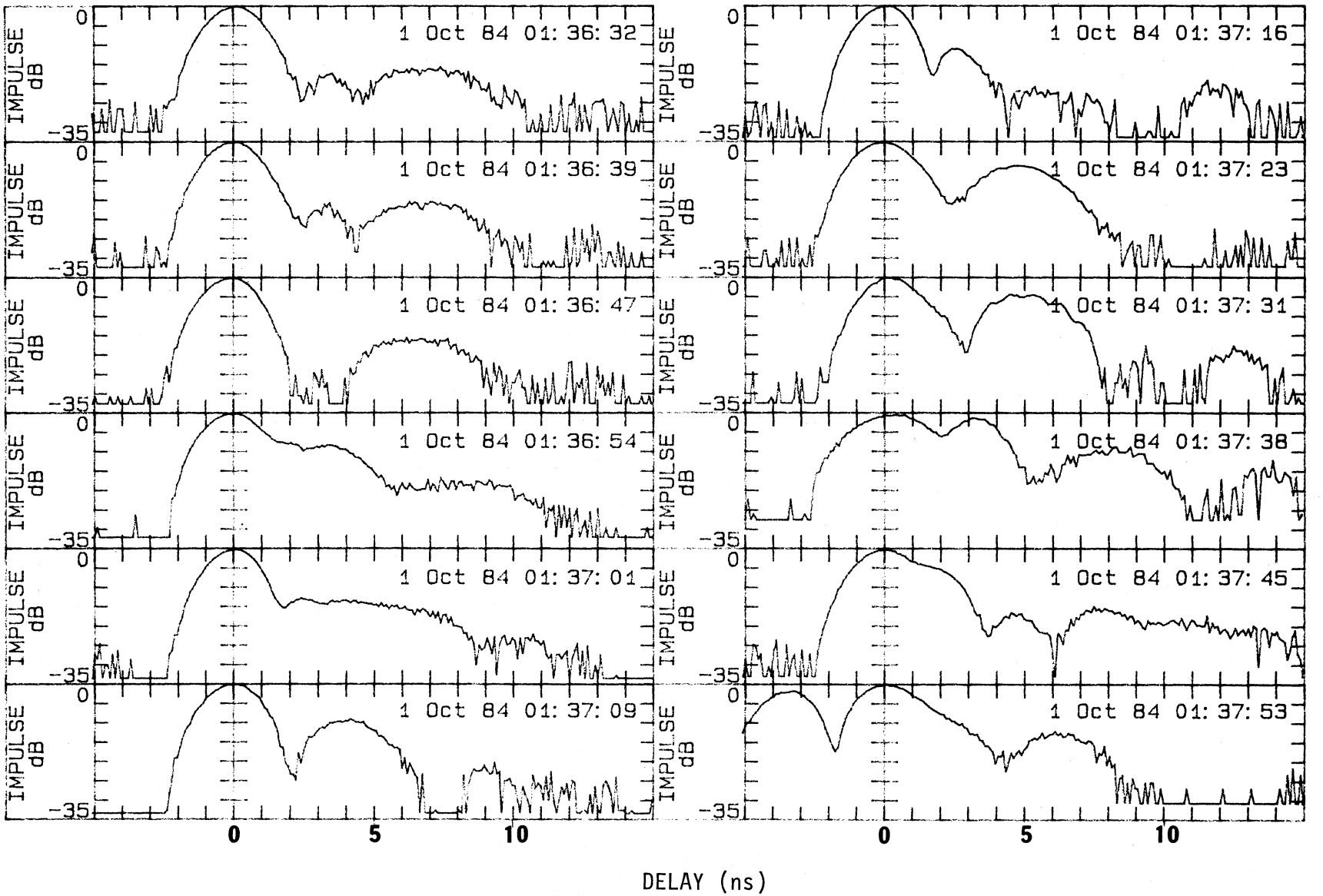

Figure 41. Impulse measurements on 17th Street (run #11) beginning at 01:36:22, October 1, 1984.

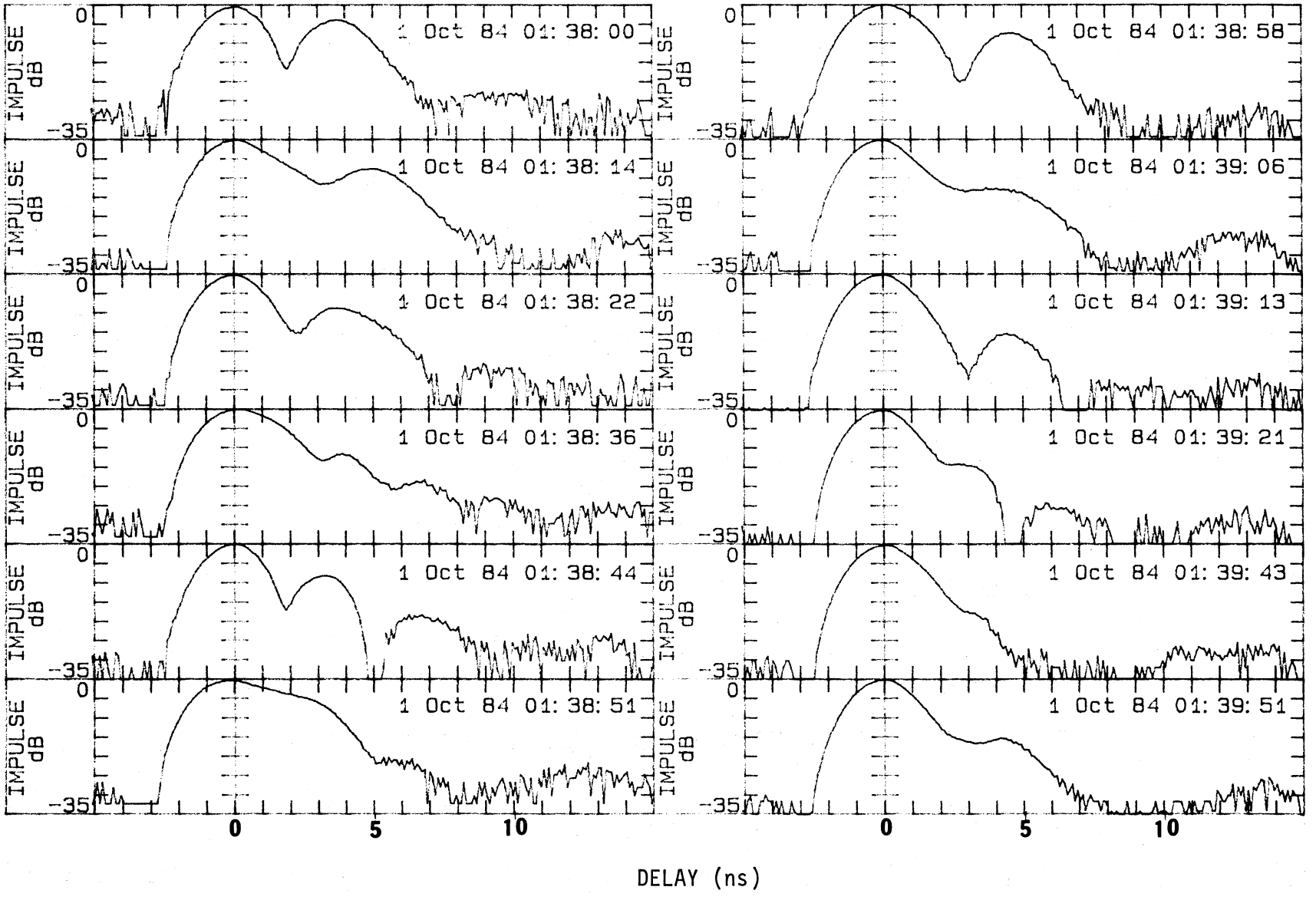

Figure 42. Impulse measurements on 17th Street (run #11) beginning at 01:38:00, October 1, 1984.

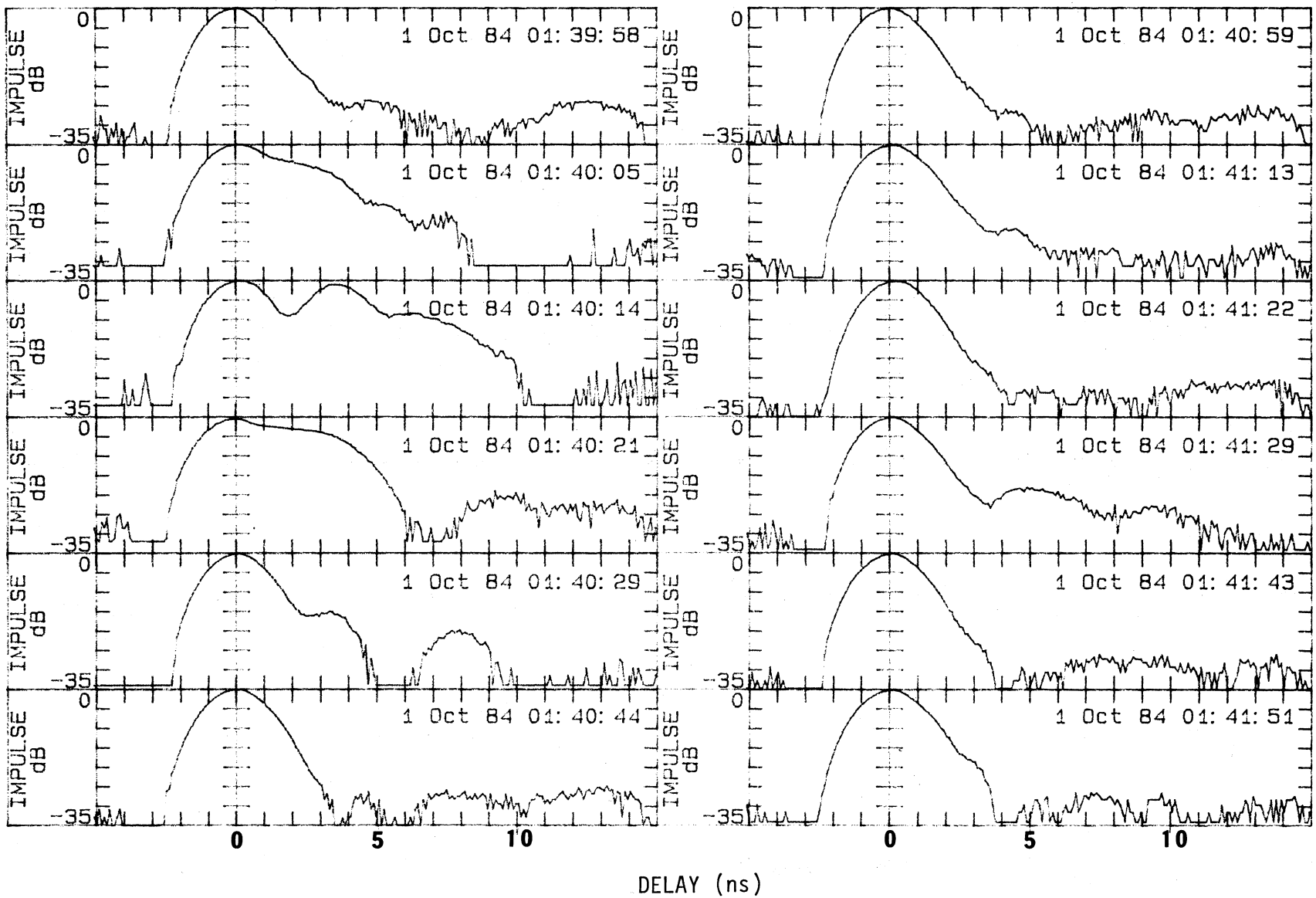

Figure 43. Impulse measurements on 17th Street (run #11) beginning at 01:39:58, October 1, 1984.

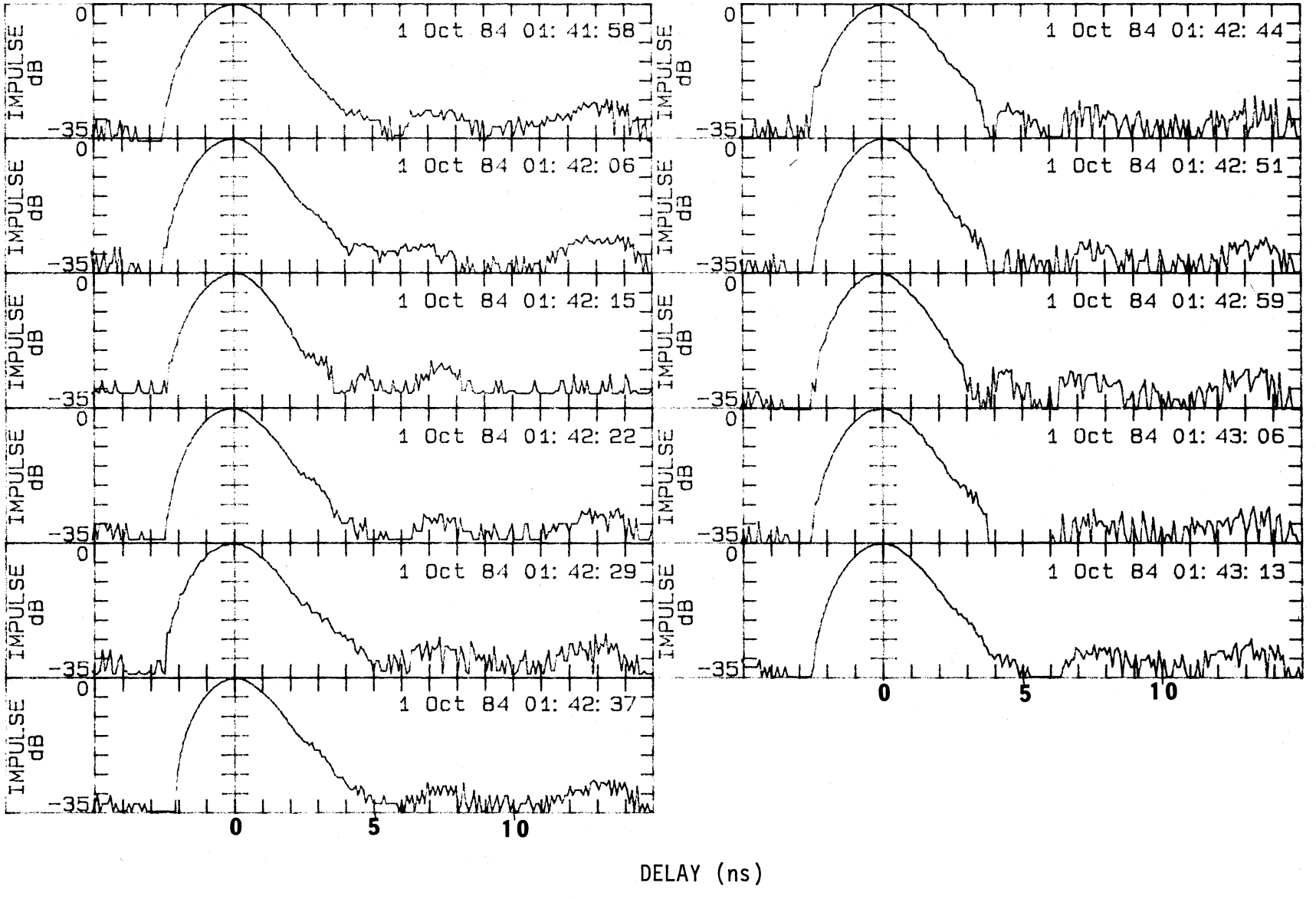

Figure 44. Impulse measurements on 17th Street (run #11) beginning at 01:41:58, October 1, 1984.

caused further hardware deterioration, so occurrences of the failure to achieve word sync were more numerous. The successful impulse recordings are shown on Figures 45 and 46. Since it was anticipated that multipath signals would occur with longer delay times, especially at the shorter path lengths, the delay time axis is extended from 15 ns to 25 ns. Table 3 lists the times the transmitter terminal arrived at the middle of the indicated street intersections. The strongest and longest delayed multipath was recorded at 23:23:35 when the transmitter was about 20-30 m west of the Welton Street intersection. A multipath peak of -2 or -3 dB with a delay of around 9 ns from the direct path is seen at this time. Data for the wide-beam receiving antenna are very limited. Preliminary indications are that distortion may restrict the maximum usable bandwidth to less than 40 MHz or less than a 20 Mb/s data rate. Bit error rate (BER) will be measured for the channel during the next series of measurements using a phase-shift-keyed carrier modulation to verify the relationship of multipath distortion to BER (Violette et al., 1983b).

4. SUMMARY AND CONCLUSIONS

Measurements were conducted at frequencies in the micro/millimeter-wave bands to obtain data on propagation characteristics in urban and suburban environments. The measurements were made for two distinctly different configurations, namely, (1) nonline-of-sight and (2) line-of-sight (LOS) paths. The non-LOS paths were concerned with absorption by buildings and signal loss for other propagation modes, such as by diffraction from edges of obstructions using test frequencies of 9.6, 28.8, and 57.6 GHz. Attenuation of rf energy when passing through material used in domestic buildings, plasterboard, and plywood was small. However, when there was a high moisture (water) content within the material, a very high rf absorption was observed. Two paths obstructed by reinforced concrete buildings without windows attenuated the direct propagated energy beyond the detection threshold or more than 80 dB at the higher two frequencies. Signal levels above the -132 dBm detection threshold were recorded when the rf energy was transported by an apparent double-edge diffraction mode over the tops of these buildings or by diffraction from objects within the common volume of the antenna beams. In general, for all the above measurements, the amount of signal loss increased with an increase in frequency.

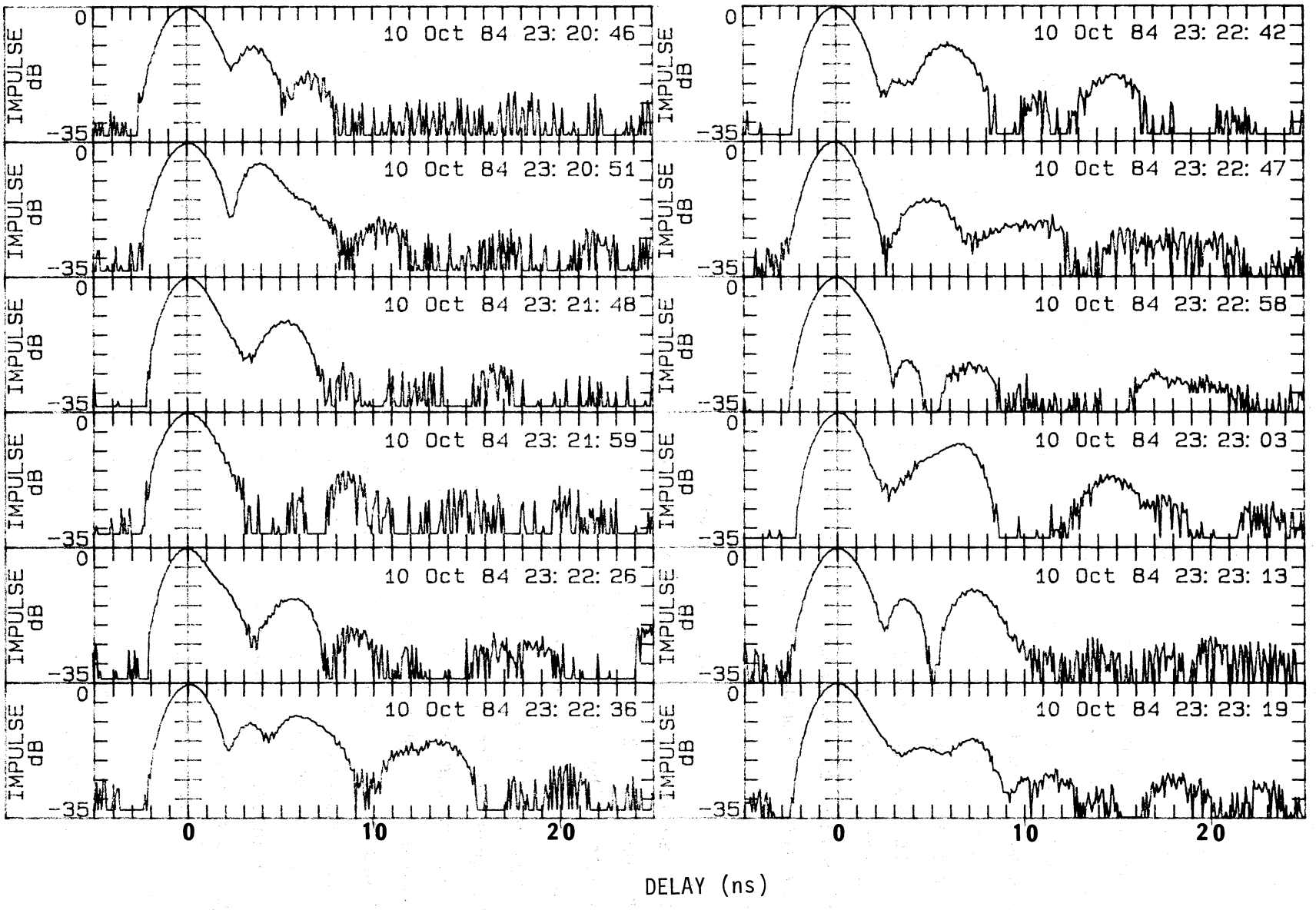

Figure 45. Impulse measurements on 17th Street beginning at 23:20:46, October 10, 1984.

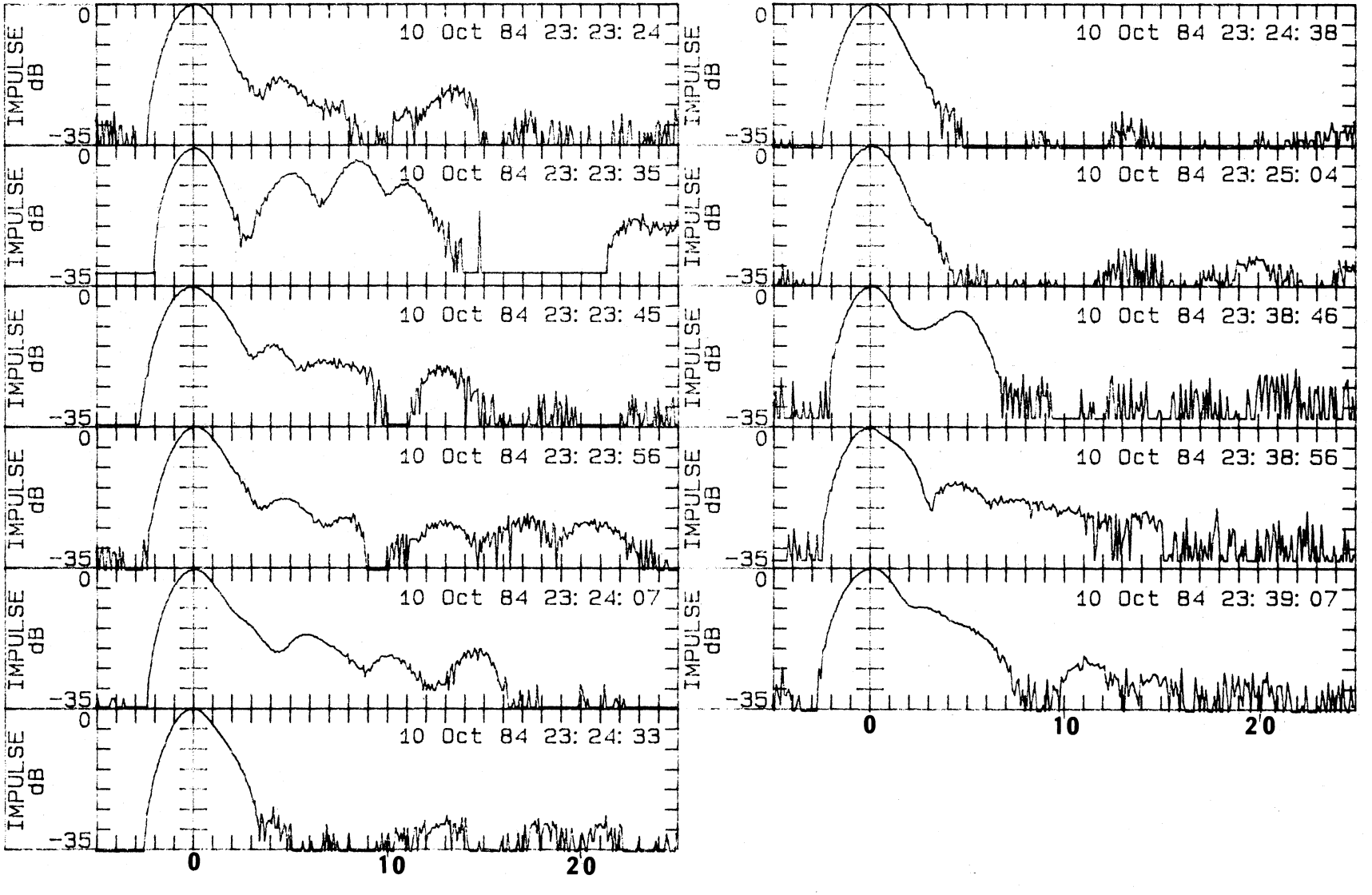

Figure 46. Impulse measurements on 17th Street beginning at 23:23:24, October 10, 1984.

Non-LOS paths through an office building constructed primarily of glass produced results that were sharply contrasting. Buildings with large areas of clear or tinted glass produced very small losses, depending on path geometry, and the signal levels could be about the same as a clear-air LOS path. Many of the recently constructed office buildings use a fused metalized coating on windows to reduce heat and light transfer into the building. A building using the metalized coating was measured, and the received signal level was reduced at least 50 dB below a LOS path.

Measurements in a variety (in density of homes) of residential areas were taken for non-LOS path lengths of from 0.1 to 1 km. These measurements were conducted during mid-summer, and the dominant absorber for nearly every path recorded was trees. As with the high absorbing commercial buildings in the path, paths obscured by tree-laden residential properties provide the strongest signal levels when a mutual LOS edge or scattering surface was illuminated in a common volume of each antenna (transmitting and receiving). Illuminated trees would predictably produce detectable signal levels that were a function of the propagated signal frequency, that is, the highest path losses at the highest frequency. For longer, non-LOS paths through residential areas, the largest signals for all measured frequencies occurred with one terminal elevated, such as positioned on a hill or overlook. This is not surprising even though the path is not LOS; the density of the obstructions is definitely less.

The second series of measurements involved only LOS paths in an urban environment. All of these measurements were recorded in Denver, Colorado, on 17th Street and used two vans, one for the transmitting terminal, the other for the receiving terminal, and a computerized data acquisition system. During recording periods, the receiving van was parked at one of two locations and the transmitting van traveled at as uniform a speed as possible (approximately 5 mph) toward the receiving terminal. Signal fading as a function of transmitter position was plotted at 11.4, 28.8, and 30.3 GHz. The highest two frequencies were used to compare fading between a very narrow bandwidth channel (3 kHz) and a wide bandwidth channel (750 MHz). As expected, the wideband channel fades were not as deep as the narrowband channel. Fades in excess of 30 dB on the narrowband channel were common and not obviously dependent on antenna polarization, vertical or horizontal linear. There was a significant difference in multipath fading when the data from the two receiving terminal

positions were compared. Fading data comparing a receiving antenna beamwidth of approximately 2.5 deg to a wide beamwidth antenna of 30 deg produced the expected increase in number of multipath components, but this test was not completed due to air-conditioning problems with the receiving van.

An important and unique millimeter-wave diagnostic tool for study of the performance of a propagation channel is the impulse probe. With the impulse probe, multipath signals can be measured in terms of amplitude and delay time with a 1-ns resolution. Not only does the impulse measurement allow an analysis of the reflection characteristics of objects, which produce multipath signals along a path, but it also allows channel distortion to be predicted, so that usable bandwidth or modulation rate limitations can be determined.

Impulse measurements recorded on the 17th Street path showed only minor distortion using a 2.3 deg receiving antenna beamwidth when the path length was less than about 350 m. However, deep fading still occurred for path lengths less than 350 m, but they are the result of strong multipath signal reflection from the street surface. Delay times relative to the direct path for street reflections are considerably less than 1 ns for the antenna heights used. Therefore, very little distortion of the impulse envelope occurred for these path lengths, and likewise very wide channel bandwidths are available before distortion from these multipath signals create a problem. For path lengths between 350 and 900 m, multipath signals nearly equal in amplitude to the direct signal were observed at delay times up to about 5 ns. As mentioned above, two receiving terminal locations were selected at random, and the number and strength of multipath signals were very different, indicating that a study of position dependence is required.

A 30-deg beamwidth antenna was installed on the receiving terminal (the same as on the transmitting terminals) which approximates the channel performance of a link with omnidirectional antennas. The main difference between omnidirectional antennas and a broadbeam directional antenna is the possibility, when using the omnidirectional antenna, of a much longer delayed multipath reflection from a surface behind either terminal. Data for the widebeam antenna were limited due to the van air-conditioner problem, but it was evident that strong, long-delay, multipath components were very numerous at path lengths of 100 to 400 m. Multipath signals within about 3 dB of the direct path with delay of nearly 10 ns were recorded. Considerable additional data

are needed to form a statistical model of channel performance in urban environments for wide beamwidth antennas.

An analytical model is presently being developed to predict multipath reflections from street and building surfaces. Given antenna heights, surface reflection coefficients, street width, and the range of the distances between terminals, signal fade statistics are predicted assuming random phase for building-reflected components. The relative phase component is computed directly from the path geometry. The channel impulse response is predicted using path delay times with amplitudes derived from the corresponding coefficients of reflection of the surfaces. The output of this model will be compared to data contained in this report as well as data to be collected in the next test series.

5. REFERENCES

Huish, P. W., and G. Pugliese (1983), A 60 GHz radio system for propagation studies in buildings, Third International Conference on Antennas and Propagation, Norwich, England, April 12-15, 1983 (Institution of Electrical Engineers, London), 219, pp. 181-185.

Hufford, G. A., R. W. Hubbard, L. E. Pratt, J. E. Adams, S. J. Paulson, and P. F. Sass (1982), Wideband propagation measurements in the presence of forests, Research and Development Technical Report CECOM 82-CS029-F, Appendix A, January.

Linfield, R. F., R. W. Hubbard, and L. E. Pratt (1976), Transmission channel characterization by impulse response measurements, OT Report 76-96, August.

Reudink, D. O. (1972), Comparison of radio transmission at X-band frequencies in suburban and urban areas, IEEE Trans., AP-20, No. 4, pp. 470-473.

Violette, E. J., R. H. Espeland, K. C. Allen, and F. Schwering (1983a), Urban millimeter wave propagation studies, Research and Development Technical Report CECOM-83-3, U.S. Army Communications-Electronics Command, Fort Monmouth, NJ 07703.

Violette, E. J., R. H. Espeland, and K. C. Allen (1983b), A diagnostic probe to investigate propagation at millimeter wavelengths, NTIA Report 83-128, August (NTIS Order No. PB84-104223).

Violette, E. J., R. H. Espeland, A. R. Mitz, F. A. Goodknight, and F. Schwering (1981), SHF-EHF propagation through vegetation on Colorado East Slope, Research and Development Technical Report CECOM-81-CS020-F, U.S. Army Communications-Electronics Command, Fort Monmouth, NJ 07703.

FORM **NTIA-29**
(4-80)

U.S. DEPARTMENT OF COMMERCE
NAT'L. TELECOMMUNICATIONS AND INFORMATION ADMINISTRATION

BIBLIOGRAPHIC DATA SHEET

	1. PUBLICATION NO.	2. Gov't Accession No.	3. Recipient's Accession No.
	NTIA Report 85-184		

4. TITLE AND SUBTITLE
Millimeter-Wave urban and suburban propagation measurements using narrow and wide bandwidth channel probes

5. Publication Date
November 1985

6. Performing Organization Code
NTIA/ITS.S3

7. AUTHOR(S)
E.J.Violette,R.H.Espeland, and G.R.Hand

9. Project/Task/Work Unit No.
9108108

8. PERFORMING ORGANIZATION NAME AND ADDRESS
NTIA/ITS.S3
U.S.Dept of Commerce
325 Broadway
Boulder, CO 80303

10. Contract/Grant No.

11. Sponsoring Organization Name and Address
NTIA
1800 G Street NW
Washington, DC

12. Type of Report and Period Covered

13.

14. SUPPLEMENTARY NOTES

15. ABSTRACT *(A 200-word or less factual summary of most significant information. If document includes a significant bibliography or literature survey, mention it here.)*

Measurements reported are part of a study of propagation characteristics for millimeter-wave communication links operating in an urban-suburban environment. Absorption data were collected for signals propagated through some common building materials at 9.6 (reference frequency), 28.8, and 57.6 GHz. At these same channel frequencies, paths at street level obstructed by office buildings and residential properties were examined in terms of received signal levels resulting from direct penetration and/or propagation by diffraction modes with terminal separation of from 0.1 to 1.2 km. Signal fading was measured for line-of-sight paths up to 0.9 km as the transmitter terminal, operating at 11.4, 28.8, and 30.3 GHz, traveled down an urban street. Narrow- and wide-beam antenna patterns and both modes of linear antenna polarization were used to compare multipath fading characteristics. A unique 30.3 GHz wide bandwidth channel impulse probe was used to record multipath signal amplitudes and delay times, relative to the direct path, for the same antenna parameters indicated above. Impulse response measurements were recorded at about 10 m intervals as the transmitter traveled along the urban street.

16. Key Words *(Alphabetical order, separated by semicolons)*
impulse; millimeter waves; multipath; propagation; urban-suburban

17. AVAILABILITY STATEMENT	18. Security Class. *(This report)*	20. Number of pages
☒ UNLIMITED.	UNCLASSIFIED	90
☐ FOR OFFICIAL DISTRIBUTION.	19. Security Class. *(This page)* UNCLASSIFIED	21. Price:

☆ U.S. Government Printing Office: 1980—678-495/529